

**An-Najah National University
Faculty of Graduate Studies**

**Design and Simulation of a Photovoltaic
System with Maximum Power Control to
Supply a Load with Alternating Current**

**By
Ja'far Saif Edden Abdel Hafeath Jallad**

**Supervisor
Prof. Marwan Mahmoud**

**This thesis is submitted in Partial Fulfillment of the Requirements
for the Degree of Master in Clean Energy and Energy
Conservation Strategy Engineering, Faculty of Graduate Studies,
at An-Najah National University, Nablus, Palestine**

2012

Design and Simulation of a Photovoltaic System with Maximum Power Control to Supply a Load with Alternating Current

By
Ja'far Saif Edden Abdel Hafeath Jallad

This Thesis was defended successfully on 27/12/2012 and approved by:

Defense Committee Members

Signature

1. Prof. Marwan Mahmoud / Supervisor



2. Dr. Abdel Karim Daud/ External Examiner



3. Dr. Imad Ibrik / Internal Examiner



Dedication

I would like to dedicate my thesis work to

My father, mother, brothers and sisters.....

All friends and colleagues.....

Everyone who works in this field.....

Acknowledgment

I would like to thank my family for constant love and support that have always given me.

Thanks go also to all my friends and fellows graduate Students.

My thanks and appreciations go to the staff of Clean Energy and Conservation Strategy Engineering Master Program in An-Najah National University

Finally, and most importantly, my furthestmost appreciation goes to my supervisor, Prof. Dr. Marwan Mahmoud for his exceptional guidance and insightful comments and observations throughout the duration of this project.

Jafar Jallad

الإقرار

أنا الموقع أدناه، مقدم الرسالة التي تحمل العنوان:

Design and Simulation of a Photovoltaic System with Maximum Power Control to Supply a Load with Alternating Current

تصميم ومحاكاة نظام خلايا شمسية مع متحكم لإيجاد القدرة القصى لتغذية الحمل بالتيار المتناوب

أقر بأن ما اشتملت عليه هذه الرسالة إنما هو نتاج جهدي الخاص، باستثناء ما تمت الإشارة إليه حيثما ورد، وأن هذه الرسالة كاملة، أو أي جزء منها لم يُقدم من قبل لنيل أي درجة أو لقب علمي أو بحثي لدى أي مؤسسة تعليمية أو بحثية أخرى.

Declaration

The work provided in this thesis, unless otherwise referenced, is the researcher's own work, and has not been submitted elsewhere for any other degree or qualification.

Student's Name:

اسم الطالب:

Signature:

التوقيع:

Date:

التاريخ:

List of Abbreviations

AC	Alternative current
DC	Direct current
kWh	Kilo watt hour
NIS	New Israeli shekel
STC	Standard Test Condition
PSH	Peak sun hour
PV	Photovoltaic
CV	Constant voltage method
CR	Charge Controller
CCM	Continues Conduction Mode
VSI	Voltage Source Inverters
FIT	Feed in Tariff
LCC	Life Cycle Cost
SPWM	Sine Pulse Width Modulation
PENRA	Palestinian Energy and natural resources Authority

Table of Contents

No.	Contents	Page
	Dedication	iii
	Acknowledgment	iv
	Declaration	v
	List of Abbreviations	vi
	Table of Contents	vii
	List of Tables	x
	List of Figures	xi
	List of Appendixes	xvi
	Abstract	xvii
	Chapter One: Introduction	1
	Chapter Two: Solar Photovoltaic Technology	6
2.1	Introduction	7
2.2	Photovoltaic Cell	7
2.2.1	Types of photovoltaic cells	8
2.3	Modeling of Photovoltaic Module by Matlab Simulink and Psim	9
2.3.1	Ideal cell	9
2.3.2	A real photovoltaic device	15
2.3.3	Model of the photovoltaic module by Matlab and Psim (Power Simulation)	15
2.3.4	R_s and R_p calculation	20
2.3.5	Impact of solar radiation on I-V characteristic curve of photovoltaic module	23
2.3.6	Impact of temperature on I-V characteristic curve of photovoltaic module	24
2.3.7	Impact of shading on I-V characteristic curve of photovoltaic module	25
2.4	The Photovoltaic Array	28
2.5	Summary	30
	Chapter Three: DC – DC Convertor and Battery	32
3.1	Introduction	33
3.2	Power Electronics in a PV System	33
3.3		35
3.3.1	DC-DC switch mode converters	35
3.3.2	Control of DC-DC converters	36
3.3.3	Steady state analysis	38
3.4		39
3.4.1	Buck converter	39
3.4.2	Output voltage ripple in a buck converter	42

No.	Contents	Page
3.5		43
3.5.1	Boost converter	43
3.5.2	Output voltage ripple in a boost converter	46
3.6	Buck versus Boost in a PV System	47
3.7	Battery	48
3.8	Charge Controllers	51
3.8.1	Series controllers	52
3.8.2	Shunt controllers	52
3.8.3	MPPT charge controllers	53
3.9	Calculation of Boost Converter Parameters	53
	Chapter Four: Maximum Power Point Tracking (MPPT) Techniques	56
4.1	Introduction	57
4.2	Maximum Power Point Tracking (MPPT) Techniques	58
4.2.1	Perturb and observe	59
4.2.2	Incremental conductance	61
4.2.3	Open-circuit voltage	64
4.2.4	Short -circuit current	65
4.3	Simulation and Validation of the Buck Converter with MPPT Controller by using Simulink and Psim Software	66
4.4	Discussion	69
	Chapter Five: Voltage Source Inverters (VSI)	73
5.1	Introduction	74
5.2	DC/AC Inverter Analysis	74
5.2.1	Single phase full bridge DC/AC inverter	74
5.2.2	Six step inverter	79
5.3	Modulation Strategy	83
5.3.1	Sine PWM	83
5.3.2	Simulation and validation the sine PWM by using Psim	86
	Chapter Six: Design of PV System for Electrification of a Household in Palestine	89
6.1	Introduction	90
6.2	Ambient Temperature in Palestine	92
6.2	Solar Energy in Palestine	93
6.3	Calculation Electricity Consumption	94
6.4	The Average Daily of Solar Radiation Intensity	96
6.5	Installation of the PV System	96
6.5.1	PV generator sizing	96
6.5.2	Selection of the battery block	99
6.5.3	Charge regulator (CR) sizing	100

No.	Contents	Page
6.5.4	Inverter sizing	102
6.6	Types of Solar PV Systems	103
6.6.1	Stand-alone PV	103
6.6.2	Grid tie inverter	105
	Chapter Seven: Economic Analysis of the Standalone and Grid Tie PV system	107
7.1	Economic study of the Standalone PV Systems	108
7.1.1	Determining the cost of producing one kWh from Standalone PV System	108
7.1.2	Economic factors	110
7.1.3	Cost of producing one kWh from standalone PV system for a house	112
7.2	Grid Tie System Tariffs	114
7.2.1	Net metering tariff	114
7.2.2	Feed in tariff	115
7.2.3	Evaluation the economic impact of a house grid tie feed in tariff PV system	116
7.3	Environment impact of PV system	114
	Chapter Eight: Modeling of the Standalone and Grid Tie PV system	120
8.1	Introduction	121
8.2	Standalone PV System	121
8.2.1	Battery charging algorithm	124
8.2.1.1	Trickle charge – 1 st stage (from T ₀ to T ₁)	125
8.2.1.2	Bulk charge - 2 nd stage (from T ₁ to T ₂)	126
8.2.1.3	Over charge – 3 rd stage (from T ₂ to T ₃)	126
8.2.1.4	Float charge – 4 th stage (from T ₃ until the end)	126
8.2.2	Off - grid inverter	131
8.3	Grid Tie PV System	133
	Conclusions and Future Scope of Work	142
	References	144
	Appendixes	149
	الملخص	ب

List of Tables

No.	Table	Page
Table (2.1)	Electrical characteristics data of the MSX-50 solar module at 25 °C, 1.5AM, 1000W/m ² . Taken from the datasheet [4]	16
Table (3.1)	Specification of Boost Controller	54
Table (6.1)	Hourly average solar radiation of typical summer day (31/7/2012)[22]	90
Table (6.2)	Ambient temperature in Tulkarm[22]	93
Table (6.3)	Monthly solar energy on horizontal surface for Tubas District –2011[23]	94
Table (6.4)	The electrical load for typical household	95
Table (6.5)	Specification of Kyocera KC130GHT-2 module at standard conditions	96
Table (7.1)	Cost of elements and installation of standalone PV system	112

List of Figures

No.	Figure	Page
Figure (2.1)	Photovoltaic cell [2]	8
Figure (2.2)	The main industrialized PV technologies [3]	9
Figure (2.3)	Equivalent model of a photovoltaic cell [4]	10
Figure (2.4)	Characteristic I-V, P-V curve of a practical photovoltaic device [4]	14
Figure (2.5)	Picture of MSX-50 Photovoltaic Modules [4]	16
Figure (2.6)	I-V characteristics at 1000W/m^2 , from data sheet with different temperature	17
Figure (2.7)	PV module model in Simulink	17
Figure (2.8)	Equivalent circuit of a practical PV	18
Figure (2.9)	Simulink modeling implementation for I_o	18
Figure (2.10)	Simulink modeling implementation for I_{PV}	19
Figure (2.11)	Simulink modeling implementation for I_m	19
Figure (2.12)	PV model in Psim	20
Figure (2.13)	I-V characteristics at $T=25^\circ\text{C}$, irradiance= 1000W/m^2 , after calculation of R_s and R_p , by Simulink	22
Figure (2.14)	I-V, P-V characteristics at $T=25^\circ\text{C}$, irradiance = 1000W/m^2 , after calculation of R_s and R_p , by Psim	22
Figure (2.15)	P-V characteristics at $T=25^\circ\text{C}$, by Simulink With different irradiances[Y- axis: power, X –axis: voltage]	23
Figure (2.16)	I-V characteristics at $T=25^\circ\text{C}$, by Simulink with different irradiances[Y- axis: current, X –axis: voltage]	24
Figure (2.17)	I-V characteristics at $T=25^\circ\text{C}$, by Psim with different irradiances	24
Figure (2.18)	I-V characteristics at 1000W/m^2 , by Psim with different temperature	25
Figure (2.19)	Two PV module with series connection at variable irradiance at 1000W/m^2 and 500W/m^2 , by Matlab - Simulink	26
Figure (2.20)	I-V characteristics at variable irradiance at 1000W/m^2 and 500W/m^2 , by Matlab – Simulink [Y- axis: current, X –axis: voltage]	26
Figure (2.21)	P-V Characteristics at variable irradiance at 1000W/m^2 and 500W/m^2 , by Matlab – Simulink [Y- axis: power, X –axis: voltage]	26

No.	Figure	Page
Figure (2.22)	A PV module with bypass and blocking diodes	27
Figure (2.23)	Relation between the PV cell, a module and an array	28
Figure (2.24)	PV array model, Nser is number of series of PV modules; Npar is number of parallel PV modules	29
Figure (2.25)	I-V Characteristics at T=25°C, G=1000W/m ² , by Simulink for Nser = 15, Npar = 2 [Y- axis: current, X -axis: voltage]	30
Figure (2.26)	P-V Characteristics at T = 25°C, 1000W/m ² , by Simulink for Nser = 15, Npar = 2 [Y- axis: power, X -axis: voltage]	30
Figure (3.1)	Block diagram of a power electronic system[10]	34
Figure (3.2)	Block diagram of a power processor	35
Figure (3.3)	The principle of PWM control	37
Figure (3.4)	The principle of switching [10]	37
Figure (3.5)	Buck converter [10]	40
Figure (3.6)	Buck converter circuit for: a) t_{on} and b) t_{off} CCM[10]	40
Figure (3.7)	Inductor voltage and current of the buck converter [10]	41
Figure (3.8)	Output voltage ripple in a buck converter [10]	43
Figure (3.9)	Boost converter [10]	44
Figure (3.10)	Boost converter circuit for a) t_{on} and b) t_{off} in CCM [10]	44
Figure (3.11)	Inductor voltage and current of the boost converter	45
Figure (3.12)	The effect of parasitic elements in a boost converter	46
Figure (3.13)	Output voltage ripple in a boost converter [10]	47
Figure (3-14)	Number of cycles for different discharge depths[12]	50
Figure (3.15)	Series charge controller	52
Figure (3.16)	Shunt charge controller	52
Figure (3.17)	MPPT controller	53
Figure (3.18)	Boost converter circuit	54
Figure (4.1)	PV module is directly connected to a (variable) resistive load [14]	57
Figure (4.2)	I-V curves of BP SX 150S PV module and various resistive loads at (1000W/m ² , 25oC) [14]	58

No.	Figure	Page
Figure (4.3)	P-V Characteristics of a module [15]	59
Figure (4.4)	P&O flow chart[15]	60
Figure (4.5)	Design P&O algorithm by Psim	60
Figure (4.6)	Incremental Conductance flow chart [15]	62
Figure (4.7)	Incremental conductance by psim	63
Figure (4.8)	Open Circuit voltage flow chart[15]	64
Figure (4.9)	Constant voltage flow chart [16]	65
Figure (4.10)	Short circuit current flow chart [15]	65
Figure (4.11)	PV system with a constant voltage MPPT by Simulink	66
Figure (4.12)	Voltage compensator	67
Figure (4.13)	The power output from PV with constant voltage MPPT controller[Y- axis: power, X –axis: time (sec)]	67
Figure (4.14)	MPP voltage regulation of PV by constant voltage MPPT controller [Y- axis: voltage, X –axis: time (sec)]	68
Figure (4.15)	Current of PV by using constant voltage MPPT controller [Y- axis: current, X –axis: time (sec)]	68
Figure (4.16)	PV system with a constant voltage MPPT by Psim	69
Figure (4.17)	The output power, voltage and current of PV system with P&O MPPT at variation radiation $G = (1000W/m^2, 800W/m^2)$ by Psim	69
Figure (4.18)	Variation of MPP with changing irradiance but temperature constant	70
Figure (4.19)	Variation of MPP with changing temperature but irradiance constant	70
Figure (5.1)	Equivalent circuit of the full bridge single-phase inverter	75
Figure (5.2)	Topology of a single-phase inverter with filter and load	75
Figure (5.3)	Output current for S1, S2 ON; S3, S4 OFF for $t_1 < t < t_2$	76
Figure (5.4)	Output current for S3, S4 ON; S1, S2 OFF for $t_2 < t < t_3$ [6]	76
Figure (5.5)	Single-phase output voltage	77
Figure (5.6)	Fundamental component[19]	77
Figure (5.7)	Output voltage and current with blanking time[19]	78
Figure (5.8)	Harmonic of output voltage when α is a 10[20]	79

No.	Figure	Page
Figure (5.9)	Three-phase six-step inverter	80
Figure (5.10)	Waveforms of the switching functions	81
Figure (5.11)	Phase voltage normalized spectrum [19]	82
Figure (5.12)	Shows the waveform of the sine triangle and the voltage reference comparison	84
Figure (5.13)	Sine triangle, voltage reference and phase voltage [20]	84
Figure (5.14)	Three phase voltage source inverter (VSI) simulation in Psim	87
Figure (5.15)	The waves of three phase voltage source inverter (VSI) simulation in Psim in figure(5.14) : I_{RL1a} , I_{RL1b} , I_{RL1c} , V_{car} , V_a , V_{gate}	88
Figure (6.1)	The global irradiation (kW/m^2) versus time (hours)-2012[22]	92
Figure (6.2)	The daily ambient temperature curve-2012[22]	93
Figure (6.3)	Monthly solar energy for Tubas district-2011 on horizontal surface	94
Figure (6.4)	The configuration of PV generator for household	98
Figure (6.5)	The configuration of battery blocks of the PV system for household	100
Figure (6.6)	Charge controller specifications	101
Figure (6.7)	Inverter specifications	103
Figure (6.8)	Stand - alone PV operation [25]	104
Figure (6.9)	Grid tie inverter[28]	105
Figure (7.1)	The cash flow which represent initial, operational cost and salvage value	110
Figure (7.2)	Cash flow of standalone PV system for a house	113
Figure (7.3)	Grid tie net metering tariff.	115
Figure (7.4)	Grid tie feed in tariff	116
Figure (7.5)	Cash flow of grid tie PV system for a house	118
Figure (8.1)	Charge controller system	122
Figure (8.2)	PV system consists: PV panel, MPPT (P&O) controller and buck-boost converter	123
Figure (8.3)	Voltage output from PV system before charge controller [Y- axis: voltage(volt), X –axis: time (sec)]	123
Figure (8.4)	Battery charger	124
Figure (8.5)	Boost power converter, $L=10e-6$, $C=100e-6$	124
Figure (8.6)	Current and voltage curves in the four stages of battery charge [31]	125

No.	Figure	Page
Figure (8.7)	Battery charging algorithm with two main stages	128
Figure (8.8)	Battery charging controller blocks	128
Figure (8.9)	V-Charge block, values PID controller is (P=0.65, I=150, D= 2.7e-06)	129
Figure (8.10)	Battery charging at voltage constant mode (V=48volts) [Y- axis voltage(volt), X –axis: time (sec)]	129
Figure (8.11)	I-Charge block, values PID controller is (P = 0.75, I = 50, D = 3*2.7e-06)	130
Figure (8.12)	Battery charging at current constant mode (I=100A) [Y- axis: current(A), X –axis: time (sec)]	130
Figure (8.13)	Inverter designing for solar PV system	131
Figure (8.14)	Dc link voltage after boost-converter VSTEADY \approx 192volts [Y- axis: voltage(volt), X –axis: time (sec)]	132
Figure (8.15)	Output voltage v-AC [Y- axis: voltage(volt), X –axis: time (sec)] And current i-AC[Y- axis: current(A), X –axis: time (sec)] from off-grid inverter	133
Figure (8.16)	One phase on grid inverter	133
Figure (8.17)	VSC main controller block	135
Figure (8.18)	IC conductance mppt controller block	135
Figure (8.19)	IC conductance mppt algorithm	136
Figure (8.20)	Output power (kW), output voltage(volt) from PV array and Mppt duty cycle with changing a radiation(Kw/m ²), [X –axis: time (sec)]	137
Figure (8.21)	Output power (kW) from the grid tie PV system with variable radiations, [X –axis: time (sec)]	138
Figure (8.22)	Grid tie voltage (volt) and current (A) output with difference radiation, [X –axis: time (sec)]	139
Figure (8.23)	50Hz Voltage and current output of grid tie PV system, [X –axis: time (sec)]	140
Figure (8.24)	Vdc mean and Vdc ref with modulation index, [X –axis: time (sec)]	141

List of Appendixes

No.	Appendix	Page
Appendix A	Specifications of the MSX-50 Photovoltaic Module	150
Appendix B	M-file code that calculate R_s and R_p	152
Appendix C	Perturb and Observe Algorithm	157
Appendix D	Specifications of the Standalone PV system elements	159
Appendix E	Charge controller algorithm BY M-file	173
Appendix F	Table of interest at $i = 10\%$	176

Design and Simulation of a Photovoltaic System with Maximum Power Control to Supply a Load with Alternating Current

By

Ja'far Saif Edden Abdel Hafeath Jallad

Supervisor

Prof. Marwan Mahmoud

Abstract

Photovoltaic system is an important topic that can be researched and studied in Palestine because a solar energy potential is available. This thesis deals with the design and simulation of an efficient standalone PV system for an electrical home loads. It provides theoretical study of photovoltaic and modeling techniques using equivalent electric circuits. The research includes discussion of various MPPT algorithms and control methods to maximize the obtained solar power. Simulations by Matlab Simulink to verify the DC-DC converter design with MPPT control to be efficient as battery charge controller is investigated. The best inverter model that would be chosen for generating a sinusoidal output current supply for a household load is discussed.

This thesis selects a 4.5kWh-day energy load for a household as a case study to find the optimum design and configuration. The system is comprised of polycrystalline PV modules each rated at 130W to obtain a total peak power of 1.56 kW. In addition, one inverter of 3 kW and battery storage of 11.7 kWh is included in the system.

Design of a grid tie PV system by using matlab Simulink and testing the dynamic behavior on this system at varying solar radiation is included in this thesis.

Based on the economic evaluation, the cost of energy generated by a standalone PV system were studied is 2.1 (NIS/kWh) while the cost of energy generated by grid tie PV system is 0.72(NIS/kWh).

Chapter One

Introduction

Chapter One

Introduction

The world energy consumption and the resulting CO₂ emissions are increasing substantially and this increase puts in danger the ecological stability of our earth, making this an important topic in the society, both in a political and social aspect. The energy production has mainly been based on energy sources like oil, gas and coal, which until recently was looked upon as close to inexhaustible. As the world energy consumption is growing with a high rate and the fossil fuels reserves are decreasing, needing renewable energy resources has gained more important research. The sun is a non-polluting resource responsible for the sustained life on earth and can give us efficient renewable energy in Palestine because a potential is available.

In this master thesis a standalone PV system will be studied. A standalone PV system is used in the places where no electrical grid is available. The PV system will utilize the solar energy as the power source and transfer the power into the battery through conditioning by power electronics, after that the energy is stored in battery then converted by another stage of power electronics to be used in a home load. The power electronics is an essential part of a PV system, and it is necessary to understand how to utilize and control this part for optimization of the power generation. This issue will support teaching in control of power electronics, through learning many control strategies and know the suitable parameters to obtain more efficient performance for a standalone PV

system by using a Matlab Simulink and Psim (Power simulation) software's.

The main objective of the present work is to design a standalone PV system by using Matlab Simulink program and simulate this system on real conditions (radiation, load home...) as a case study. To achieve this objective the mathematical models were studied which characterize each part of system such as PV module, DC-DC converters, Maximum Power Point Tracking (MPPT) algorithms, Charge controller, battery and inverter. After that the suitable rated value for all components in a standalone PV system was calculated according to the energy consumption in kWh for a home load. In addition, economical study was made to know the cost in NIS/ kWh for a standalone PV system and compare it with other PV system which is a grid tie PV system considering the feed in tariff.

The work carried out in this thesis has been summarized in seven chapters:

In chapter one, the study begins with an introduction to this thesis, it gives information about objective, procedure and the main outline of the research. In chapter two, the study describes the types of PV cells and the mathematical modeling and simulation of PV module by Matlab Simulink to illustrate the I-V, P-V curve of a practical photovoltaic device and how it responses in function of radiation and temperature.

Chapter three handles the importance of power electronics (DC-DC converter) applications in photovoltaic systems. This chapter explains the

principles of operation and contraction of types of DC-DC converter to be capable to design mathematically a suitable value of its parameters to work in the best conditions. The type of battery with the main terms illustrating its performance is illustrated. Finally the types of charge regulator and their function are presented.

Chapter four illustrates the importance of using Maximum Power Point Tracking (MPPT) technologies in PV systems and explains their main types showing how can MPPT used in Psim and Matlab Simulink.

Chapter five handles DC/AC inverter analysis single phase and three phase with Sine Pulse Width Modulation (SPWM) strategy. After that a simulation of the Sine PWM in three phase inverter was made by using Psim.

Chapter six shows the potential of solar energy in Palestine. It illustrates calculations of the daily energy consumption for a home, as a case study, to determine ratings of the PV system elements. Finally a description of the main PV system types: Stand-alone PV system and grid tie is described.

Chapter seven is shows the economical study to determine cost of NIS/ kWh for standalone and grid tie PV system is carried out. Finally, an evaluation of the environmental impacts when using PV systems is illustrated.

Chapter eight is focused on modeling the standalone PV system by Simulink with shows the response of all components to produce AC voltage to home load. And design a grid tie PV system by using matlab Simulink and observe how the system works with a dynamics behavior of changing radiations.

Chapter Two

Solar Photovoltaic Technology

Chapter Two

Solar Photovoltaic Technology

2.1 Introduction

Photovoltaic offer consumers the ability to generate electricity in a clean, quiet and reliable way. Photovoltaic systems are comprised of photovoltaic cells, devices that convert light energy directly into electricity. Because the source of light is usually the sun, they are often called solar cells. The word photovoltaic comes from “photo” meaning light and “voltaic” which refers to producing electricity. Therefore, the photovoltaic process is “producing electricity directly from sunlight. Photovoltaic are often referred to as PV [1].

This chapter discusses the fundamentals of PV cells and modeling of a PV cell using an equivalent electrical circuit. The models are implemented using MATLAB and Psim (Power simulation) software to study PV characteristics and simulate a real PV module.

2.2 Photovoltaic Cell

Solar cells are made from semiconductor materials (pn junction, usually silicon), which are specially treated to form an electric field, positive on one side (backside) and negative on the other (towards the sun). When solar energy (photons) hits the solar cell, electrons are knocked loose from the atoms in the semiconductor material, creating electron-hole pairs. If electrical conductors are then attached to the positive and negative sides,

forming an electrical circuit, the electrons are captured in the form of electric current I_{ph} (photocurrent).

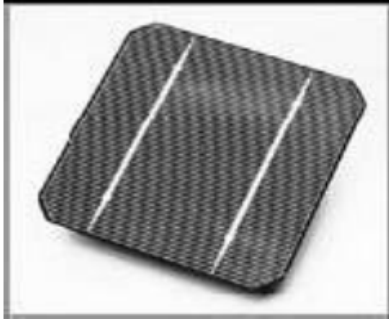


Figure (2.1): Photovoltaic cell [2].

A typical PV cell made of crystalline silicon is 12 centimeters in diameter and 0.25 millimeters thick. In full sunlight, it generates 4 amperes of direct current at 0.5 volts or 2 watts of electrical power[2].

2.2.1 Types of photovoltaic cells

There are essentially two types of PV technology, crystalline and thin-film. Crystalline can again be classified into two types:

- Mono crystalline Cells: These are made using cells cut from a single cylindrical crystal of silicon. While mono crystalline cells offer the highest efficiency (approximately 18% conversion of incident sunlight), their complex manufacturing process makes them slightly more expensive.
- Polycrystalline Cells: These are made by cutting micro-fine wafers from ingots of molten and recrystallized silicon. Polycrystalline cells are cheaper to produce, but there is a slight compromise on efficiency (approximately 14% conversion of incident sunlight).

Thin film PV is made by depositing an ultrathin layer of photovoltaic material onto a substrate. The most common type of thin-film PV is made from the material a-Si (amorphous silicon), but numerous other materials such as CIGS (copper indium/gallium selenide) CIS (copper indium selenide), CdTe (Cadmium Telluride) [3].

The efficiency of this type varies approximately in the range from 2%- 10%.

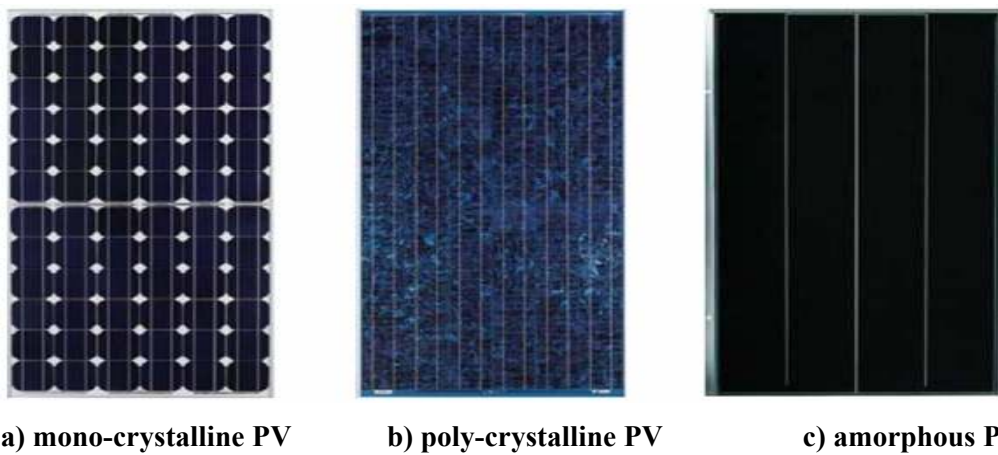


Figure (2.2): The main industrialized PV technologies [3].

2.3 Modeling of Photovoltaic Module by Matlab Simulink and Psim

The use of equivalent electric circuits makes it possible to model characteristics of a PV cell. The method used here is implemented in MATLAB and PSIM programs for simulations. The same modeling technique is also applicable for modeling a PV module.

2.3.1 Ideal cell

Solar cells consist of a p-n junction fabricated in thin wafer or layer of semiconductors, whose electrical characteristics differ very little from a

diode represented by the equation of Shockley. Thus the simplest equivalent circuit of a solar cell is a current source in parallel with a diode as shown in Figure (2.2). The output of the current source is directly proportional to the light falling on the cell (photocurrent $I_{PV, cell}$). So the process of modeling this solar cell can be developed based on equation (2.1), (2.2) and (2.3):

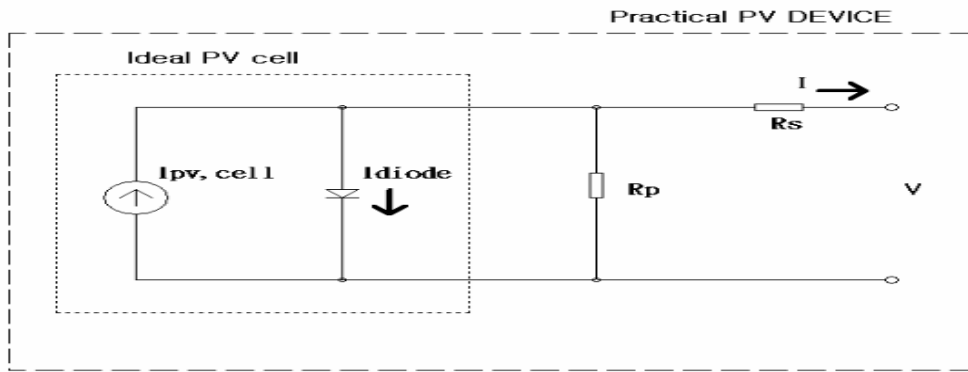


Figure (2.3): Equivalent model of a photovoltaic cell [4].

$$I = I_{PV,CELL} - I_{diode} = I_{PV,CELL} - I_{0,CELL} \left[\exp\left(\frac{q \times V}{\alpha k T}\right) - 1 \right] \quad (2.1)$$

Where:

- ❖ $I_{PV, cell}$: the current generated by the incident light.
- ❖ I_{diode} : the Shockley diode equation.
- ❖ $I_{0, cell}$ [A]: the reverse saturation or leakage current of the diode [A].
- ❖ q : the electron charge [$1.60217646 \cdot 10^{-19}$ C].
- ❖ k : the Boltzmann constant [$1.3806503 \cdot 10^{-23}$ J/K].
- ❖ T [K]: the temperature of the p-n junction.
- ❖ α : the diode ideality factor which lies between 1 and 2 for mono crystalline silicon.

The basic equation (2.1) of the elementary PV does not represent the I-V characteristic of practical PV module. Practical module are composed of several connected PV cells requires the inclusion of additional parameters R_s and R_p is the equivalent series resistance of the module and the equivalent parallel resistance respectively, with these parameters equation (2.1) becomes equation (2.2).

$$I = I_{PV} - I_0 \left[\text{EXP} \left(\frac{V + R_s \times I}{V_T \times \alpha} \right) - 1 \right] - \frac{V + R_s \times I}{R_p} \quad (2.2)$$

The light-generated current of the array depends linearly on solar irradiation and is also influenced by temperature according to equation (2.3).

$$I_{PV} = (I_{PV,n} + K_I \Delta T) \frac{G}{G_n} \quad (2.3)$$

Where:

$I_{PV,n}$ (in amperes): the light-generated current at the nominal condition (usually 25 °C and 1000 W/m²).

$\Delta T = T - T_n$ (T and T_n being the actual and nominal temperatures [in Kelvin], respectively)

K_I : the Temperature coefficient of I_{SC} .

G: the irradiance (W/m²).

G_n : the irradiance at standard operating conditions.

The diode saturation current I_0 dependence on temperature can be expressed as shown in equation (2.4).

$$I_0 = I_{0,n} \left(\frac{T_n}{T} \right)^3 \text{EXP} \left[\frac{qE_g}{\alpha k} \left(\frac{1}{T_n} - \frac{1}{T} \right) \right] \quad (2.4)$$

Where:

E_g : the band gap energy of the semiconductor .

$I_{0,n}$: the nominal saturation current expressed by (2.5).

$I_{0,n}$: the nominal saturation current expressed by equation

$$I_{0,n} = \frac{I_{SC,n}}{\left[\text{EXP} \left(\frac{V_{OC,n}}{V_{T,n} \times \alpha} \right) - 1 \right]} \quad (2.5)$$

From equation (2.4) and (2.5) I_0 can be expressed as shown in equation (2.6).

$$I_0 = \frac{I_{SC,n} + K_I \Delta T}{\text{EXP} \left(\frac{V_{OC,n} + K_V \Delta T}{V_T \times \alpha} \right) - 1} \quad (2.6)$$

Where:

$V_{OC,n}$: open circuit voltage.

$I_{SC,n}$: the short circuit current.

V_T : the thermal voltage.

T_n : the temperature at standard operating conditions.

K_I : the Temperature coefficient of I_{SC} .

K_V : the Temperature coefficient of V_{OC} .

$V_T = N_s \times kT/q$ is the thermal voltage of the module with N_s cells connected in series. [Cells connected in parallel increase the current and cells connected in series provide greater output voltages]. If the module is composed of N_p parallel connections of cells the photovoltaic and saturation currents may be expressed as:

$$I_{pv} = I_{pv,cell} \times N_p \quad (2.7)$$

$$I_0 = I_{0,cell} \times N_p \quad (2.8)$$

In equation (2.2) R_S is the equivalent series resistance of the module (unknown) and R_p is the equivalent parallel resistance (unknown), so they have to be calculated. Equation (2.2) originates the I-V curve seen in figure (2.4), where three remarkable points are highlighted:

- a) Open- circuit ($V_{oc}, 0$).
- b) Short circuit ($0, I_{sc}$).
- c) Maximum power point (V_{mp}, I_{mp}).

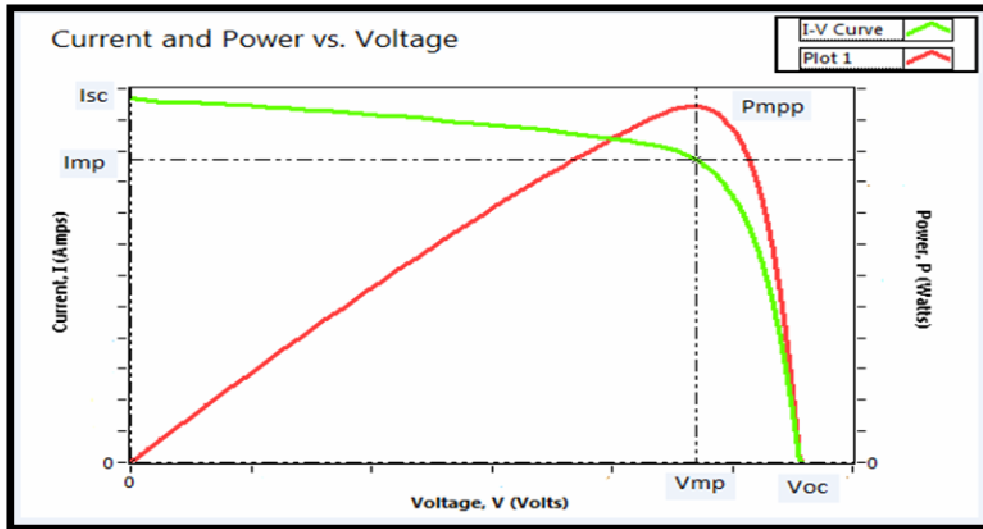


Figure (2.4): Characteristic I-V, P-V curve of a practical photovoltaic device [4].

a) **Open-circuit:** This point is obtained when the terminals of the module are disconnected. The module presents a voltage called (V_{OC}). Expressed analytically using equation (2.9).

$$V_{OC} = \frac{\alpha \times k \times T_{CELL}}{q} \ln \frac{I_{PV}}{I_0} \quad ; \quad I_{PV} > I_0 \quad (2.9)$$

b) **Short-circuit:** The terminals of the module are connected with an ideal conductor, through which flows a current called (I_{SC}). In this situation, the voltage between module terminals is zero.

$$I_{SC} = I_{PV} = K \times G \quad (2.10)$$

Where, K is a constant.

c) **Maximum power point “MPP”:**

Here the voltage versus current product is the maximum. V_{MP} is related to V_{OC} through the relation (2.11):

$$V_{MP} \approx 0.8 \times V_{oc} \quad (2.11)$$

And I_{MP} is related to I_{SC} through the relation (2.12):

$$I_{MP} \approx 0.9 \times I_{SC} \quad (2.12)$$

The best conditions, are the "standard operating conditions" happen at irradiance equal to 1000W/m^2 , cells temperature equals to 25°C , and spectral distribution (Air Mass) AM is equal to 1.5 [4].

2.3.2 A real photovoltaic device

PV cells are the basic building blocks of PV modules. For almost all applications, the one-half volt produced by a single cell is inadequate. Therefore, cells are connected together in series to increase the voltage. Several of these series strings of cells may be connected together in parallel to increase the current as well.

So in a real photovoltaic model; must include the effects of series and parallel resistance of the PV, so when the first Kirchhoff law is applied to one of the nodes of the equivalent circuit, the current supplied by a PV, at a specified temperature as shown in equation (2.2) [6]:

In (2.13) R_s is the equivalent series resistance of the module and R_p is the equivalent parallel resistance [4].

2.3.3 Model of the photovoltaic module by Matlab and Psim (Power Simulation)

MSX-50 solar PV module, pictured in Figure (2.5), is chosen for a MATLAB and Psim simulation model. The module is made of 36 multi-

crystalline silicon solar cells in series and provides 50W of nominal maximum power. Table (2.1) shows its electrical specification and figure shows its I-V characteristics from data sheet. The data sheet MSX-50 solar PV module in appendix (A).

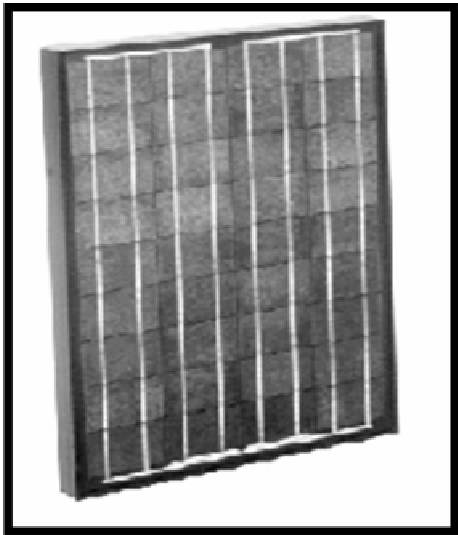


Figure (2.5): Picture of MSX-50 Photovoltaic Modules [4].

Table(2.1): Electrical characteristics data of the MSX-50 solar module at 25 °C, 1.5AM, 1000W/m². Taken from the datasheet [4].

Electrical Characteristics	
Maximum Power (Pmax)	50W
Voltage at Pmax (Vmp)	17.1V
Current at Pmax (Imp)	2.92A
Open-circuit voltage (Voc)	21.1V
Short-circuit current (Isc)	3.17A
Temperature coefficient of Isc	(0.065±0.015)%/°C
Temperature coefficient of Voc	-(80±10)mV/°C
NOCT	47±2°C

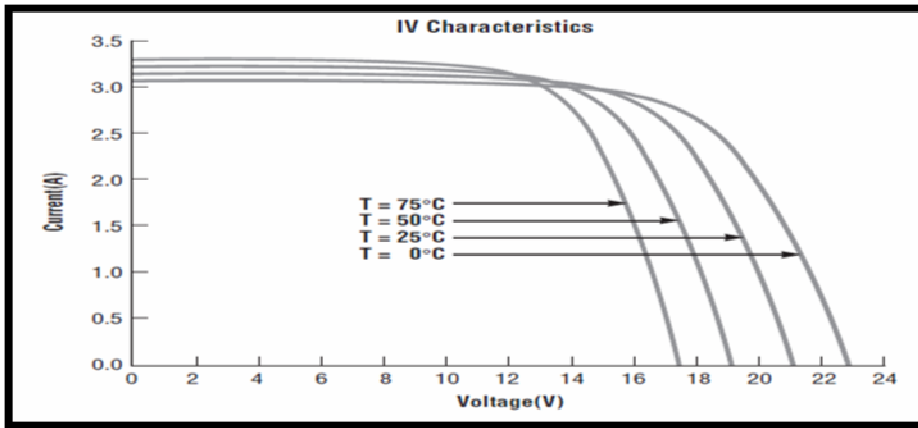


Figure (2.6): I-V characteristics at $1000\text{W}/\text{m}^2$, from data sheet with different temperature.

The model of the photovoltaic panel has been implemented in Simulink as shown in figure (2.7). The temperature and the irradiance are specified. The simulation allows having the curve I-V and P-V characteristics. The Simulink model and Psim uses a current source, voltage source and the value of the resistance in series and parallel of the PV [4].

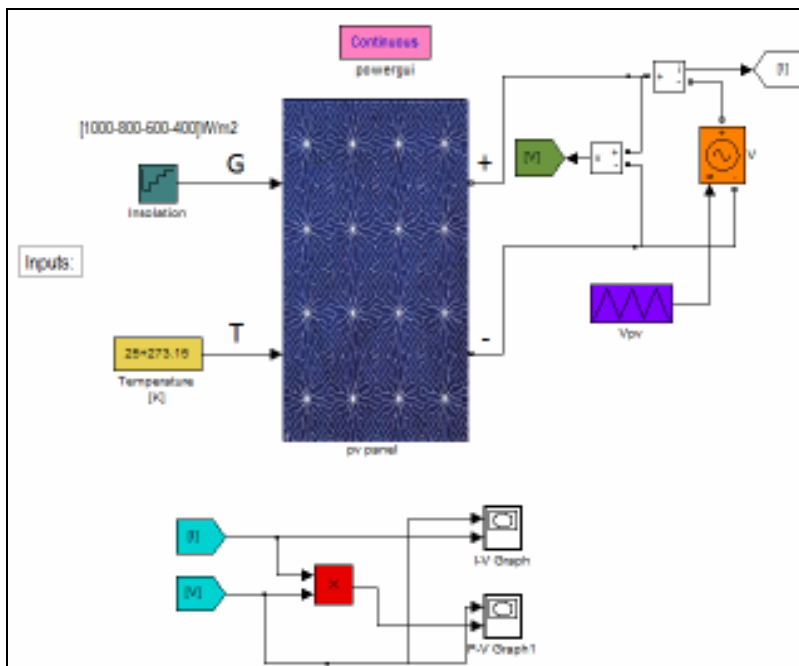


Figure (2.7): PV module model in Simulink.

Inside the block PV panel we can see a schematic circuit and some blocks which represented the equation of PV module as figure shown in (2.8), (2.9), (2.10) and (2.11).

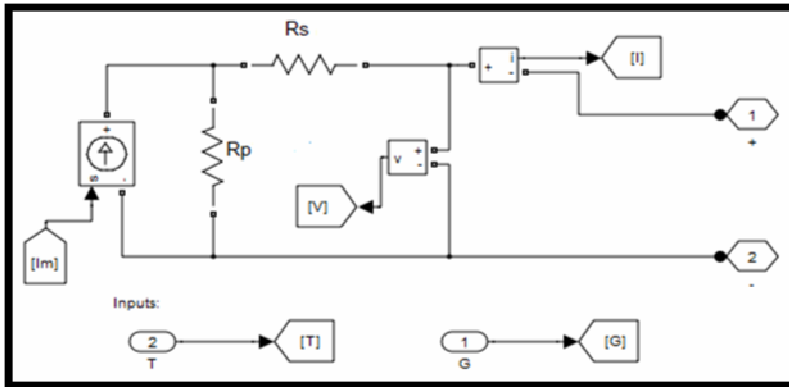


Figure (2.8): Equivalent circuit of a practical PV

Figure (2.9) shows the Simulink model for the reverse current saturation (I_0) at the reference temperature which is given by the equation (2.13) [5]:

$$I_0 = \frac{I_{sc,n} + K_I \Delta T}{\text{EXP} \left(\frac{V_{oc,n} + K_V \Delta T}{V_T \times \alpha} \right) - 1} \quad (2.13)$$

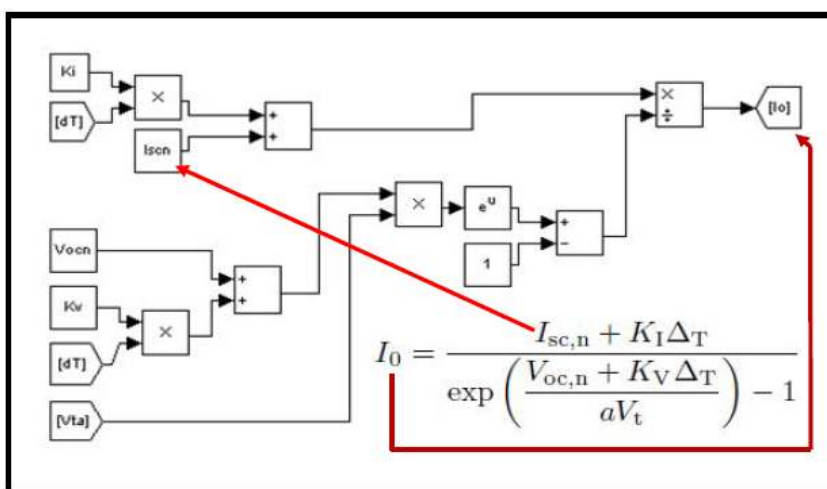


Figure (2.9): Simulink modeling implementation for I_0 .

Figure (2.10) shows the Simulink model for the light generated current of the photovoltaic cell which depends linearly on the influence of temperature and solar radiation as given by the equation (2.14) [5]

$$I_{PV} = (I_{PV,n} + K_I \Delta T) \frac{G}{G_n} \quad (2.14)$$

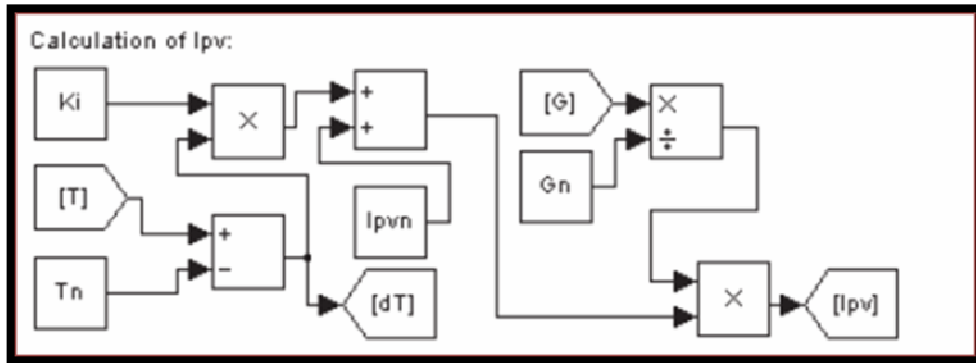


Figure (2.10): Simulink modeling implementation for I_{PV} .

Figure (2.11) shows the Simulink model for the model current I_m which given by the equation (2.15) [5]:

$$I_m = I_{PV} - I_0 \left[\text{EXP} \left(\frac{V + R_s \times I}{V_T \times \alpha} \right) - 1 \right] \quad (2.15)$$

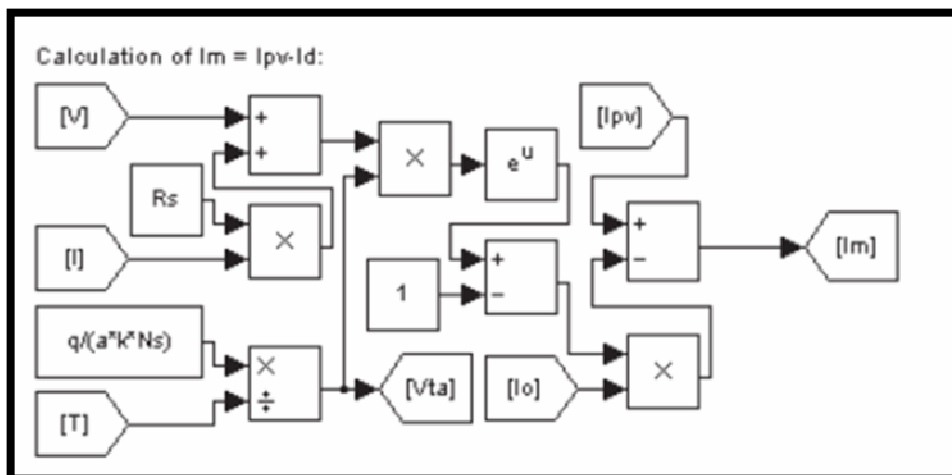


Figure (2.11): Simulink modeling implementation for I_m

In figure (2.12) shown the PV model built by Psim software.

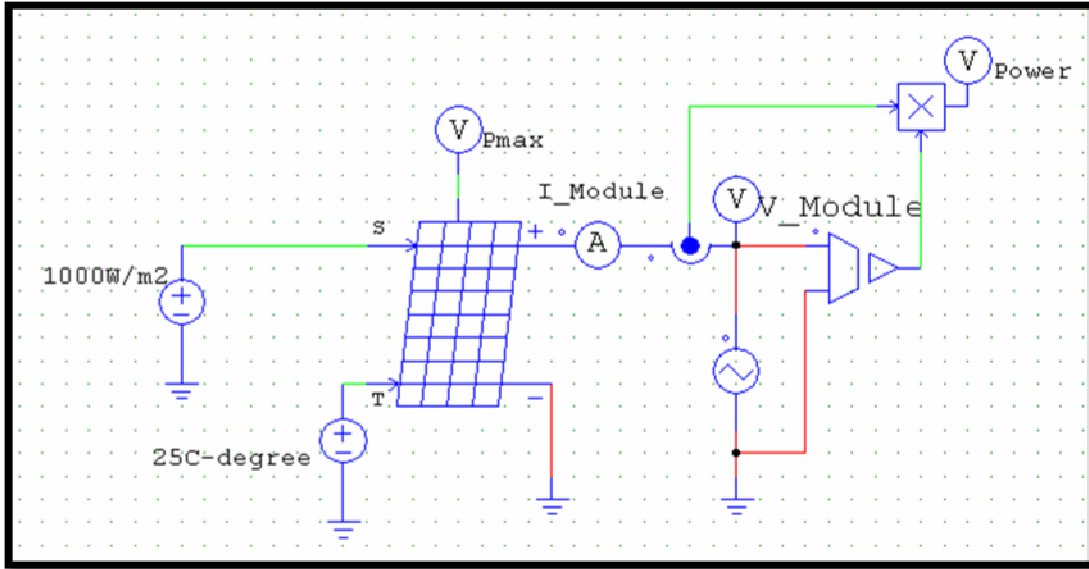


Figure (2.12): PV model in Psim.

2.3.4 R_s and R_p calculation

Two parameters remain unknown in equation (2.2), which are R_s and R_p . A few authors have proposed ways to mathematically determine these resistances. Although it may be useful to have a mathematical formula to determine these unknown parameters, any expression for R_s and R_p will always rely on experimental data. This procedure proposes a method for adjusting R_s and R_p based on the fact that there is an only pair $\{R_s, R_p\}$ that warranties that $P_{\max,m} = P_{\max,e} = V_{mp}I_{mp}$ at the (V_{mp}, I_{mp}) point of the I-V curve, i.e., the maximum power calculated by the I-V model of $(P_{\max,e})$ is equal to the maximum experimental power from the datasheet $(P_{\max,e})$ at the MPP. Conventional modeling methods found in the literature take care of the I-V curve but forget that the P-V (power versus voltage) curve must match the experimental data too.

The relation between R_s and R_p , the only unknowns of (2.2), may be found by making $P_{\max,m} = P_{\max,e}$ and solving the resulting equation for R_s , as shown.

$$P_{\max,m} = V_{mp} \left\{ I_{PV} - I_0 \left[\exp \left(\frac{q}{kT} \frac{V_{mp} + R_s I_{mp}}{\alpha N_s} \right) - 1 \right] - \frac{V_{mp} + R_s I_{mp}}{R_p} \right\} = P_{\max,e} \quad (2.16)$$

$$R_p = \frac{V_{mp} (V_{mp} + R_s I_{mp})}{\left\{ V_{mp} I_{PV} - V_{mp} I_0 \exp \left[\frac{V_{mp} + R_s I_{mp}}{\alpha N_s} - \frac{q}{kT} \right] + V_{mp} I_0 - P_{\max,e} \right\}} \quad (2.17)$$

The equation (2.17) means that for any value of R_s there will be a value of R_p that makes the mathematical I-V curve cross the experimental (V_{mp}, I_{mp}) point.

The goal is to find the value of R_s (and hence R_p) that makes the peak of the mathematical P-V curve coincide with the experimental peak power at the (V_{mp}, I_{mp}) point. This requires several iterations until $P_{\max,m} = P_{\max,e}$. Initial guesses for R_s and R_p are necessary before the iterative process starts. The initial value of R_s may be zero. The initial value of R_p may be given by:

$$R_{p,\min} = \frac{V_{mp}}{I_{sc,n} - I_{mp}} - \frac{V_{oc,n} - V_{mp}}{I_{mp}} \quad (2.18)$$

Equation (2.18) determines the minimum value of R_p , which is the slope of the line segment between short-circuit and the maximum-power remarkable points. Although R_p is still unknown, it surely is greater than $R_{p,\min}$ and this is a good initial guess.

We use a code by m-file in matlab to calculate the values of R_s and R_p that makes the mathematical P-V curve coincide with the experimental

peak power at the (V_{mp}, I_{mp}) point. The value of R_s and R_p are reached when the iteration stopped for P_{max} calculated is equal to P_{max} estimated. The iterative method gives the solution $R_s=0.235\Omega$ and $R_p=350.90396\Omega$ for the MSX-50 solar module. Figure(2.13) Shows the I-V characteristic at standard conditions where V_{MP} , I_{MP} , V_{OC} and I_{SC} values are shown using the calculated values of R_s and R_p by Simulink and figure (2.13) Shows the I-V, P-V characteristic by Psim at the same values[4]. The m-file code that calculate R_s and R_p are in the appendix (B).

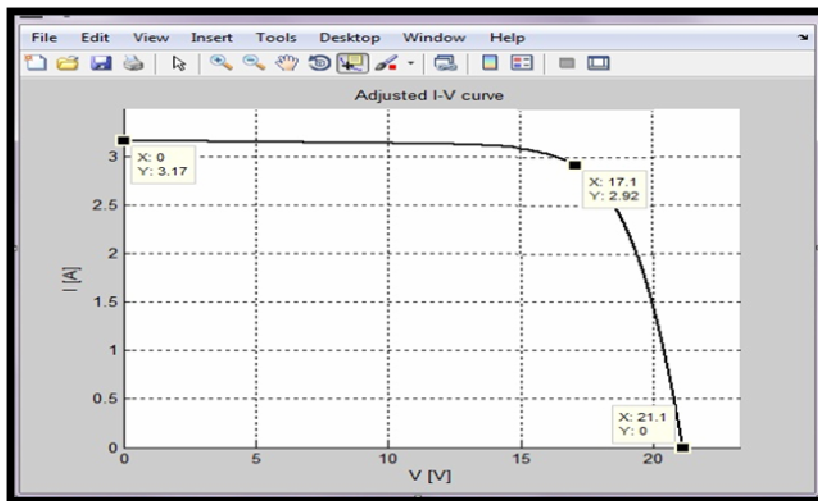


Figure (2.13): I-V characteristics at $T=25^{\circ}$ C, irradiance= $1000\text{W}/\text{m}^2$, after calculation of R_s and R_p , by Simulink.

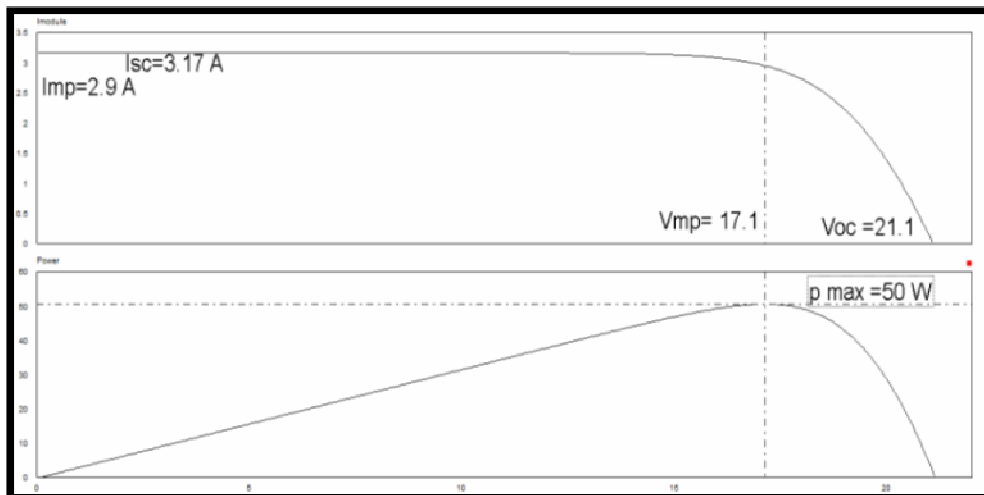


Figure (2.14): I-V, P-V characteristics at $T=25^{\circ}$ C, irradiance = $1000\text{W}/\text{m}^2$, after calculation of R_s and R_p , by Psim.

2.3.5 Impact of solar radiation on I-V characteristic curve of photovoltaic module

Standard sunlight conditions on a clear day are assumed to be 1000 watts of solar energy per square meter (1000 W/m^2). This is sometimes called "one sun," or a "peak sun." Less than one sun will reduce the current output of the module by a proportional amount. For example, if only one-half sun (500 W/m^2) is available, the amount of output current is roughly cut in half [6].

For maximum output, the front surface of the photovoltaic modules should be pointed as straight toward the sun as possible.

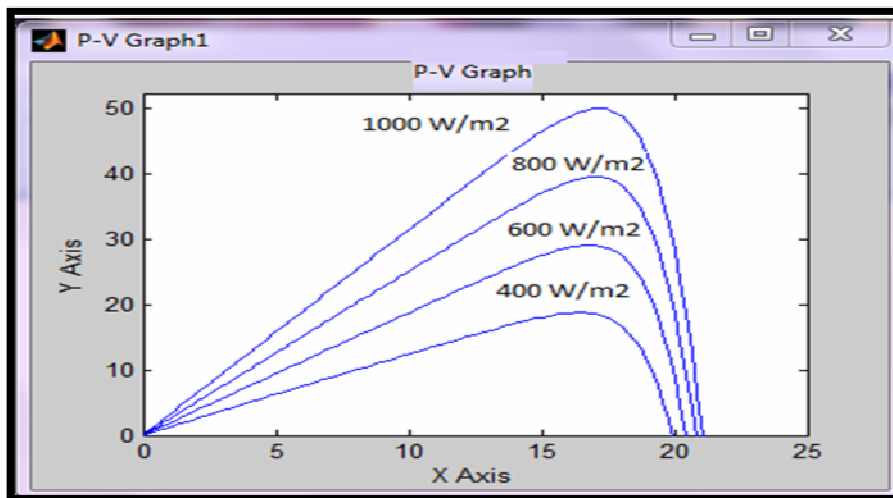


Figure (2.15): P-V characteristics at $T=25 \text{ C}$, by Simulink With different irradiances[Y- axis: power(watt), X –axis: voltage(volt)].

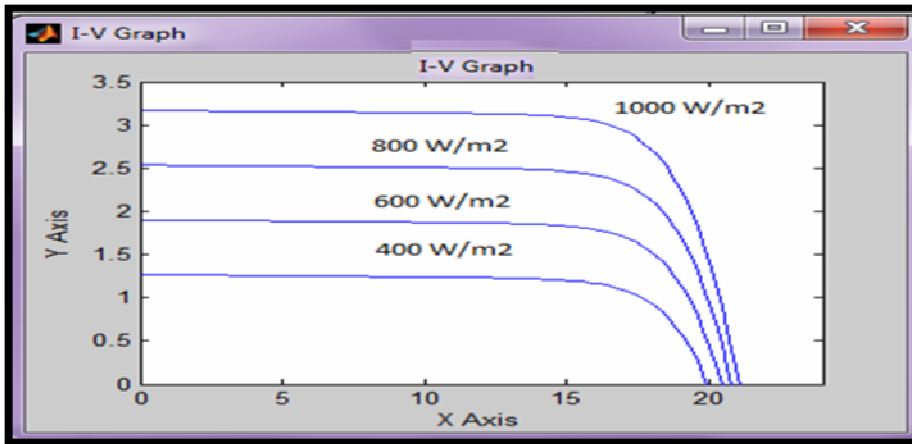


Figure (2.16): I-V characteristics at $T=25^{\circ}\text{C}$, by Simulink with different irradiances[Y- axis: current(A), X –axis: voltage(volt)].

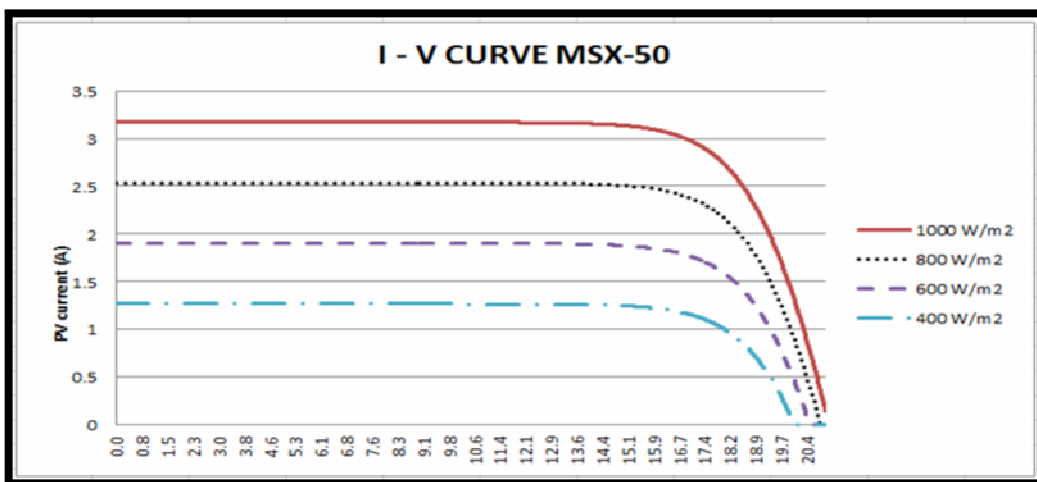


Figure (2.17): I-V characteristics at $T=25^{\circ}\text{C}$, by Psim with different irradiances[Y- axis: current(A), X –axis: voltage(volt)].

2.3.6 Impact of temperature on I-V characteristic curve of photovoltaic module

The temperature of the PV cell is an important parameter that has to be taken into consideration in PV system operation. The PV cell has given temperature coefficients for both the current and the voltage (α). The current coefficient is mostly negligible; hence it is mainly the voltage temperature coefficient that is considered during calculations. For silicon based cells the coefficient (α) = $2\text{mV}/\text{C}^{\circ}$ _ per cell]6[.

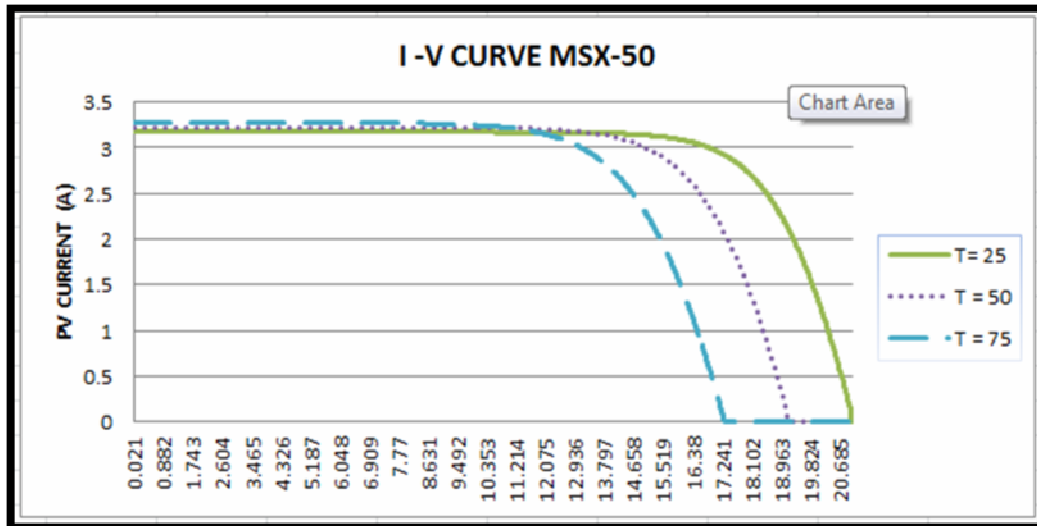


Figure (2.18): I-V characteristics at 1000w/m², by Psim with different temperature[Y- axis: current(A), X –axis: voltage(volt)].

2.3.7 Impact of shading on I-V characteristic curve of photovoltaic module

Solar PV panel is a power source having non-linear internal resistance. A major challenge in using a PV source containing a number of cells in series is to deal with its non-linear internal resistance. The problem gets all the more complex when the array receives non-uniform insolation. Cells under shade absorb a large amount of electric power generated by cells receiving high insolation and convert it into heat. This heat may damage the low illuminated cells under certain conditions. To relieve the stress on shaded cells, bypass diodes are added across the module[7]. In figure (2.19) shows two PV module with series connection at variable irradiance at 1000W/m² and 500W/m², and the figure (2.20), (2.21) shows the effect of shading in the I-V,P-V characteristic curve .

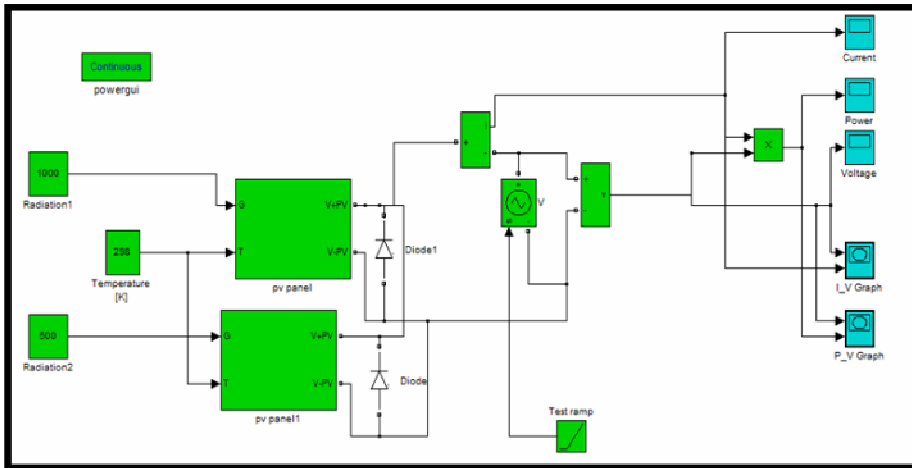


Figure (2.19): Two PV module with series connection at variable irradiance at 1000W/m^2 and 500W/m^2 , by Matlab - Simulink.

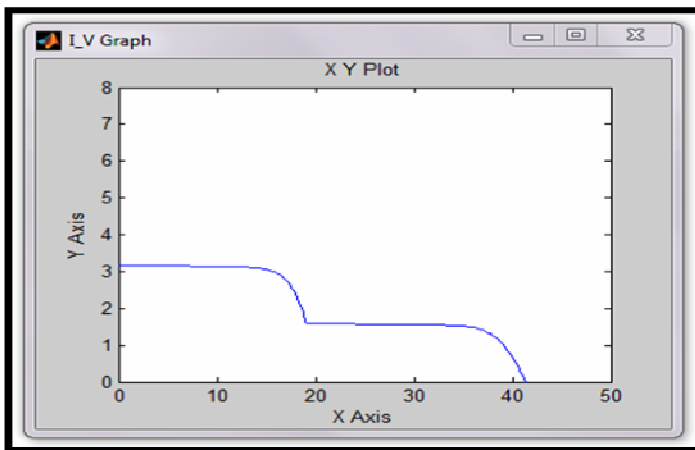


Figure (2.20): I-V characteristics at variable irradiance at 1000W/m^2 and 500W/m^2 , by Matlab – Simulink [Y- axis: current(A), X –axis: voltage(volt)].

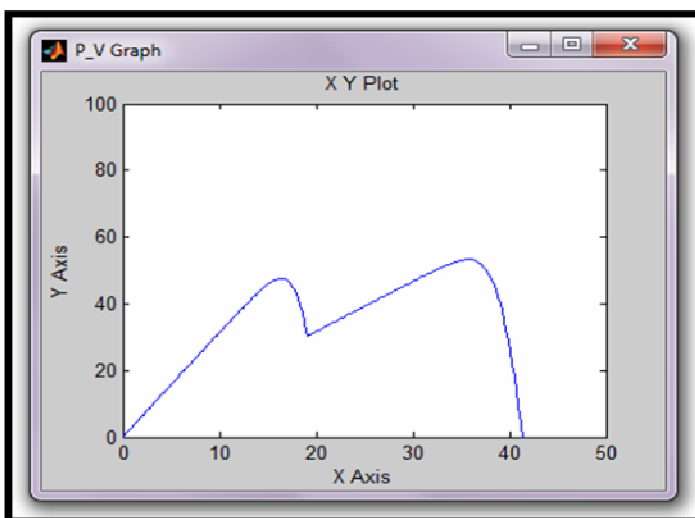


Figure (2.21): P-V Characteristics at variable irradiance at 1000W/m^2 and 500W/m^2 , by Matlab – Simulink [Y- axis: power(watt), X –axis: voltage(volt)].

The first function of the by-pass diodes is the protection of the module against Hot-Spot and destruction of cells. As a general rule, one diode is required for about 18 to 24 cells. The second function of the by-pass diode is to reduce the reverse voltage across the sub-module, therefore limiting the shading voltage drop within the string to the normal voltage of one sub-module (-0.7V) [8].

During the night, when none of the modules are illuminated, an energy storage (like a battery) connected directly in series with the modules makes the cells forward biased. This might lead to a discharge of the energy storage. To prevent this from happening a blocking diode can be connected in series with the module. But during normal illumination level this diode represents a significant power loss[6].

The placement of bypassing and blocking diodes in the system is shown in figure (2.22).

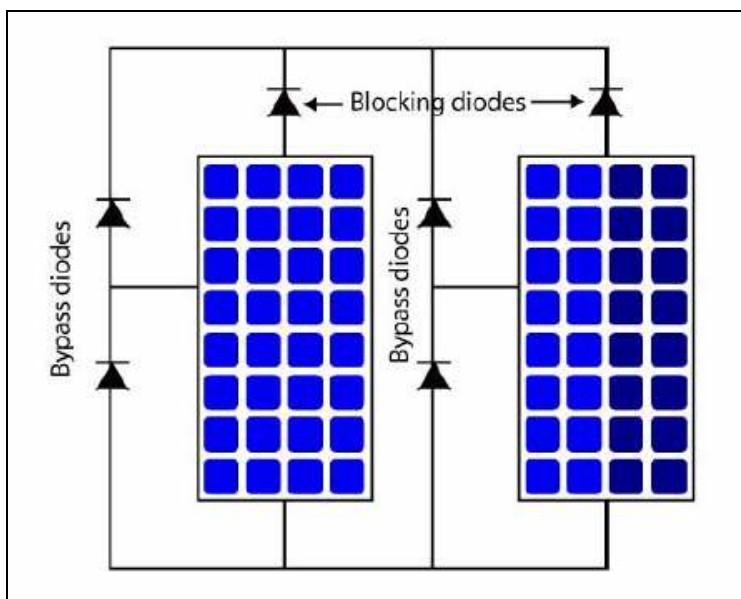


Figure (2.22): A PV module with bypass and blocking diodes.

2.4 The Photovoltaic Array

If the output voltage and current from a single module is smaller than desired, the modules can be connected into arrays. The connection method depends on which variable that needs to be increased. For a higher output voltage the modules must be connected in series, while connecting them in parallel in turn gives higher currents. It is important to know the rating of each module when creating an array. The highest efficiency of the system is achieved when the MPP of each of the modules occurs at the same voltage level [9].

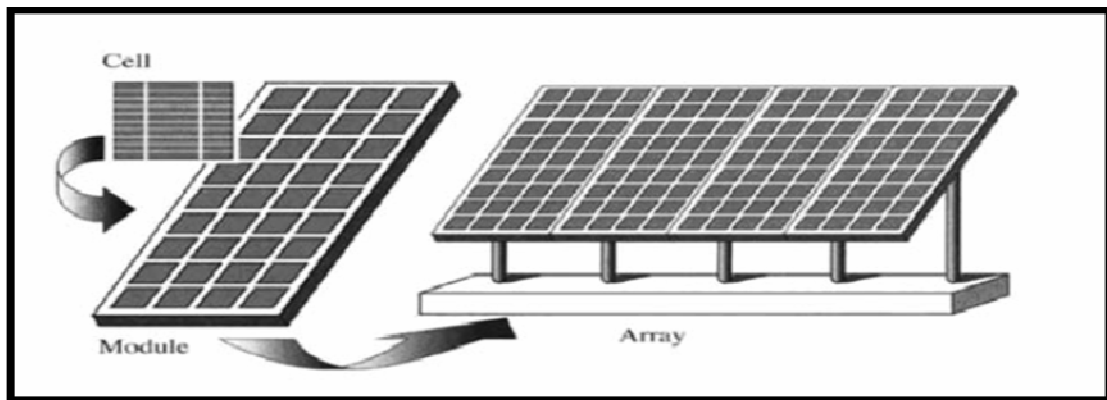


Figure (2.23): Relation between the PV cell, a module and an array.

The simulation of the photovoltaic array is realized with Simulink block. The input parameters required to modify the PV module to be an array are:

N_{ser} : number of modules in series.

N_{par} : number of modules in parallel.

In figure (2.24) shows the modification in the PV module to be an array.

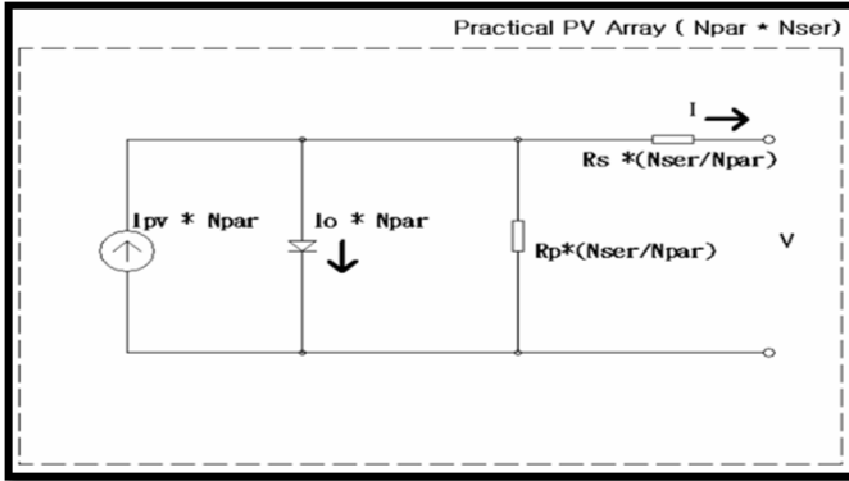


Figure (2.24): PV array model, N_{ser} is number of series of PV modules; N_{par} is number of parallel PV modules.

If the array is composed of N_{par} parallel connections of PV modules, the photovoltaic and saturation currents may be expressed as:

$$I_{pv, array} = I_{pv, module} \times N_{par} \quad (2.19)$$

$$I_{0, array} = I_{0, module} \times N_{par} \quad (2.20)$$

If the array is composed of N_{ser} series connections of PV modules, the output voltage may be expressed as:

$$V_{array} = V_{module} \times N_{ser} \quad (2.21)$$

The resistance of a PV array may be expressed as:

$$R_{s, array} = R_{s, module} \times (N_{ser} / N_{par}) \quad (2.22)$$

$$R_{p, array} = R_{p, module} \times (N_{ser} / N_{par}) \quad (2.23)$$

If we take as an example $N_{ser} = 2$ and $N_{par} = 15$, just to verify the validation of the array model we will have the results of simulation shown

in figure (2.25) for I-V characteristic curve at $T = 25^{\circ}\text{C}$ and $G = 1000\text{W}/\text{m}^2$, the $I_{sc} = 6.34\text{A}$ ($3.17\text{A} \times 2$) as expected for $N_{par} = 2$, $V_{oc} = 316.5\text{V}$ ($21.1\text{V} \times 15$) as expected for $N_{ser} = 15$. Figure (2.26) shows P-V characteristic for the same conditions where the value of the peak power is as expected to be $1500\text{W} = (15 \times 2 \times 50\text{W})$.

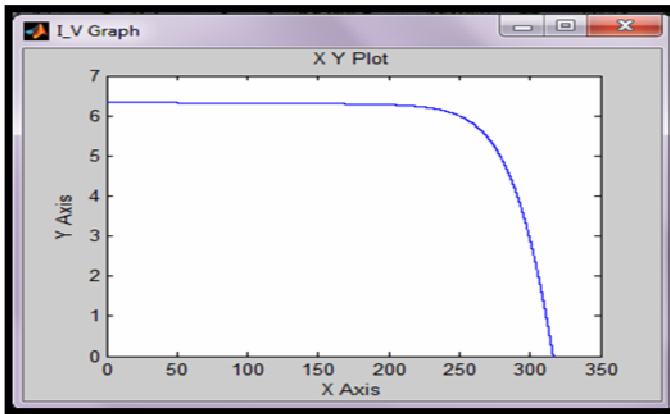


Figure (2.25): I-V Characteristics at $T=25^{\circ}\text{C}$, $G=1000\text{W}/\text{m}^2$, by Simulink for $N_{ser} = 15$, $N_{par} = 2$ [Y- axis: current(A), X -axis: voltage(volt)].

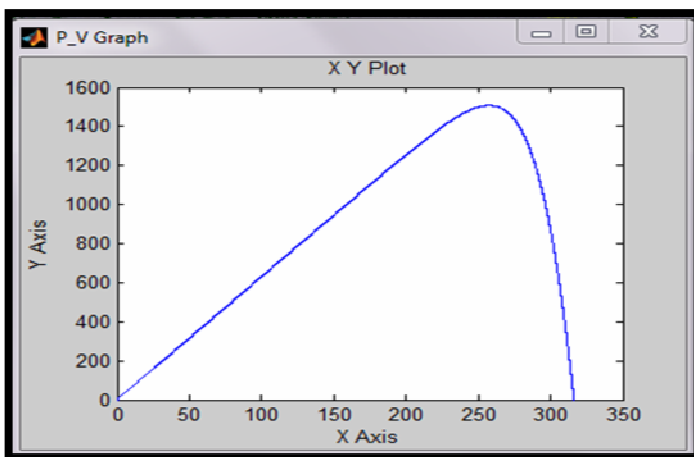


Figure (2.26): P-V Characteristics at $T = 25^{\circ}\text{C}$, $1000\text{W}/\text{m}^2$, by Simulink for $N_{ser} = 15$, $N_{par} = 2$ [Y- axis: power(watt), X -axis: voltage(volt)].

2.5 Summary

In this Chapter, a MATLAB Simulink / Psim PV system simulator based on an improved single-diode model is proposed. To reduce the

computational time, the input parameters are reduced to four and the values of R_p and R_s are estimated by an efficient iteration method. Furthermore the inputs to the simulator are information available on standard PV module datasheets. Simulation results show a matching between the Simulink model, Psim model and the manufacturers published curves.

Chapter Three
DC – DC Converter and Battery

Chapter Three

DC – DC Convertor and Battery

3.1 Introduction

The world energy consumption is increasing while fossil fuel is limited. The main resource of the world energy in the near future is going to be renewable energy sources such as wind, solar and geothermal energy. Although these new energy technologies are promising, their energy production is still more expensive than conventional energy productions. In this case power electronic technologies are needed to reduce the losses as much as possible, and to deliver and distribute the power very efficiently. Power electronics had changed rapidly during the last thirty years and the number of application is increasing due to developments of the main components of power electronics, which all semiconductor devices and the microprocessor technology.

The power electronics application in photovoltaic system is using the most efficient technique to extract the maximum power from the PV cell. This is achieved by using MPPT (Maximum Power Point Tracking) control unit in the converter or inverter side. The MPPT techniques will be explained in the following chapter.

3.2 Power Electronics in a PV System

The voltage produced by the photovoltaic cells will vary according to the sunlight intensity (irradiance), but the system output requires a constant voltage value to be able to process and control the electric energy

in the system (i.e. the voltages, currents, frequency) there is a need for a power electronic interface. A typical setup of a power electronic system is shown in figure (3.1). The power flows from the input to the output through a processor stage, which is controlled through a negative feedback signal from either the input or the output (or both)[10].

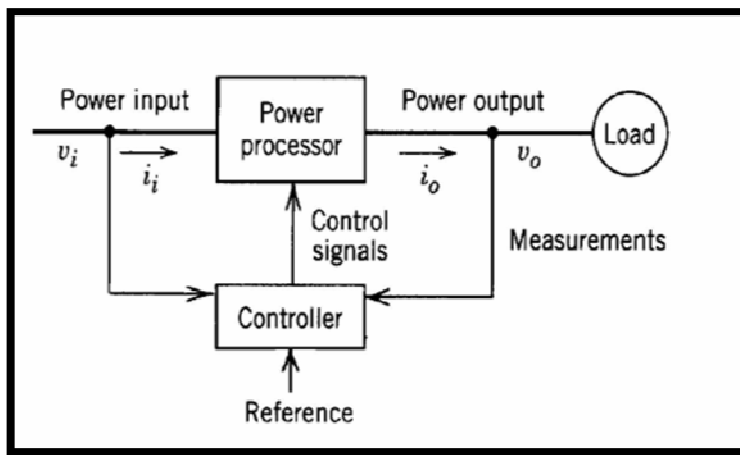


Figure (3.1): Block diagram of a power electronic system[10]

The power input can be a DC as well as an AC signal. The output depends on the requirement from the load. In a PV system the power input will always be a DC signal given by the functionality of the PV cell (which is varying with the amount of energy absorbed from the sun).

The power processor can be described as a power conversion stage. It typically consists of one or more converters, often with an energy storage element included. A PV system intended for grid connection usually has a power processor as shown in figure (3.2). In the system considered in this master thesis Converter 1 corresponds to a DC-DC converter, while Converter 2 is a DC-AC converter (inverter, we will discuss it in chapter 5). This way the output is connected directly to an AC load or to the grid.

The controller can be implemented to control both the converters separately to ensure a stable interface between each of the stages, i.e. between the input and converter 1 and converter 2 and the output.

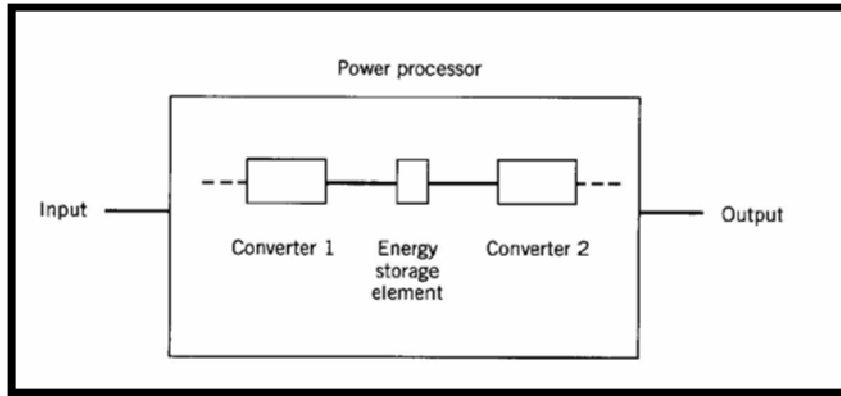


Figure (3.2): Block diagram of a power processor.

3.3.1 DC-DC switch mode converters

The purpose of DC-DC Switch Mode Converters in general DC power supplies is to convert unregulated DC input to regulated or controlled DC output at a desired voltage level. In such systems the input is often fluctuating due to rectification and the output is requiring a constant output. In a PV system, on the other hand, the DC-DC converter is actually controlling the input by considering the unregulated output. By help of MPP Tracking (which will be explained later) the converter adjusts its operation according to the output value to find the optimal operating voltage of the PV module [10].

There are several different kinds of DC-DC converters in use in the industry today, but most of them are based on two basic converter topologies:

- Buck converter (step-down)
- Boost converter (step-up)

Each of the topologies will be explained later in this chapter.

3.3.2 Control of DC-DC converters

The voltage transformation in a DC-DC switch mode converter is done by utilizing switches, hence the name "switch mode converters". The switches are controlled to be on and off for a certain amount of time through a method called pulse width modulation (PWM). The switching period $T_s = t_{on} + t_{off}$ (and hence the frequency) is held constant while the ratio of the on time to the switching time is varied. This ratio is called the switch duty ratio (D), or duty cycle. By using switch mode control in the circuit in figure (3.3 a), the output voltage V_o will be a constant pulse as shown in figure (3.3 b). Because of inductive and capacitive circuit elements in the converter topologies the output voltage may have a certain amount of ripple, but the average output voltage should be constant (given as the dashed line V_o).

The switch control signal can be generated by comparing a control value (which most often is an amplified error) to a repetitive waveform V_{st} . The control value may be the difference between the actual and the desired output voltage V_o as seen in figure (3.3).

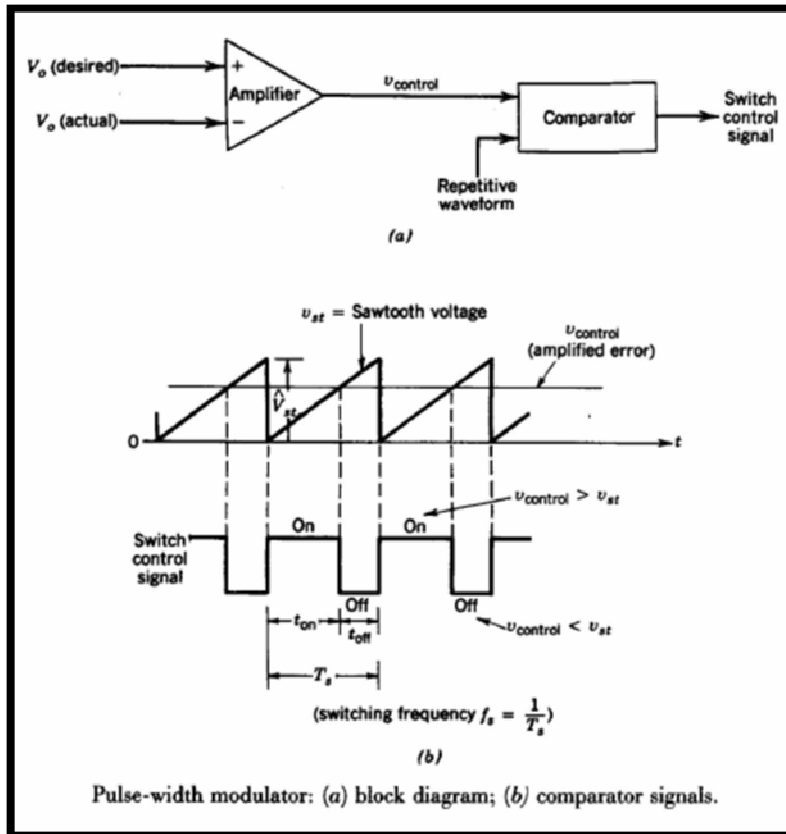


Figure (3.3): The principle of PWM control.

The effects of the comparison are:

- when $V_{\text{control}} > V_{\text{st}}$: switch on
- when $V_{\text{control}} < V_{\text{st}}$: switch off

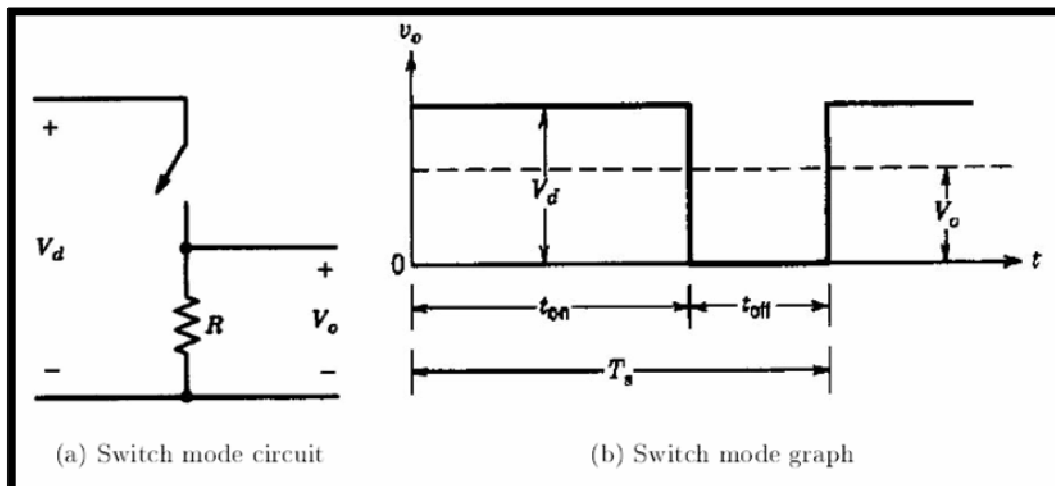


Figure (3.4): The principle of switching [10].

The duty cycle D can now be defined in two different ways:

$$D = \frac{t_{on}}{T_s} = \frac{V_{control}}{V_{st}^{\wedge}} \quad (3.1)$$

The frequency (T_s) can also be varied in a PWM switching mode. This method might make it hard to filter the ripple components in the converter waveforms.

Common for both the converter topologies is the direction of transferred energy. The energy is unidirectional, which means that it can be transferred in one direction only. As there is seldom a requirement of a bidirectional flow in a grid connected PV system, the buck and boost converter topologies are more than sufficient for this application.

In the following sections the converter topologies will be analyzed with steady state conditions, the switches are assumed to be ideal and losses in the capacitors and inductors are neglected. In addition the switching time is assumed much shorter than the electric time constant of the circuit. Then the model analysis will be extended to include perturbation in the converter operation.

3.3.3 Steady state analysis

When analyzing each of the converter topologies, it is first assumed that they operate in steady state. This implies a constant duty cycle, which means that the current starts from the same value at the beginning of every switching cycle. Due to the inductor the current will charge and discharge through one cycle and steady state condition implies that $\Delta I_{on} = \Delta I_{off}$.

The change in current is the only factor deciding whether or not the system is in steady state. In a DC-DC converter with an optimal design it is assumed that the switching ripples are very small compared to the average values, often less than 1 %. This is often referred to as the small or linear ripple approximation [10].

3.4.1 Buck converter

The buck converter is often referred to as a step-down converter, and as the name implies, the converter produces a lower DC voltage output than the input. The circuit of the buck converter can be seen in figure (3.5).

This circuit is an improved version of the circuit in figure (3.4 a). The resistive load is replaced by a diode to overcome the problem of stored inductive energy that will normally appear in the circuit. In figure (3.4 a) this energy can harm the switch because there are no other components that can dissipate it. Secondly a low-pass filter is used to reduce the output voltage fluctuations as much as possible. This is achieved by wise selection of filter parameters to reduce the corner frequency f_c (this will also be explained later). The output voltage V_o will be as in figure (3.4 b).

The buck converter will have different circuit schemes for each of the switch positions. To obtain the relationship between the input and output of the converter (and hence the duty cycle) the current through the inductor will be examined. The filter capacitor is assumed to be so large that $v_o(t) = V_o$, which means that no current will flow through it.

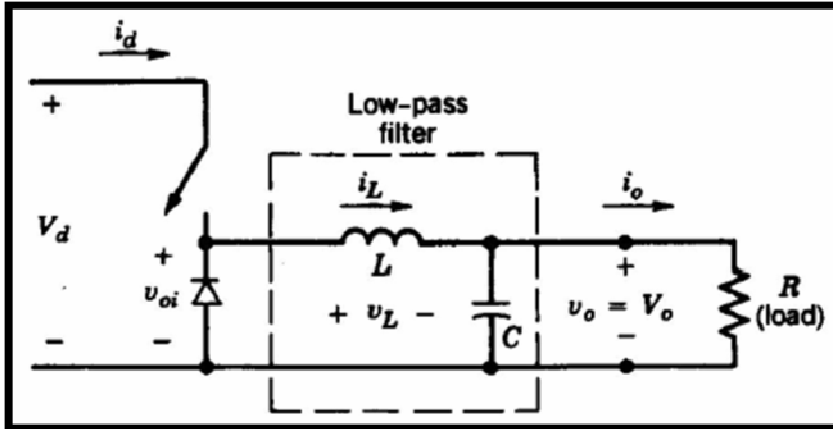


Figure (3.5): Buck converter [10].

Thus it can be concluded that the inductor current equals the output current for both switch positions. The earlier assumption about the system being in steady state implies that the voltage and current waveforms repeat for each time period T_s . This can be seen by considering each of the circuits in figure (3.6).

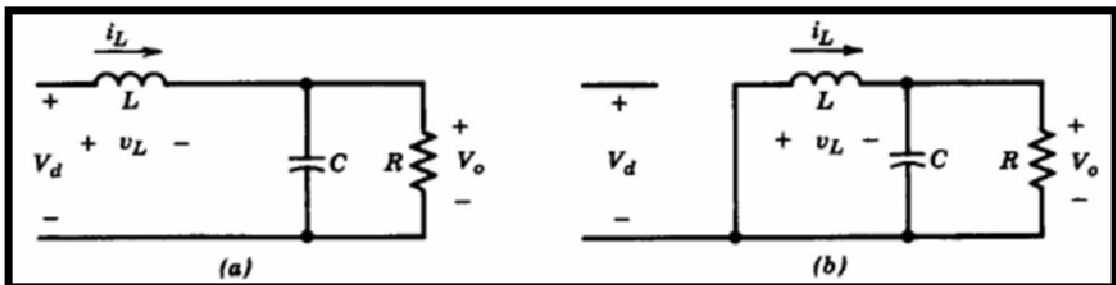


Figure (3.6): Buck converter circuit for: a) t_{on} and b) t_{off} CCM[10].

When the switch is on, the input voltage V_d leads to a linear increase in the inductor current. As the switch is turned off, the diode becomes forward biased and the stored energy in the inductor makes the current continue to flow. But as the energy is transferred from the inductor to the load, the current is decreasing again. The inductor voltage is given as:

$$v_L = L \frac{di_L}{dt} \quad (3.2)$$

As the inductor voltage is repeating itself for each time period, the change for each period is zero:

$$(\mathbf{i}_L)_{\text{on}} = (\mathbf{i}_L)_{\text{off}}$$

$$\int_0^{t_{\text{on}}} v_L dt = \int_{t_{\text{on}}}^{T_s} v_L dt \quad (3.3)$$

By considering the voltage curve in figure (3.7) the equation can easily be solved:

$$(V_d - V_o) t_{\text{on}} = V_o (T_s - t_{\text{on}}) \quad (3.4)$$

Where,

V_d : input voltage as seen in figure (3.6).

V_o : output voltage as it seen in figure (3.6).

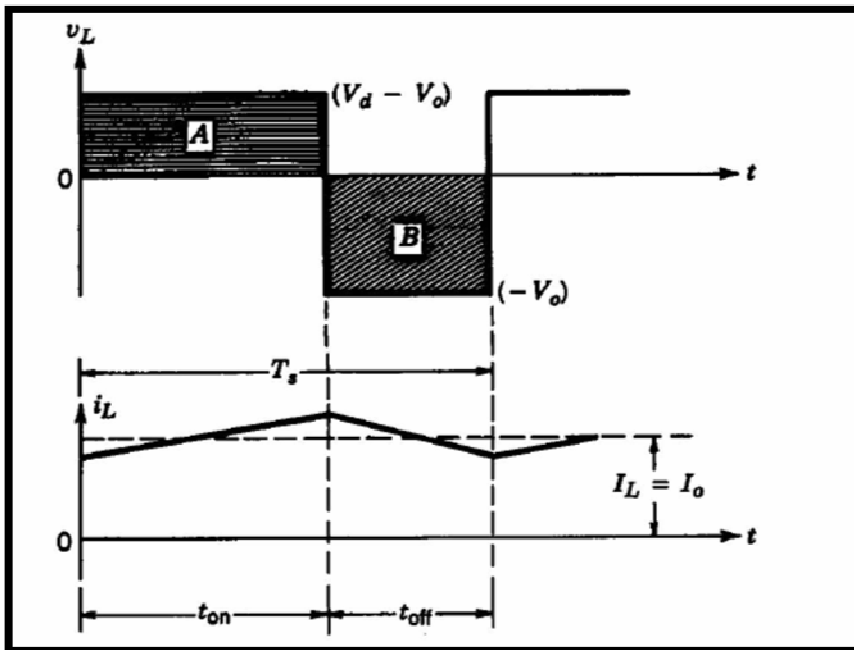


Figure (3.7): Inductor voltage and current of the buck converter [10].

By some rearrangement, the relationship between the input and the output voltage is found:

$$\frac{V_o}{V_d} = \frac{T_{on}}{T_s} = D \quad (3.5)$$

The buck converter is actually equivalent to a transformer where the turn's ratio is changed by varying the duty cycle. This can be shown mathematically by considering the power input and output. Neglecting the losses in the circuit gives the following relations:

$$P_d = P_o$$

$$V_d I_d = V_o I_o$$

$$\frac{V_o}{V_d} = \frac{I_d}{I_o} = D \quad (3.6)$$

This is also referred to as a POPI (Power In - Power Out) type converter [10].

3.4.2 Output voltage ripple in a buck converter

The theoretical value of the filter capacitor is assumed to be so large that the output voltage is constant. But in a realistic buck converter this will not be the case, and there will be produced a ripple in the output voltage.

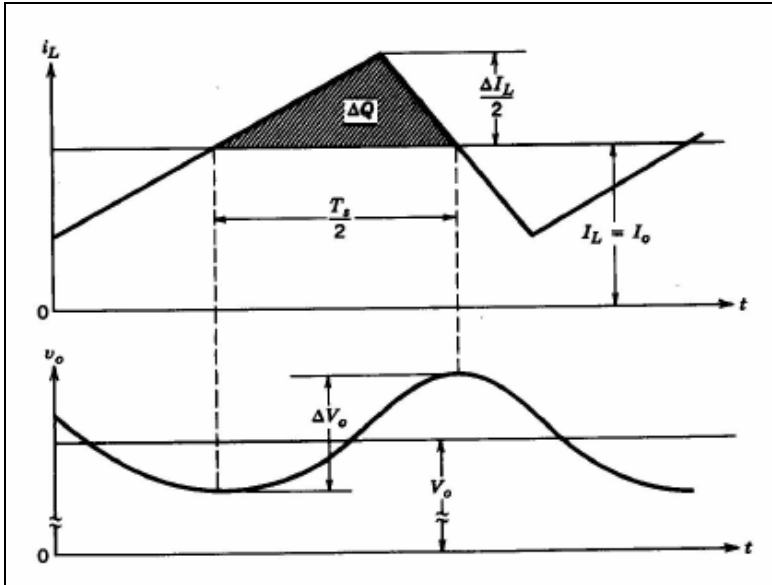


Figure (3.8): Output voltage ripple in a buck converter [10].

The inductor current consists of two components, an average component flowing through the resistive load, and a ripple component assumed to flow through the capacitor. The ripple current introduces an additional charge ΔQ , which can describe the ripple voltage:

$$\Delta V_o = \frac{Q_c}{C} = \frac{1}{C} \left(\frac{1}{2} \frac{T_s}{2} \frac{\Delta I_L}{2} \right) = \frac{1}{8C} \Delta I_L T_s \quad (3.7)$$

To minimize the ripple, the low-pass filter has to be selected so that the corner frequency $f_c = \frac{1}{2\pi\sqrt{LC}} \ll f_s$. This deduction is done assuming the ESR, which is the resistive part of the capacitor and inductor impedances, to be negligible [10].

3.5.1 Boost converter

As opposed to the buck converter, the boost converter produces an output voltage which is higher than the input voltage. The circuit is according to figure (3.9).

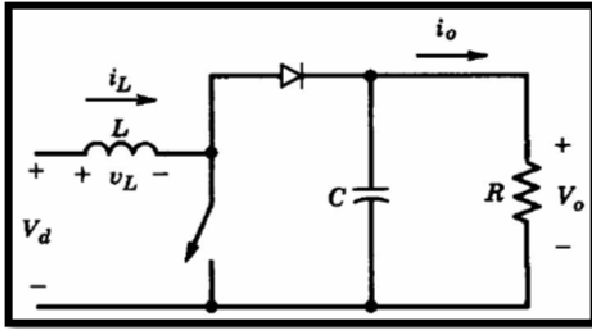


Figure (3.9): Boost converter [10].

This topology also has different circuit schemes depending on the state of the switch, as seen in figure (3.10). When the switch is on the output stage is isolated from the input caused by the reverse biased diode. The input will supply the inductor with a constant voltage, and the inductor current will increase according to equation (3.2)

. When the switch is turned off, the output will be supplied both by the input and the inductor, and the current through the inductor will decrease because of this energy transfer.

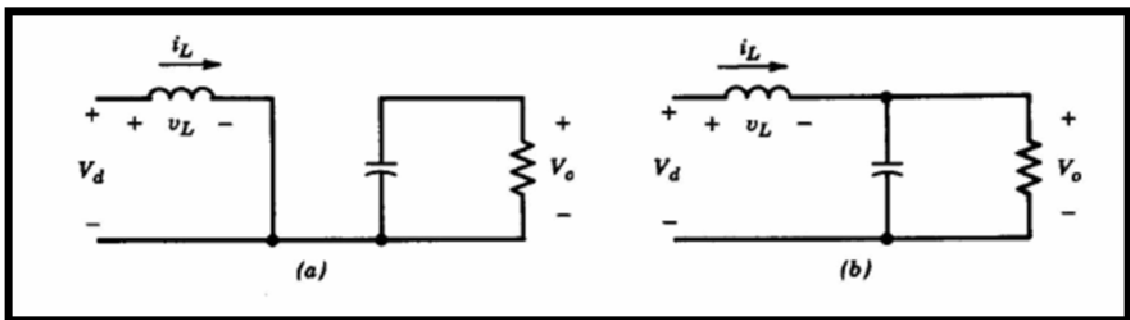


Figure (3.10): Boost converter circuit for a) t_{on} and b) t_{off} in CCM [10].

The voltage and current graphs of the inductor through one time period is shown in figure (3.11). The shapes are equal to those of the buck converter, but the voltage of the inductor is different due to the placement of the switch and the diode.

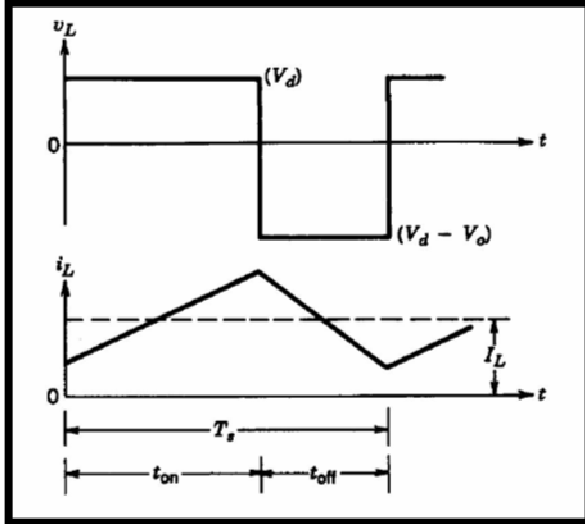


Figure (3.11): Inductor voltage and current of the boost converter.

The same considerations regarding the inductor current can be done for this converter as in the previous section, which leads to the connection.

Using Faraday's law for the inductor boost converter

$$V_d t_{on} = (V_o - V_d)(T_s - t_{on}) \quad (3.8)$$

After some rearrangements the equation becomes:

$$\frac{V_d}{V_o} = (1 - D) = \frac{I_o}{I_d} \quad (3.9)$$

The last term of the equation is yielded from the assumption of no power loss in the circuit (i.e. P_{in} equals P_{out}), and as for the buck it is referred to as a POPI converter [11].

Parasitic elements in a boost converter there will be losses due to the switches, the diode, the capacitor and the inductor. When the duty cycle gets close to one, the output voltage will theoretically increase against infinity, but due to the parasitic elements the ratio of V_o on V_d will

actually go to zero. The ideal and the real characteristic of the conversion ratio versus duty ratio is shown in figure (3.12).

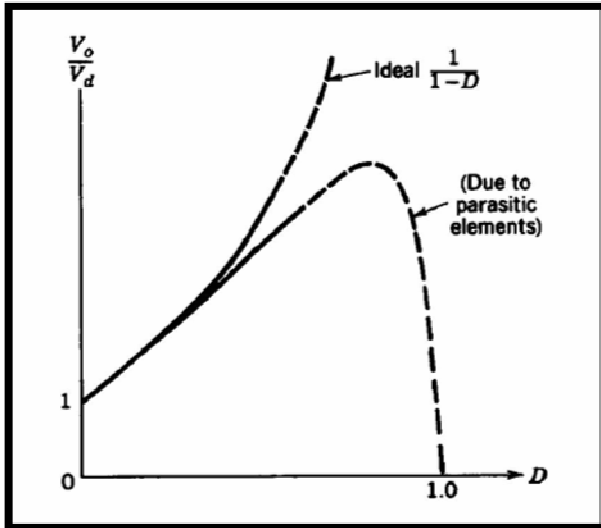


Figure (3.12): The effect of parasitic elements in a boost converter.

In general the parasitic elements will seldom have a big impact because the duty ratio goes into saturation before entering the steep slope of the parasitic curve [10].

3.5.2 Output voltage ripple in a boost converter

The output voltage ripple will also be present in a boost converter due to the capacitor value. When the switch is on the stored energy in the capacitor will be sent to the load, causing a discharge and decreased voltage. When the switch is off the capacitor is charged again by the input. The ripple voltage ΔV_o can be written as:

$$\Delta V_o = \frac{Q_c}{C} = \frac{I_o D T_s}{C} = \frac{V_o D T_s}{R C} \quad (3.10)$$

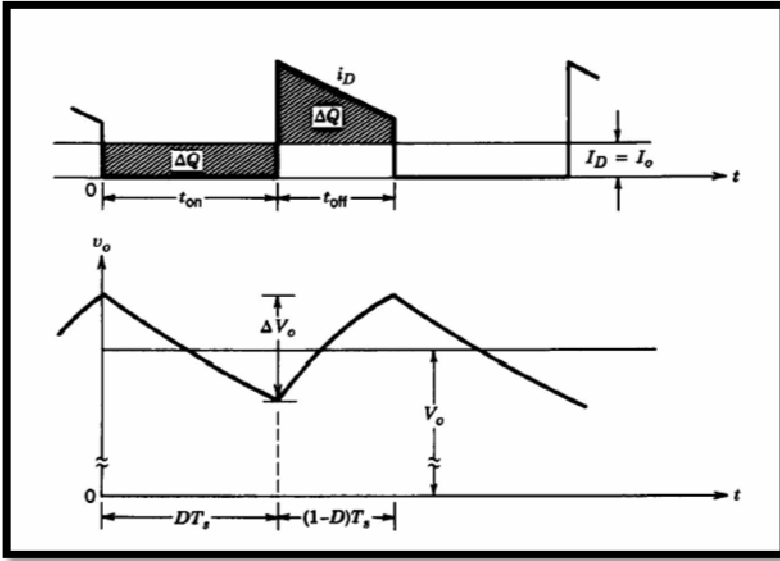


Figure (3.13): Output voltage ripple in a boost converter [10].

This equation can also be utilized to find a capacitor value suitable for the circuit, choosing a worst case tolerated value of the ripple ΔV_o .

Normally the values D and R are dependent on the operation, but when calculating for a specific point of operation these values are known [10].

3.6 Buck versus Boost in a PV System

In grid connected systems with varying input from the source (like PV or wind), the input voltage might be either higher or lower than the AC voltage. This makes both buck and boost operation necessary, depending on the input voltage. Both converter topologies are applicable for MPPT. In real systems, however, the boost converter is the one most utilized. Normally the DC link voltage will be at least 350 V, and if enough modules

cannot be connected in series to obtain this voltage level in small systems, a boost stage is necessary.

It has been presented in earlier studies that the efficiency for a boost converter operating in CCM(Continuous Conduction Mode) varies slightly for varying duty cycle, while the efficiency variation for a buck converter is considerable [11].

For a boost converter the current through the inductor will equal the input current, while for a buck converter it will equal the output current. This can also be seen in the figures (3.6) and (3.10).

3.7 Battery

Batteries store direct current electrical energy in chemical form for later use. In PV system, the energy is used at night and during periods of cloudy weather.

A battery is charging when energy is being put in and discharging when energy is being taken out. A cycle is considered one charge-discharge sequence, which often occurs over a period of one day in residential PV systems. The following types of batteries are commonly used in PV system[12]:

1- Lead-acid batteries

2- Liquid vented

3- Alkaline batteries

4- Nickel Cadmium

5- Nickel iron

The performance of storage batteries is described below [13]:

Ampere-hour capacity: The number of amp-hours a battery can deliver is simply the number of amps of current it can discharge, multiplied by the number of hours it can deliver that current. System designers use amp-hour specifications to determine how long the system will operate without any significant amount of sunlight to recharge the batteries. This measure of "days of autonomy" is an important part of design procedures. Theoretically, a 200 amp-hour battery should be able to deliver either 200 amps for one hour, 50 amps for 4 hours, 4 amps for 50 hours, or one amp for 200 hours.

Charge and discharge rates: If the battery is charged or discharged at a different rate than specified, the available amp-hour capacity will increase or decrease. Generally, if the battery is discharged at a slower rate, its capacity will probably be slightly higher. More rapid rates will generally reduce the available capacity. The rate of charge or discharge is defined as the total capacity divided by some number. For example, a discharge rate of C/20 means the battery is being discharged at a current equal to 1/20th of its total capacity. In the case of a 400 amp-hour battery, this would mean a discharge rate of 20 A.

Temperature: Batteries are rated for performance at 80°F. Lower temperatures reduce amp-hour capacity significantly. Higher temperatures result in a slightly higher capacity, but this will increase water loss and decrease the number of cycles in the battery life.

Depth of discharge: This describes how much of the total amp hour capacity of the battery is used during a charge-recharge cycle.

As an example, "shallow cycle" batteries are designed to discharge from 10% to 25% of their total amp-hour capacity during each cycle.

In contrast, most "deep cycle" batteries designed for photovoltaic applications are designed to discharge up to 80% of their capacity without damage. Even deep cycle batteries are affected by the depth of discharge. The deeper the discharge, the smaller the number of charging cycles the battery will last, Figure (3-14) [12].

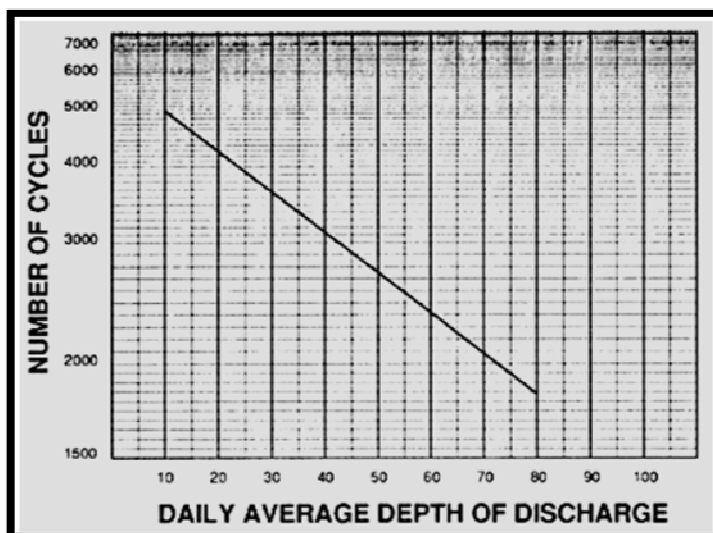


Figure (3-14): Number of cycles for different discharge depths[12].

3.8 Charge Controllers

The most important feature of charge controller is to measure the battery voltage and protects the battery against the overcharging. This can be achieved by the following ways.

Switching off the PV array when the charge cut-out voltage is exceeded, short-circuiting the PV array with a shunt controller and adjusting the voltage with an MPP charge controller.

The reserve diode which prevents the battery to be discharged via the array during low irradiation level is integrated to the charge controller.

Operation of batteries over long time of operation requires a charge controller to be flexible. The charge cut-off and discharge cut-off voltages are dependent on the state of charge of the battery.

The main jobs of the charge controller are [13]:

- ❖ Allow the optimum charge for the battery.
- ❖ Protect the battery from the overcharge.
- ❖ Prevent the battery from unwanted discharge and from deep discharge.
- ❖ Get information of state of charge of batteries.

3.8.1 Series controllers

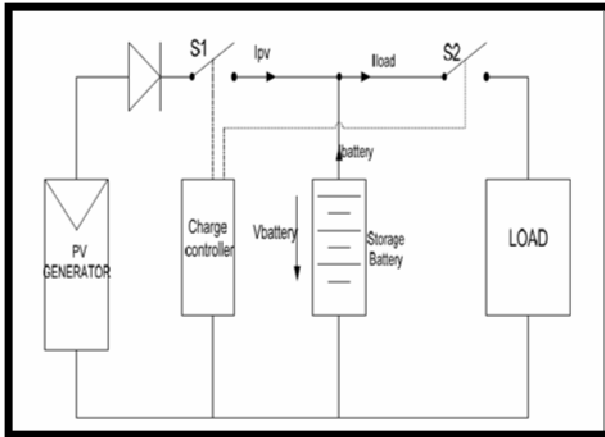


Figure (3.15): Series charge controller

When the voltage level reaches to the charge cut-off level the power from the PV generator is blocked by the switch in S1 in Figure (3.15). After the voltage drops again below the charging cut-off voltage level S1 switches back on [10].

3.8.2 Shunt controllers

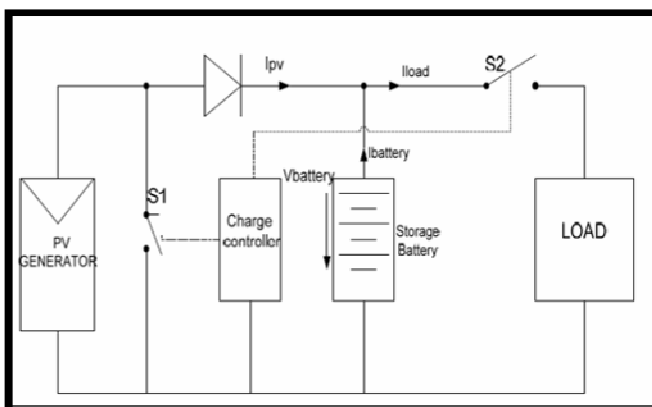


Figure (3.16): Shunt charge controller

When the charge cut-off voltage is reached charge controller continuously reduces the power of the module. Since it reduces the power continuously the unwanted power is short-circuited via the array, this

creates heat in the system. This method is usually used for battery when charging is safe and swift [10].

3.8.3 MPPT charge controllers

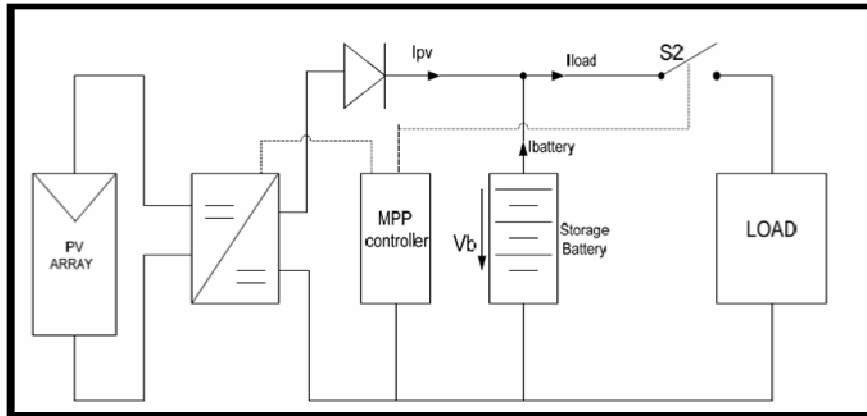


Figure (3.17): MPPT controller

During the operation of the PV array the temperature and irradiation are changing continuously, this result in changing the I-V curve of the PV array consecutively the maximum power point of the curve should be tracked to exploit the energy from the PV more efficiently. MPP tracker is used with DC/DC converter by regulation the voltage every a few minutes and passes through the characteristics of PV array to determine the maximum point. DC/DC converter gets the power from the specified point on the curve [10].

3.9 Calculation of Boost Converter Parameters

Figure (3.18) shows the Circuit of the boost converter. The input of the boost converter is the photovoltaic output voltage. The inductance and the capacitor need to be specified. The switching command of the IGBT (S) as it shown in figure (3.18) is obtained from the MPPT controller.

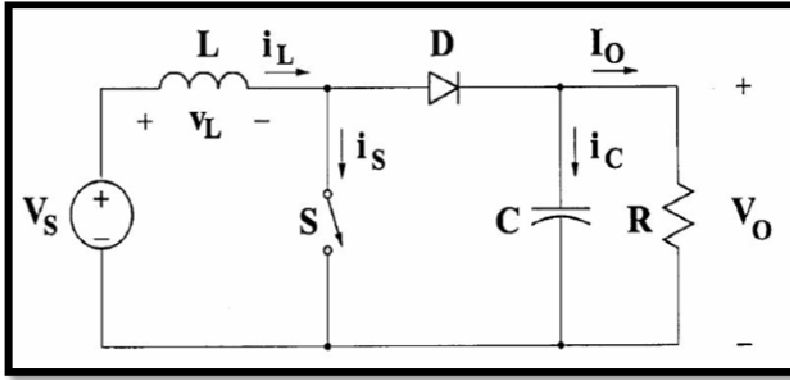


Figure (3.18): Boost converter circuit.

We take a case study to design boost converter parameters. The design specifications of boost controller are shown in table (3.1). The specifications are for a variable value of input voltage of the boost controller where the input voltage comes from the renewable source of the hybrid system and the output voltage of the boost controller is fixed 120V DC.

Table (3.1): Specification of Boost Controller.

Parameter	Value
Input Voltage	0-48Vdc
Output Voltage	120Vdc
Output Current	4.5A
Switching frequency	10kHz

Based on the specification for input voltage and output voltage as shown in table (3.1), the required duty cycle can be determined by using Equation (3.11).

In this boost controller circuit, the duty cycle of the boost controller changes with the value of its input voltage. Therefore, in order to determine the value of minimum inductor L_{min} and minimum capacitor C_{min} of the boost controller, the minimum of the duty cycle D of the boost controller is

used in which this duty cycle can be achieved when the input voltage of the boost controller is at maximum value and the output voltage is fixed at 120V.

For the boost converter the input-output ratio is calculated by;

$$V_s \times D \times T + (V_o - V_s) \times (1 - D) \times T = 0$$

$$\frac{V_o}{V_{in}} = \frac{1}{1-D} \quad (3.11)$$

$$D = \frac{V_o - V_{in}}{V_o}$$

$$D_{max} = (120-0)/120 = 1$$

$$D_{min} = (120-48)/120 = 0.6$$

The minimum inductance can be determined by using Equation (3.12).

$$L_{min} = \frac{D(1-D)^2 R}{2f} \quad (3.12)$$

$$L_{min} = \frac{0.6(1-0.6)^2 \times 10}{2 \times 30 \times 10^3} = 16 \mu H$$

The capacitance is calculated using Equation (3.13). Let the peak-to-peak ripple voltage equal to 0.05.

$$\Delta V_o = 0.05$$

$$C_{min} = \frac{V_o D}{\Delta V_o R f} \quad (3.13)$$

$$C_{min} = \frac{120 \times 0.6}{0.05 \times 10 \times 30 \times 10^3} = 4.8 \text{ mF} \approx 5 \text{ mF}$$

Chapter Four

**Maximum Power Point
Tracking (MPPT) Techniques**

Chapter Four

Maximum Power Point Tracking (MPPT) Techniques

4.1 Introduction

When a PV module is directly coupled to a load, the PV module's operating point will be at the intersection of its I-V curve and the load line which is the I-V relationship of load. For example in figure (4.1), a resistive load has a straight line with a slope of $1/R_L$ as shown in figure (4.2). In other words, the impedance of load dictates the operating condition of the PV module. In general, this operating point is seldom at the PV module's MPP. Thus it is not producing the maximum power.

A study shows that a direct-coupled system utilizes a more 31% of the PV capacity. A PV array is usually oversized to compensate for a low power yield during winter months.

This mismatching between a PV module and a load requires further over-sizing of the PV array and thus increases the overall system cost. To mitigate this problem, a maximum power point tracker (MPPT) can be used to maintain the PV module's operating point at the MPP. MPPTs can extract more than 97% of the PV power when properly optimized [14].

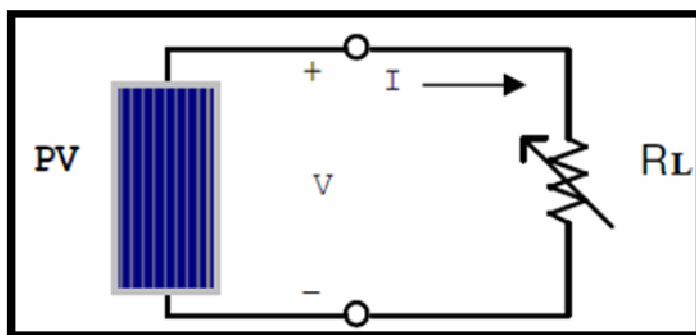


Figure (4.1): PV module is directly connected to a (variable) resistive load [14].

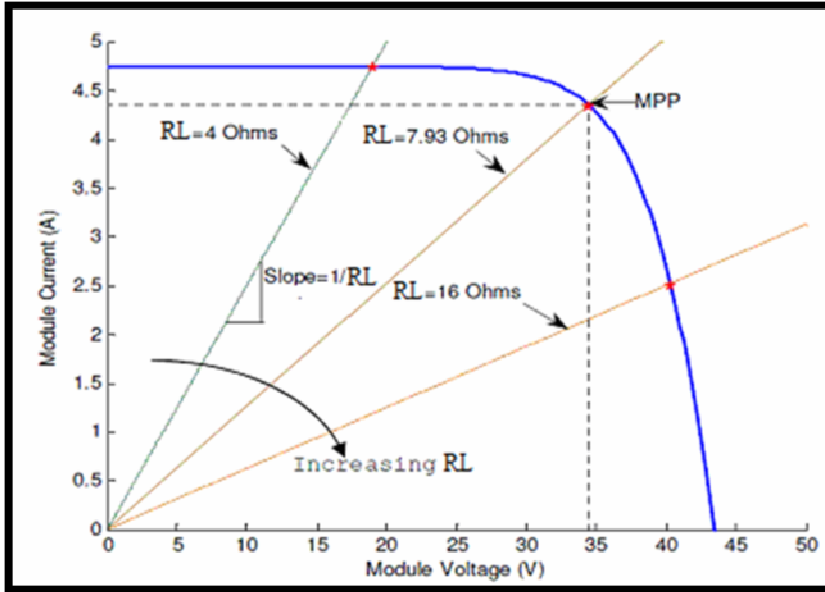


Figure (4.2): I-V curves of BP SX 150S PV module and various resistive loads at (1000W/m², 25oC) [14].

4.2 Maximum Power Point Tracking (MPPT) Techniques

The tracking algorithm works based on the fact that the derivative of the output power P with respect to the panel voltage V is equal to zero at the maximum power point as in Fig.3. The module P-V characteristics are shown in Figure (4.3) show further that the derivative is greater than zero to the left of the peak point and is less than zero to the right.

$$\frac{\partial P}{\partial V} = 0 \text{ for } V = V_{mp} \quad (4.1)$$

$$\frac{\partial P}{\partial V} > 0 \text{ for } V < V_{mp} \quad (4.2)$$

$$\frac{\partial P}{\partial V} < 0 \text{ for } V > V_{mp} \quad (4.3)$$

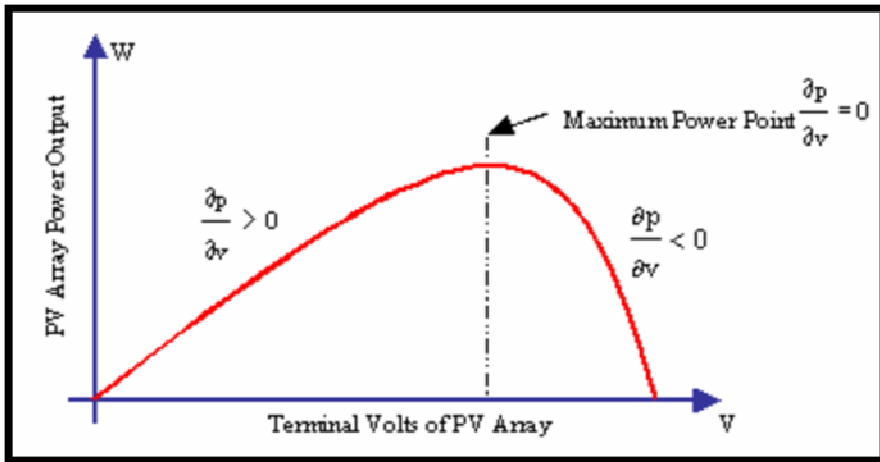


Figure (4.3): P-V Characteristics of a module [15].

In the literature, various MPPT algorithms are available in order to improve the performance of PV system by effectively tracking the MPPT. However, most widely used MPPT algorithms are considered here, they are:

- a) Perturb and Observe (P&O)
- b) Incremental conductance (In Cond)
- c) Open Circuit Voltage
- d) Short Circuit Current

4.2.1 Perturb and observe

The most commonly used MPPT algorithm is P&O method and is also known as hill-climbing algorithm. This technique employs simple feedback arrangement and few measured parameters. In this approach, the array voltage is periodically given a perturbation and the corresponding output power is compared with that at the previous perturbing cycle.

However, the operating point oscillates around the MPP as the system is continuously perturbed. This method can be implemented easily [15].

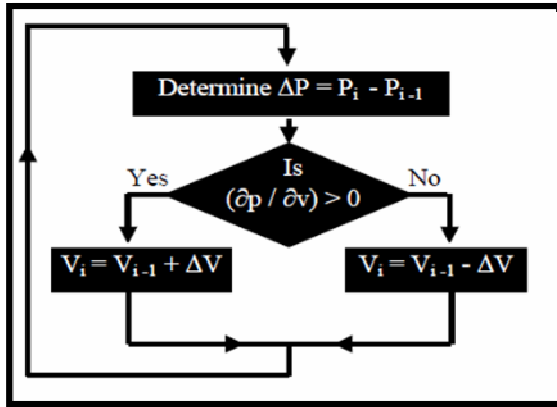


Figure (4.4): P&O flow chart[15].

In this simple algorithm, the operating voltage is perturbed with a small change $+\Delta V$ and the power output is observed. Depending on the sign of observed power, further perturbation will be given to voltage as described in Figure (4.4).

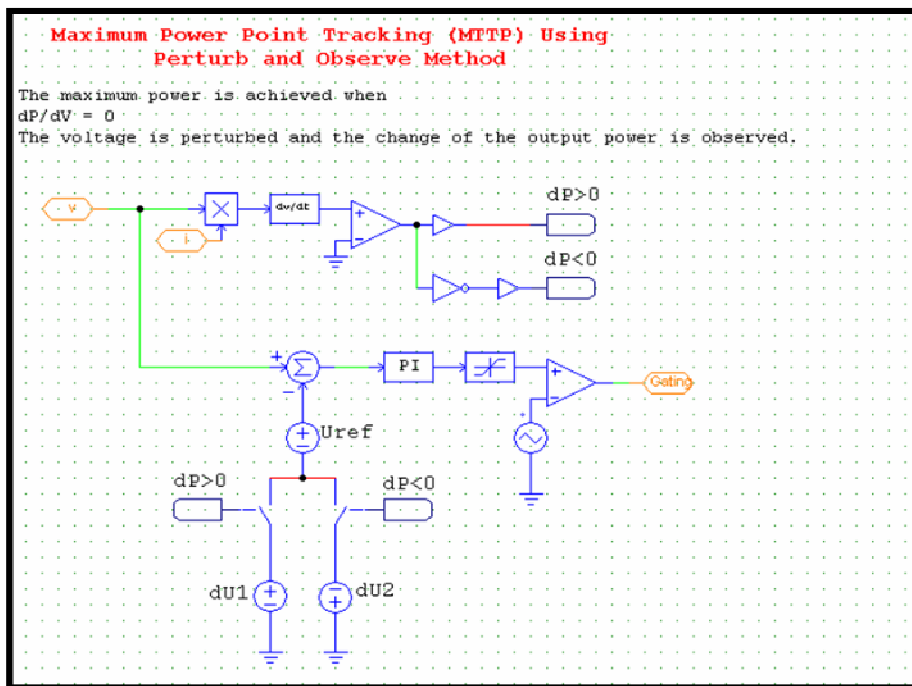


Figure (4.5): Design P&O algorithm by Psim

In Figure (4.5) shown how to design the MPPT technique by P&O algorithm using Psim software.

4.2.2 Incremental conductance

In this method, incremental conductance is compared with instantaneous conductance. We have,

$$P = V I \quad (4.4)$$

Applying the chain rule for the derivative of products yields to

$$\partial P / \partial V = [\partial (VI)] / \partial V = I [\partial V / \partial V] + V [\partial I / \partial V] = I + V [\partial I / \partial V] \quad (4.5)$$

At MPP, as $\partial P / \partial V = 0$, the equation (4.5) could be written in terms of array voltage V and array current I as

$$\partial I / \partial V = - I / V \quad (4.6)$$

Here $\partial I / \partial V$ is an incremental conductance where as I / V is an instantaneous conductance. The flow chart of incremental conductance shown in Figure (4.6) regulates the PWM control signal of the dc – to – dc converter until the condition: $(\partial I / \partial V) + (I / V) = 0$ is satisfied.

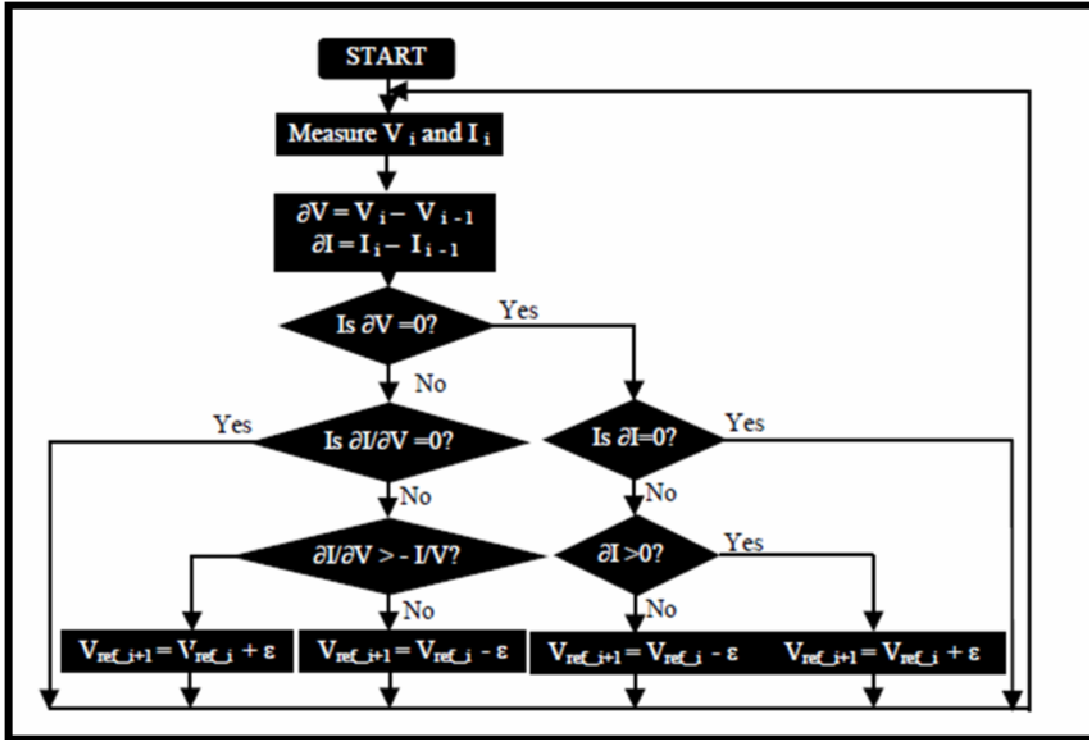


Figure (4.6): Incremental Conductance flow chart [15].

Detailed flowchart of the In Cond algorithm is depicted in Figure (4.6).

$$\diamond I/V > dI/dV \text{ for } dP/dV > 0 \quad (4.7)$$

$$\diamond I/V < dI/dV \text{ for } dP/dV < 0 \quad (4.8)$$

$$\diamond I/V = -dI/dV \text{ for } dP/dV = 0 \quad (4.9)$$

The relationship between I/V and dI/dV determines the direction of the perturbation. The incremental conductance is capable of identifying whether the MPP is reached or not. Once the MPP is reached the perturbation action stops, and it starts again only when I/V and dI/dV are not equal.

The aim is to find and adjust the module operating voltage by maintaining MPP condition through simple incremental conductance and

instantaneous conductance measurement. The microcontroller regulates the duty cycle of the converter.

The incremental conductance method can track the MPP with higher precision, and it has higher accuracy under fast changing weather conditions compared to the P&O method. However it requires more calculation process and thus slows down sampling speed. This method also requires extra sensors in order to measure the current and voltage [16].

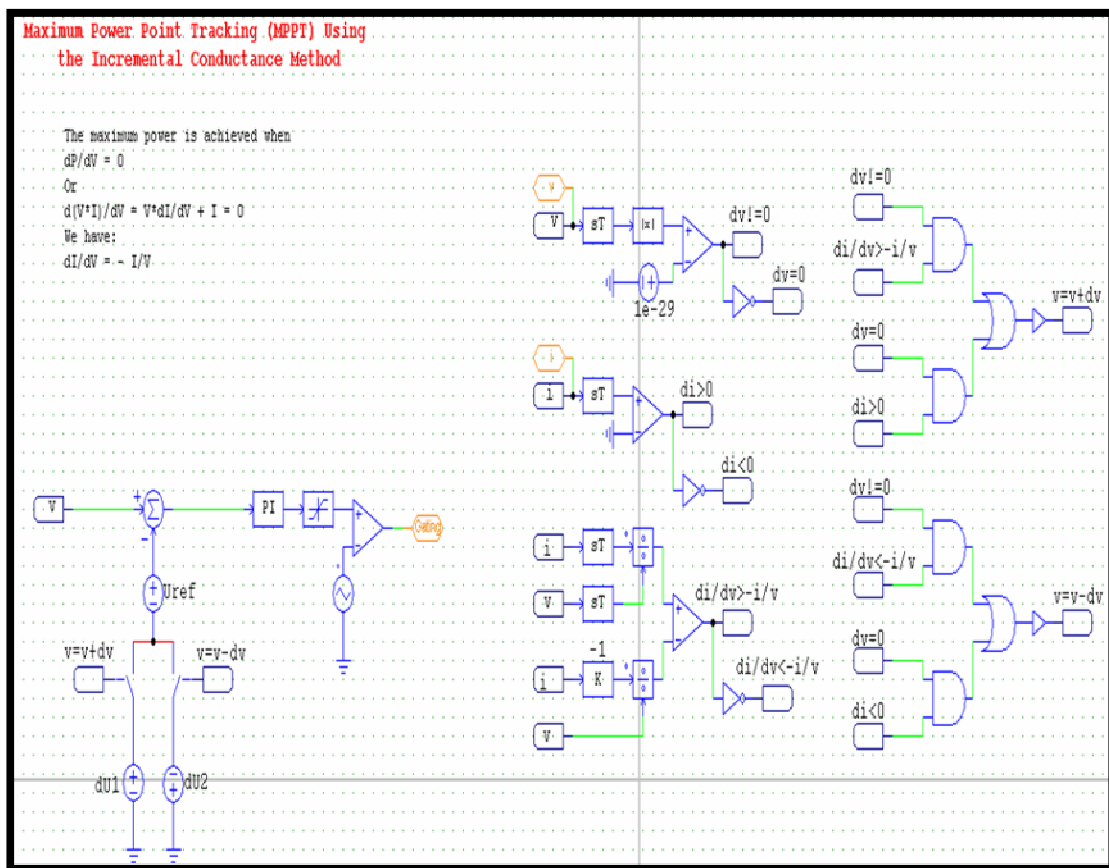


Figure (4.7): Incremental conductance by psim

In Figure (4.5) shown how to design the MPPT technique by Incremental Conductance algorithm using Psim software.

4.2.3 Open-circuit voltage

This technique is also known as constant voltage method. It uses fraction of open circuit voltage to determine the module's voltage at the maximum power point [16].

$$V_{mp} = k_1 \times V_{oc} \quad (4.10)$$

Here the factor k_1 is always <1 . Figure (4.8) shows the flow chart of this method. It looks very simple but determining best value of k_1 is very difficult and k_1 varies from 0.73 to 0.8. The common value used is 0.76; hence this algorithm is also called as 76% algorithm [16].

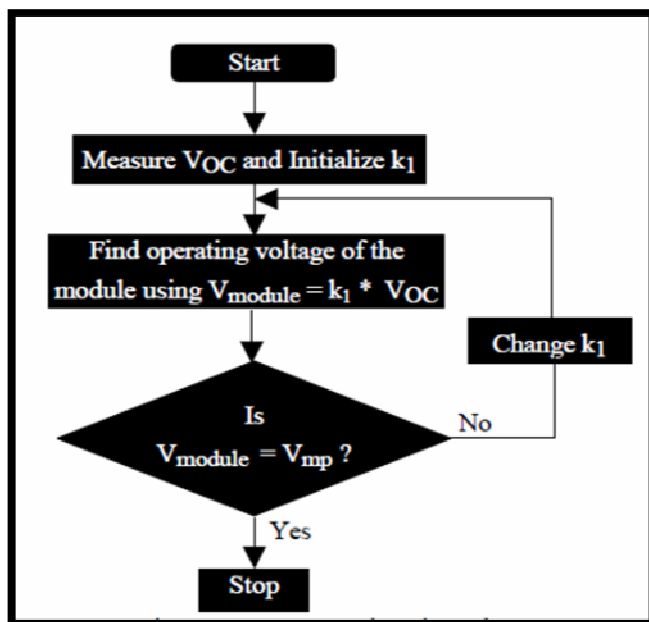


Figure (4.8): Open Circuit voltage flow chart[15].

The principle of the Constant Voltage (CV) Method is simple, the PV is supplied using a constant voltage, Temperature and Solar Irradiance impacts are neglected, the reference voltage is obtained from the MPP of the P characteristic directly. Figure (4.9) shows the CV algorithm [17].

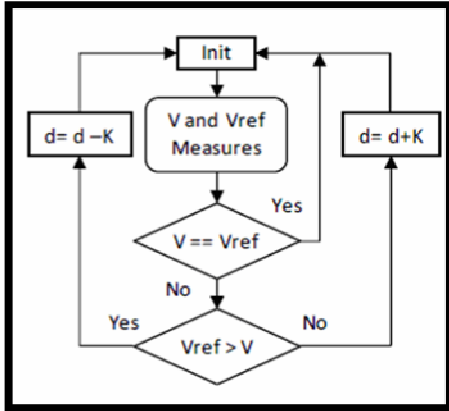


Figure (4.9): Constant voltage flow chart [16].

4.2.4 Short -circuit current

This technique is similar to the open circuit method and is also known as constant current method. It uses fraction of short circuit current to determine the module's current at the maximum power point [15].

$$I_{mp} = k_2 \times I_{SC} \quad (4.11)$$

The factor k_2 is a constant and is much closer to 1 but always < 1 .

The flow chart is shown in Figure (4.10).

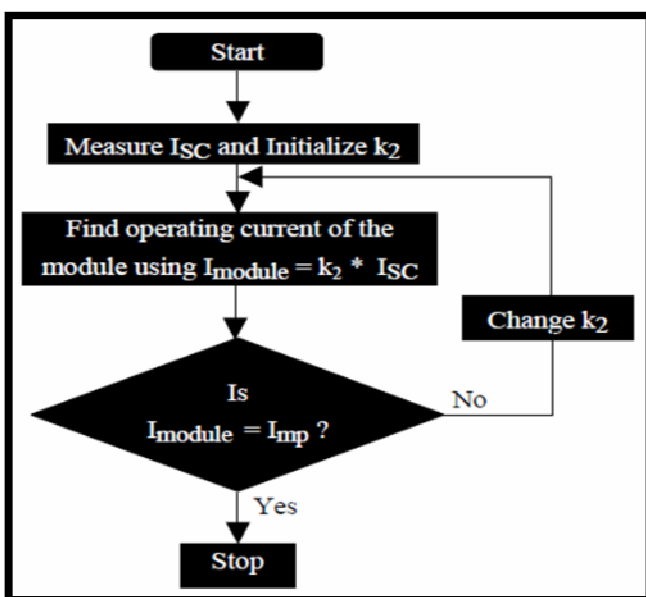


Figure (4.10): Short circuit current flow chart [15].

When the PV array output current is approximately 90% of the short circuit current, solar module operates at its MPP [15]. In other words, the common value of k_2 is 0.9.

4.3 Simulation and Validation of the Buck Converter with MPPT Controller by using Simulink and Psim Software:

In Figure (4.11) shows a PV system in Simulink which consist a PV MSX-50 Photovoltaic Module, buck convertor, load and the Constant Voltage MPPT controller.

The main specifications of a MSX-50 Photovoltaic Module are: $P_{MPP} = 50\text{Watt}$, $V_{MPP} = 17.1\text{ V}$, $I_{MPP} = 2.92\text{ A}$.

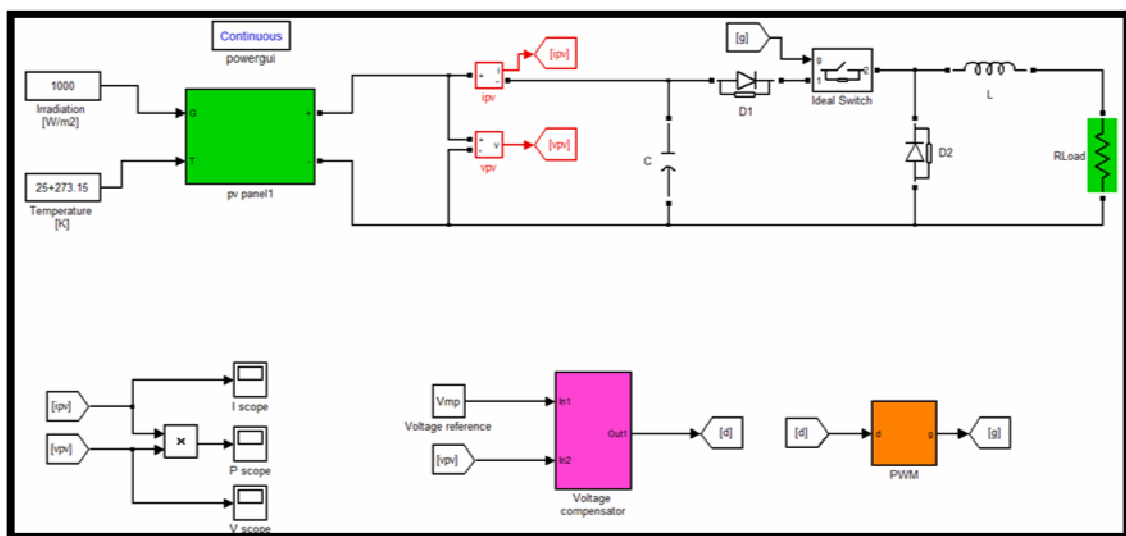


Figure (4.11): PV system with a constant voltage MPPT by Simulink.

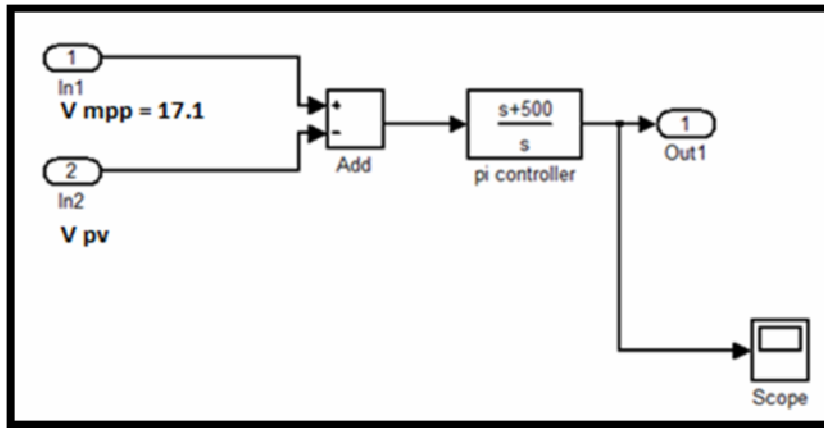


Figure (4.12): Voltage compensator

Figure (4.12) show the voltage compensator which is making a difference between a V_{MPP} from datasheet of MSX-50 Photovoltaic Module and V_{PV} from a voltage sensor to calculate an error with using PI controller. The simulations operate at 1000W/m^2 and 25°C where is the result we obtained from it as Figure (4.13), (4.14) and (4.15).

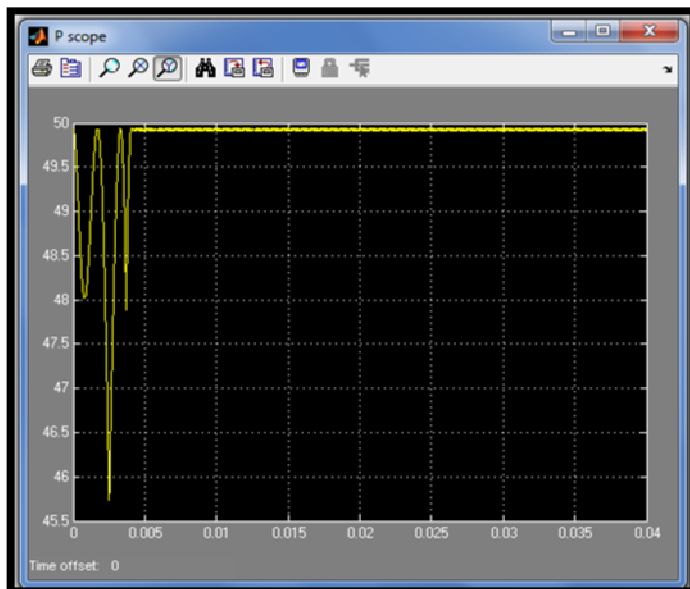


Figure (4.13): The power output from PV with constant voltage MPPT controller[Y- axis: power(watt), X –axis: time (sec)].

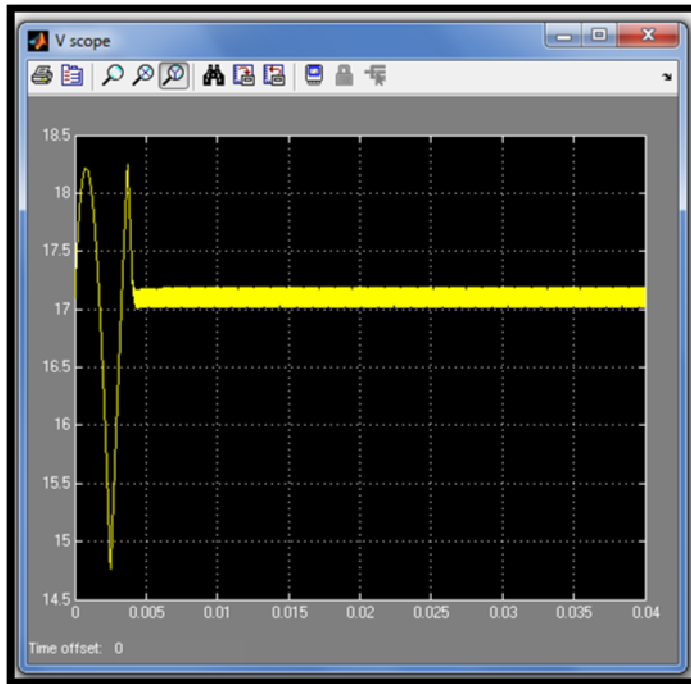


Figure (4.14): MPP voltage regulation of PV by constant voltage MPPT controller [Y- axis: voltage(volt), X –axis: time (sec)].

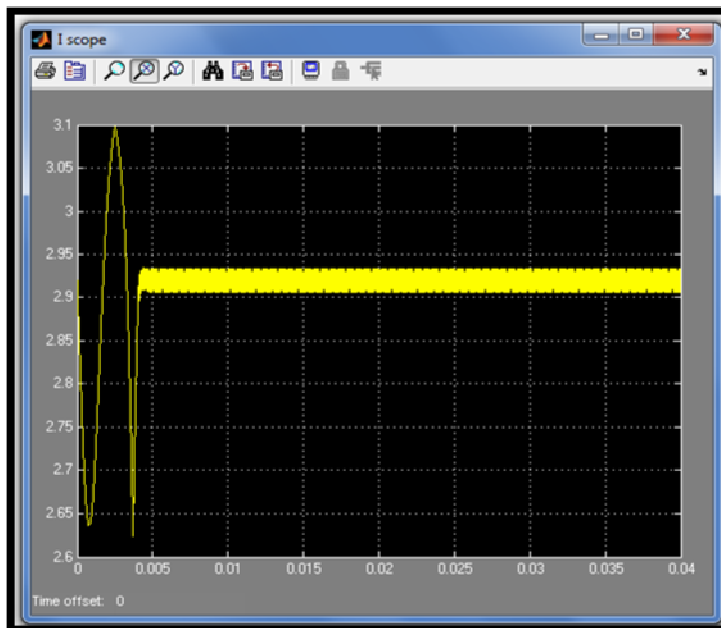


Figure (4.15): Current of PV by using constant voltage MPPT controller [Y- axis: current(A), X –axis: time (sec)].

In figure (4.16) shows a PV system in Psim which consist a PV MSX-50 Photovoltaic Module, buck convertor, load and the Perturb and Observation MPPT controller.

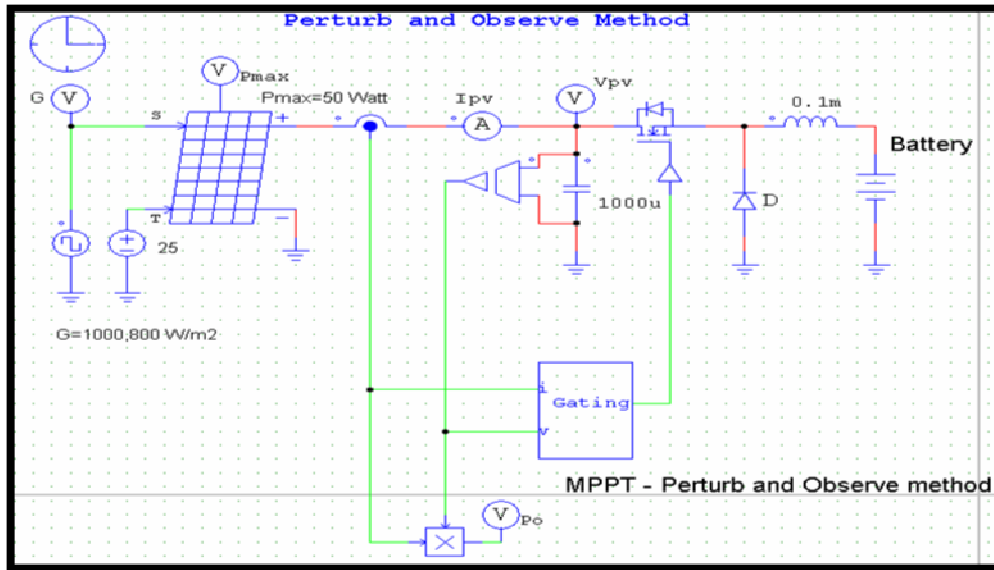


Figure (4.16): PV system with a constant voltage MPPT by Psim.

Figure (4.17) shows the results simulation of PV system in Psim.

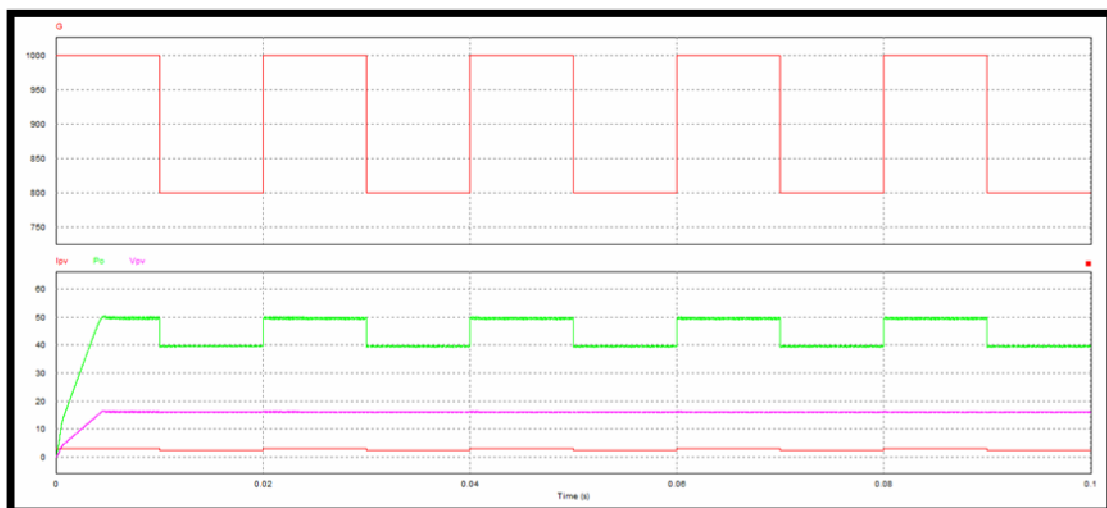


Figure (4.17): The output power(watt), voltage(volt) and current(A) of PV system with P&O MPPT at variation radiation $G= (1000\text{W}/\text{m}^2,800\text{W}/\text{m}^2)$ by Psim .

4.4 Discussion

The inclusion of tracker with PV system increases the energy output approximately 20 to 40% when compared with the system without tracker depending on how we design MPPT. Controller controls the dc-to-dc converter and performs all control functions required for MPP Tracking

process. As mentioned before in chapter two, the MPP of a module varies with radiation and temperature as illustrated in Figure (4.18) and Figure (4.19).

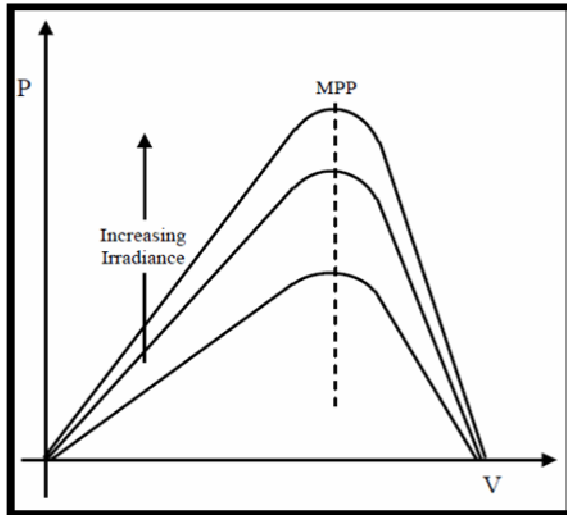


Figure (4.18): Variation of MPP with changing irradiance but temperature constant.

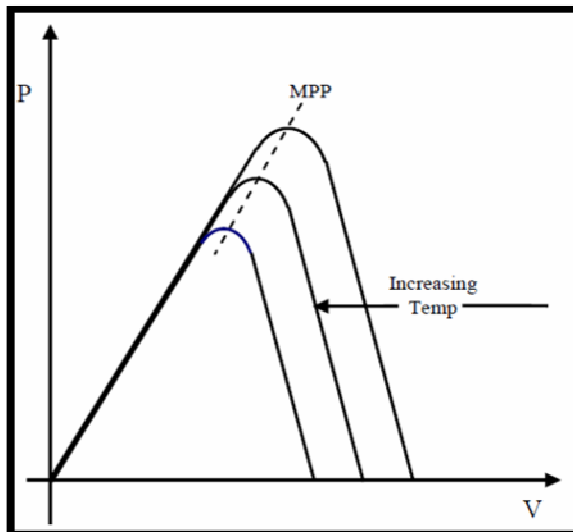


Figure (4.19): Variation of MPP with changing temperature but irradiance constant.

The variation of MPP position under changing conditions demands optimized algorithm, which in turn control the dc to- dc converter operation to increase the PV efficiency.

The Efficiency of maximum power point tracker is defined as

$$\eta_{\text{MPPT}} = \frac{\int_0^1 P_{\text{actual}}(t) dt}{P_{\text{max}}(t) dt} \quad (4.12)$$

Where P_{actual} refer to the actual power produced by the module with MPPT included where is P_{max} refer to the theoretical maximum power of the module.

The Open circuit voltage and short circuit current methods are simple and easy for implementation. However, it is very tedious to find the optimal value of k factor for the changing temperature and irradiance. These methods also suffer from low efficiencies, as it is very tedious to identify the exact MPP. Also, these methods fail to find MPP when partially shaded PV module or damaged cells are present [18]. The advantage of these methods is, response is quick as I_{SC} or V_{OC} are linearly proportional to the I_{MPP} or V_{MPP} respectively. Hence, they also give faster response for changing conditions. The P&O method is easy to implement as few parameters are to be measured and gives moderate efficiencies about 95%. However, the algorithm becomes complex when rapidly changing site conditions are present and the efficiency depends on how the method is optimized at design stage. The problems with this method are it gives arbitrary performance with oscillations around MPP particularly with rapidly changing conditions and provides slow response. Sometimes, this method is not reliable as it is difficult to judge whether the algorithm has located the MPP or not. The incremental conductance method offers high efficiencies about 98%. Even though, this method is complex and difficult

to implement, it has several advantages such as more accurate, highly efficient and operates at maximum power point. This method operates very soundly with rapidly changing atmospheric conditions as it automatically adjusts the module's operating voltage to track exact MPP with almost no oscillations. The drawbacks of this method are algorithm is complex, comparatively costlier as it requires microcontroller, and requires V and I sensors with associated peripherals [15].

Chapter Five

Voltage Source Inverters (VSI)

Chapter Five

Voltage Source Inverters (VSI)

5.1 Introduction

The purpose of DC-AC Switch Mode Inverters (Voltage source inverters (VSI)) is to produce a sinusoidal AC output from a DC input through PWM for use in the home, synchronizing with utility power whenever the electrical grid is distributing electricity. The inverter is able to control both the magnitude and the frequency of the AC output. It Converts DC power into standard AC power [6].

Inverters can be divided into three categories: PWM inverters, square wave inverters, single-phase inverters and six-step three-phase. In a PV system PWM inverters are most frequently utilized and their purpose is to keep the DC-link voltage at a constant voltage level by adjusting the DC link current.

5.2 DC/AC Inverter Analysis

In this section, inverter architectures, waveforms for single-phase inverter and six-step three-phase will be explained and analyzed for photovoltaic system. Detailed modulation strategies of the space vector modulation will be described for the three-phase inverter.

5.2.1 Single phase full bridge DC/AC inverter

In photovoltaic system, the DC/AC inverter is used to convert the power of the source by switching the DC input voltage (or current) in a pre-

determined sequence to generate AC voltage (or current) output. Figure (5.1) shows the equivalent circuit of single-phase inverter. This has four switches that turn on and off to obtain a sinusoidal output.

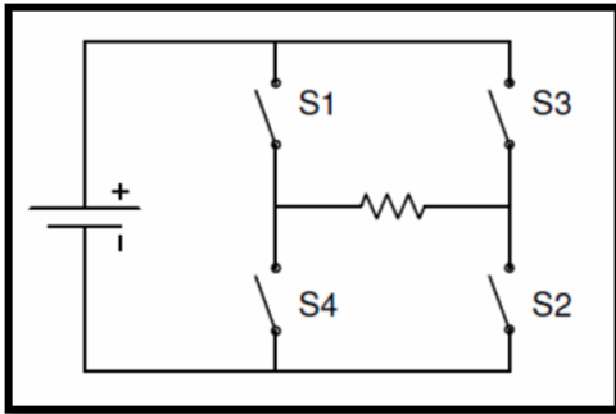


Figure (5.1): Equivalent circuit of the full bridge single-phase inverter.

The load of the inverter is a single-phase AC load or connected to single-phase grid power. The topology of the single-phase inverter is represented in figure (5.2). The single-phase inverter has four switches and four anti-parallel protective diodes. It provide path for the inductive current to flow when the switches are open and protect the switches from the large voltage by interrupting the inductive current.

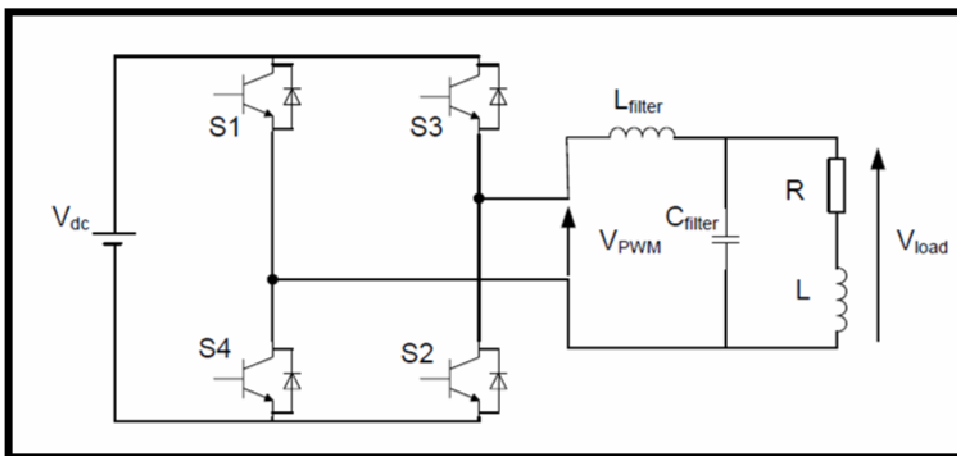


Figure (5.2): Topology of a single-phase inverter with filter and load.

To generate an AC waveform in single-phase inverter, the switches S1, S2 ON and S3, S4 off for period t_1 and t_2 as shown in figure (5.3). For that period, the output is a positive voltage.

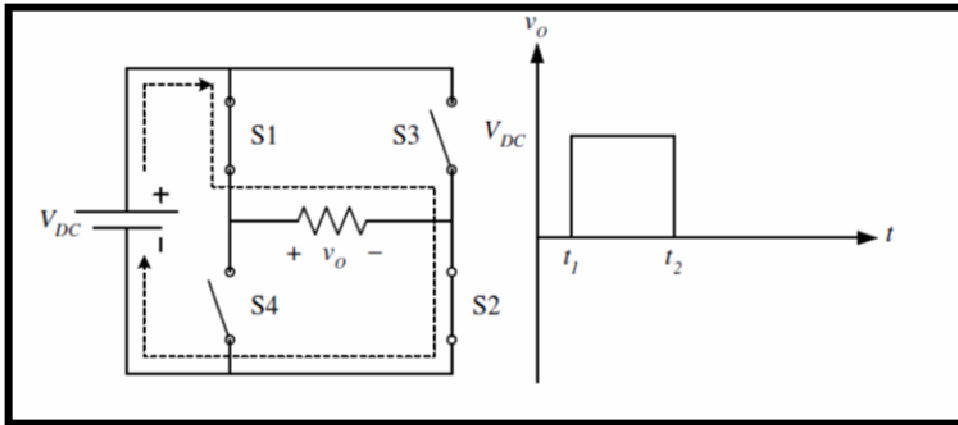


Figure (5.3): Output current for S1, S2 ON; S3, S4 OFF for $t_1 < t < t_2$.

For period t_2 to t_3 in figure (5.4), the switches S3, S4 are on and S1 and S2 are off to obtain negative voltage.

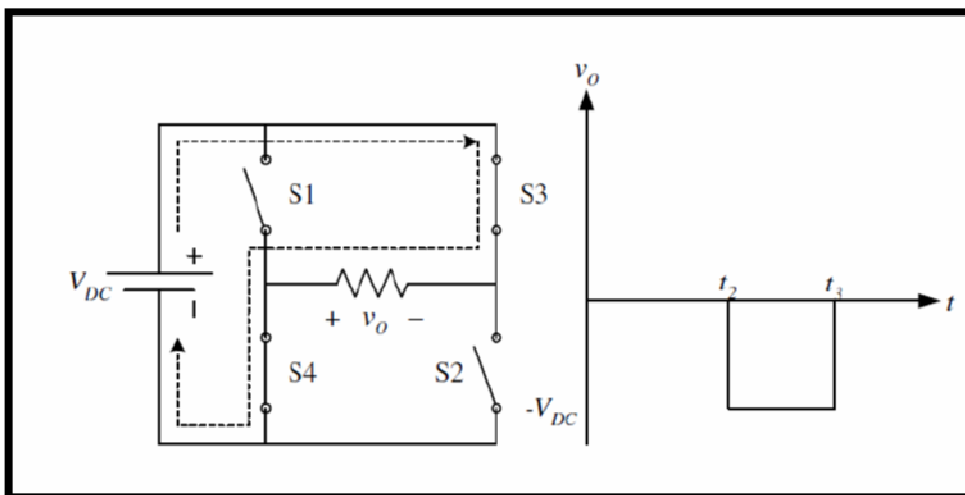


Figure (5.4): Output current for S3, S4 ON; S1, S2 OFF for $t_2 < t < t_3$ [6]

Switches S1 and S4 should not be closed simultaneously, the same for switches S3 and S2. Otherwise short circuit of the DC bus will occur.

By following the switching scheme, the inverter output voltage will alternate between positive and negative as figure (5.5), and the sinusoidal fundamental component is obtained as shown in figure (5.6).

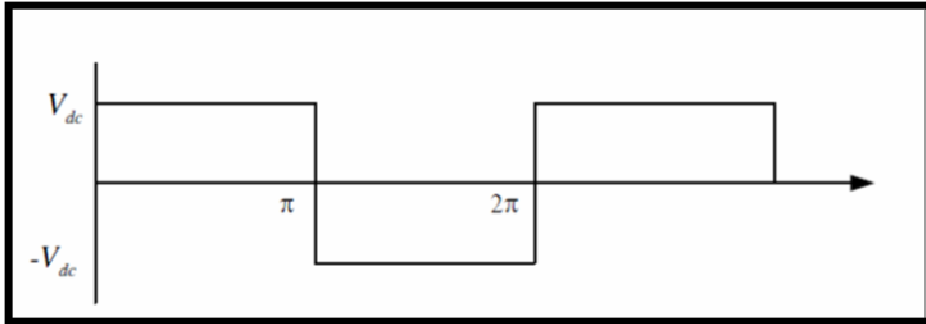


Figure (5.5): Single-phase output voltage.

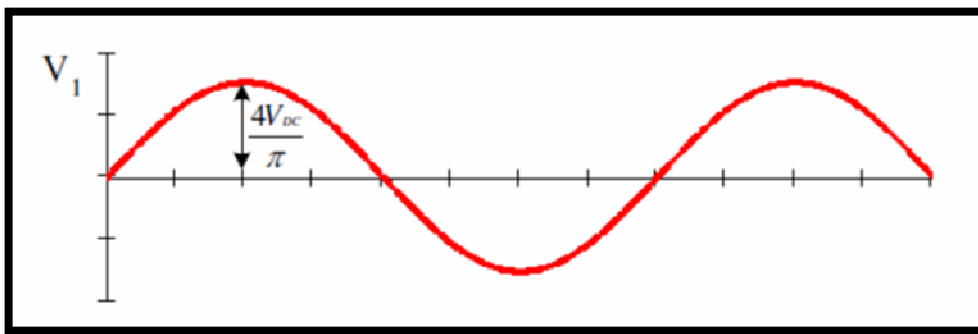


Figure (5.6): Fundamental component[19].

The load voltage is calculated by:

$$V_o = V_{DC} \text{ for period } 0 < \varphi < \pi \quad (5.1)$$

$$V_o = -V_{DC} \text{ for period } \pi < \varphi < 2\pi \quad (5.2)$$

The resulting output voltage has a fundamental alternating component and its time average is zero. The sharp transition in voltage indicates the presence of high frequency harmonics. The harmonics can be filtered with inductance and capacitor filters or controlled by implementing appropriate PWM techniques.

The instantaneous inductive load current is given in [6]

$$i_{\text{Load}}(\varphi) = \left\{ \begin{array}{l} \frac{V_{\text{DC}}}{R} - \frac{V_{\text{DC}}}{R} \left(1 + \tanh\left(\frac{\pi R}{2\omega L}\right) \right) e^{-\frac{\varphi R}{\omega L}}, \text{ for } 0 < \varphi < \pi \\ -\frac{V_{\text{DC}}}{R} + \frac{V_{\text{DC}}}{R} \left(1 + \tanh\left(\frac{\pi R}{2\omega L}\right) \right) e^{-\frac{(\varphi-\pi)R}{\omega L}}, \text{ for } \pi < \varphi < 2\pi \end{array} \right\} \quad (5.3)$$

Where R is the resistive load and L is the inductance. A blanking time is introduced in the switching cycle in order to evade a short circuit across the DC bus. The short circuit happens if S1 and S4 are on simultaneously closed due to the time delay associated with process of turning the switch OFF. The blanking time is realized by switching S1 and S3 or S4 and S2 OFF and hence the output voltage will be zero. The blanking time introduces low order harmonics to the voltage of the output, which is hard to filter out. Using the switching scheme with the blanking time, the output load voltage and current waveform is as shown in figure (5.7).

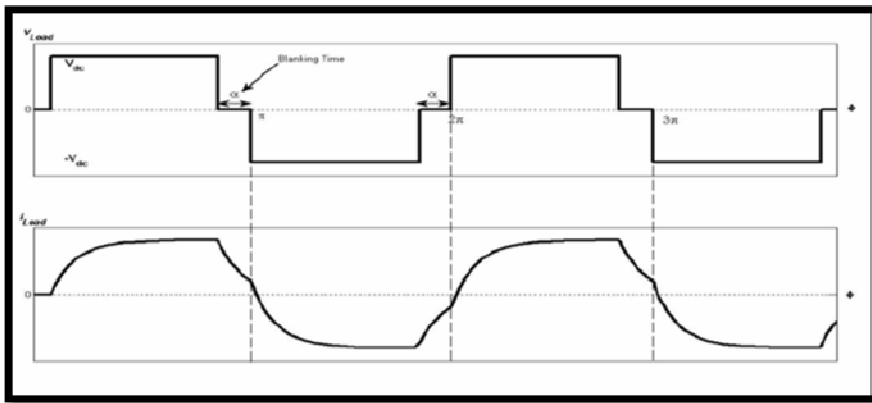


Figure (5.7): Output voltage and current with blanking time[19].

The magnitude of the n-th harmonic of the output voltage is given by Fourier analysis with .

$$V_n = 4V_{\text{DC}} \frac{\cos(n\alpha)}{n\pi} ; n = 1,2,3 \dots \quad (5.4)$$

Where α is the blanking time along with the scale of each harmonic rests on it. The blanking time is

$$\alpha = \frac{\pi}{2n} \quad (5.5)$$

The magnitude of the harmonic depends of the angle α . Figure (5.8) shows an example of voltage output harmonic spectrum when α is 10.

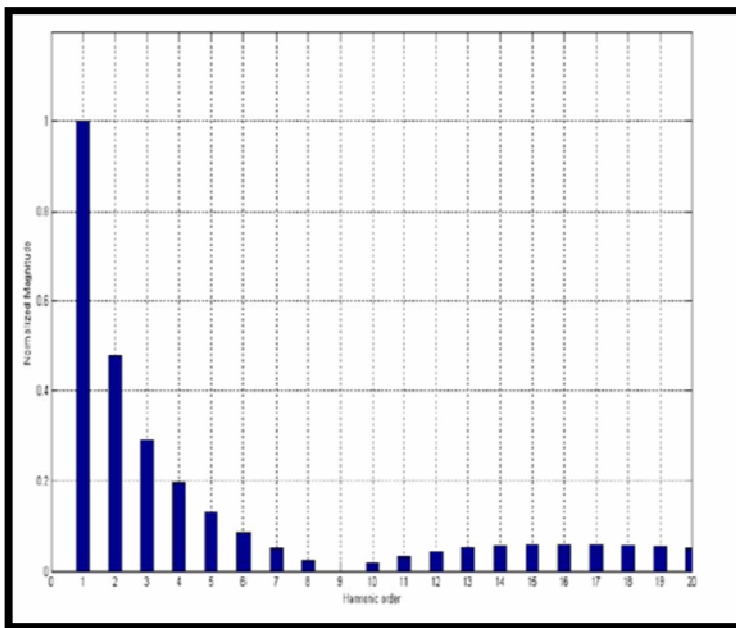


Figure (5.8): Harmonic of output voltage when α is a 10[20].

The PWM techniques provide control scheme to reduce harmonics. The technics can reduce the number of filter in high frequencies.

5.2.2 Six step inverter

The six-step inverter is used to obtain a three-phase voltage output from DC source. Three-phase voltage source inverter is a combination of three single-phase bridge circuits. A simplified diagram of a basic three-phase inverter bridge is shown in figure (5.9). There are diodes in

antiparallel in addition to the main power devices. These diodes are called the return current or feedback diodes. It provides an alternate path for the inductive current.

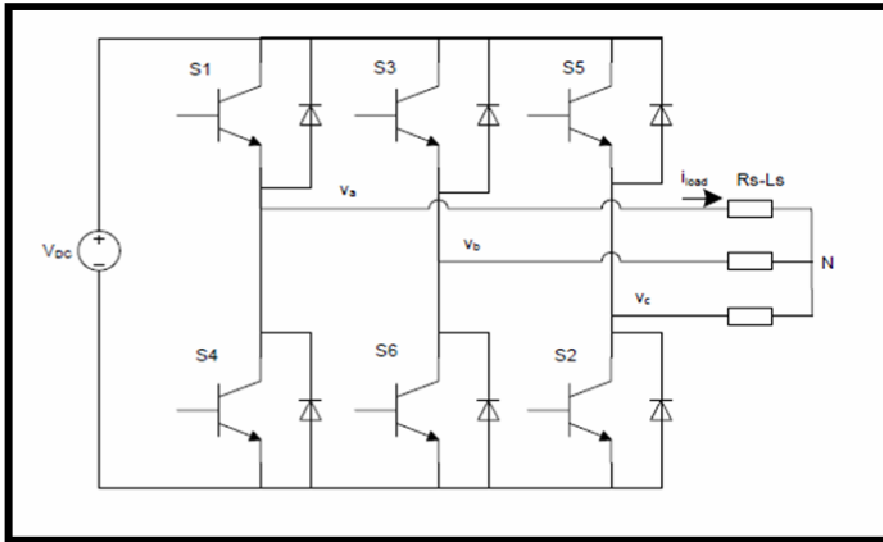


Figure (5.9): Three-phase six-step inverter.

To obtain the three-phase AC current in six-step inverter, six gating signals need to be applied to the six switches of the inverter. The waveforms of gating signals H1, H3 and H5 are shown in figure (5.10). H1, H3, H5 are 3 phase symmetrical switching function with phase shift 120° . To produce the symmetrical three phase voltages across a three phase load the devices are switched ON for 180° . The switching signals of each inverter leg are displaced by 120° with respect to the adjacent legs. The switching signals S1 and S4 are complimentary, the same for S3 and S6, S5 and S2.

The switching sequence will be $S_1S_2S_3$, $S_2S_3S_4$, $S_3S_4S_5$, $S_4S_5S_6$, $S_5S_6S_1$, $S_6S_1S_2$, $S_1S_2S_3$... for a positive sequence. The sequence will be reversed to get the negative phase sequence.

The line to neutral voltages V_{an} represented the six step of the inverter. V_{bn} and V_{cn} have the same waveform with phase shift 120° .

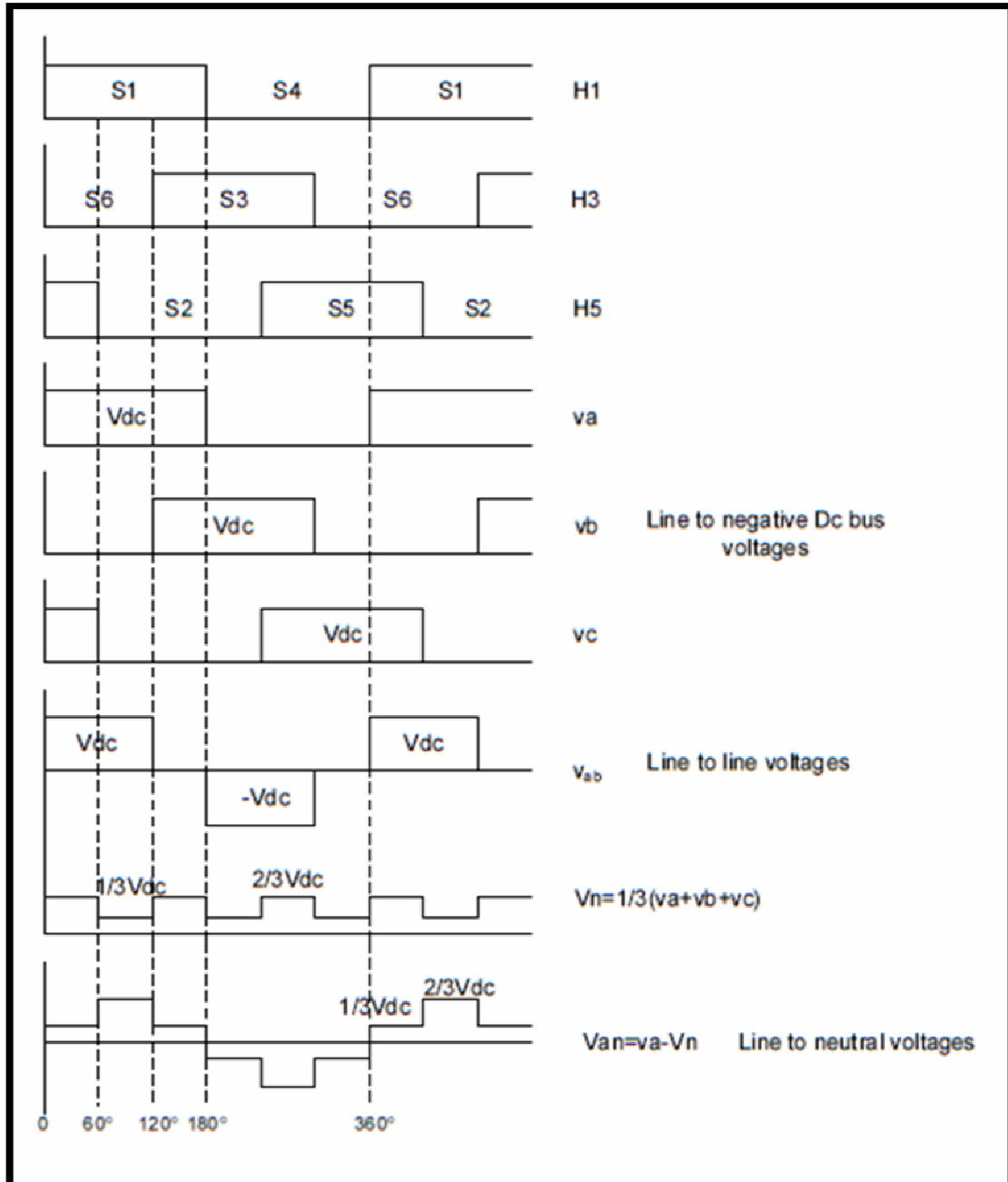


Figure (5.10): Waveforms of the switching functions.

Each switch is turned ON for 180° . The switches S_1 and S_4 , which belong to the leftmost inverter leg, produce the output voltage for phase A. The switching signals for the switches in the middle leg, S_3 and S_6 for

phase B, and are delayed by 120° from those for S_1 and S_4 respectively for a positive sequence. Similarly, for the same phase sequence, the switching signals for switches S_5 and S_2 are delayed from the switching signals for S_3 and S_6 by 120° .

It is called “six-step inverter” since there are six “steps” in the line to neutral (phase) voltage waveform as shown in figure (5.10).

For a six steps inverter, the outputs currents do not have harmonics of order three and multiples of three. Figure (5.11) represents the harmonics currents of the six steps inverter.

Control over output heft in a three-phase inverter could be attained by altering the voltage of the DC-link (V_{DC}):

$$(V_{an})_{1,peak} = 1.278 V_{DC}/2 \quad (5.6)$$

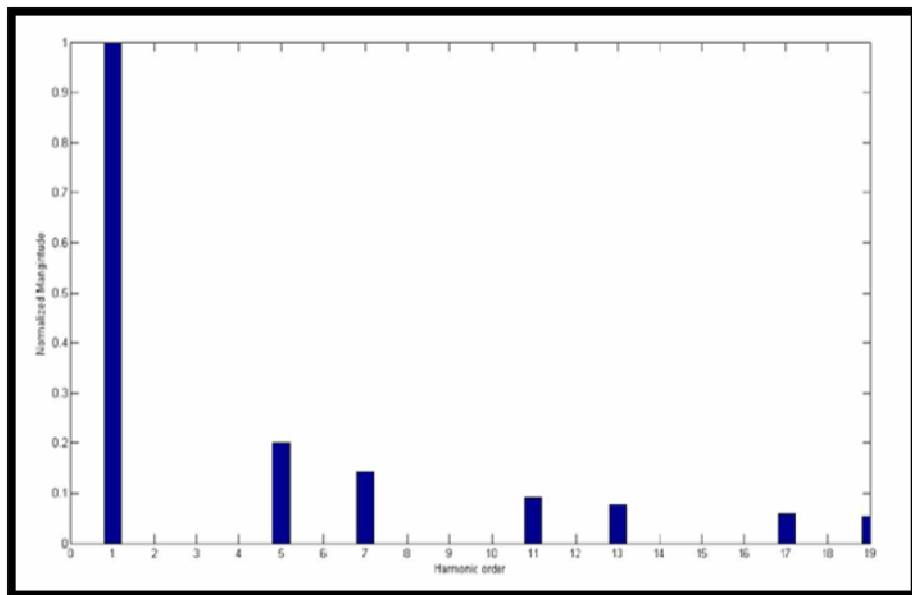


Figure (5.11): Phase voltage normalized spectrum [19].

In grid connected PV, the current output of the voltage source inverter will be injected to the grid. The output of the inverter should be in phase and have an identical frequency to the voltage of the grid[21].

5.3 Modulation Strategy

5.3.1 Sine PWM

In sine-triangle three-phase PWM inverter, three sinusoidal reference voltage waveforms at each phase are compared to the same triangular carrier. The three-reference voltages are 120° apart.

$$v_{a,ref} = V_{ref} \sin(2\pi f \times t) \quad (5.7)$$

$$v_{b,ref} = V_{ref} \sin(2\pi f \times t - 2\pi/3) \quad (5.8)$$

$$v_{c,ref} = V_{ref} \sin(2\pi f \times t + 2\pi/3) \quad (5.9)$$

With this method, switch S_1 is ON when triangular carrier is less than $v_{a,ref}$ and S_4 is OFF. The output voltage v_{a0} is equal to VDC. The same principles apply for the other legs of the converter. To summarize the principles:

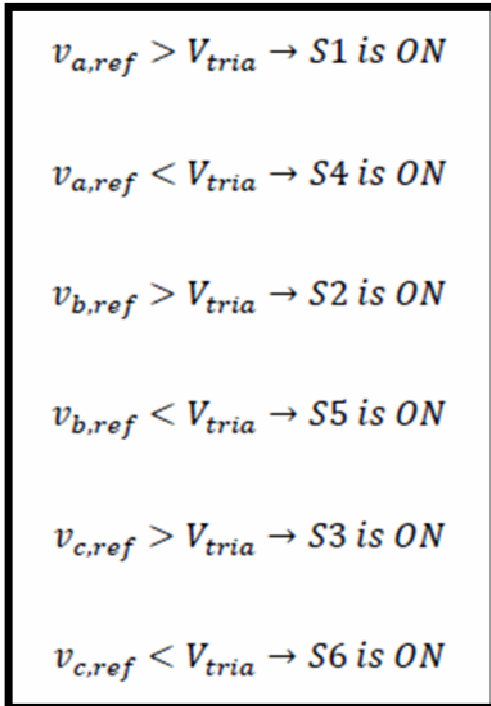


Figure (5.12): Shows the waveform of the sine triangle and the voltage reference comparison.

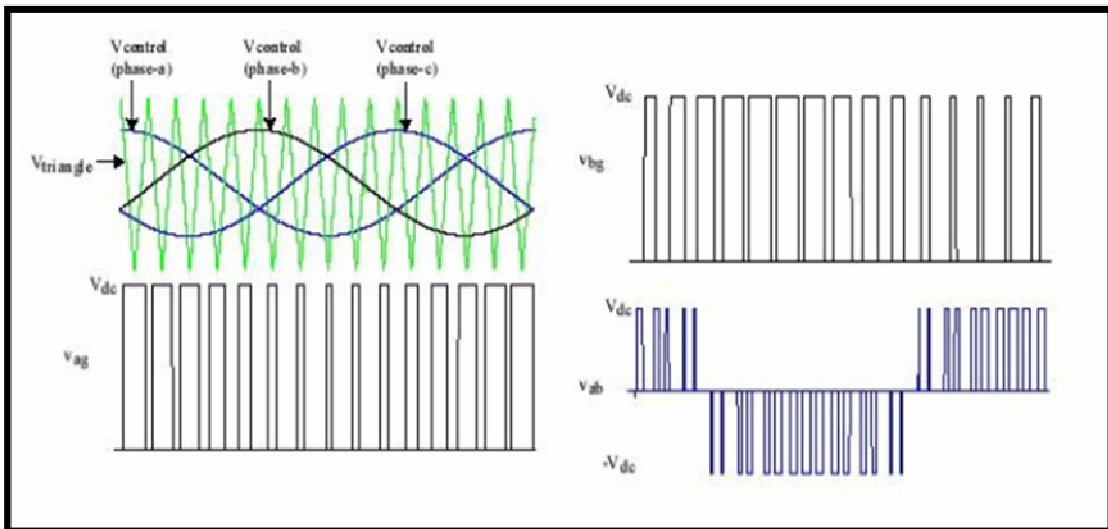


Figure (5.13): Sine triangle, voltage reference and phase voltage [20].

In sine triangle PWM, the amplitude modulation ratio (or index) m_a is defined by:

$$m_a = \frac{\text{peak amplitude of } V_{tria}}{\text{amplitude of } V_{ref}} \quad (5.10)$$

Where:

V_{tria} : the peak amplitude of the triangular carrier.

V_{ref} : the peak amplitude of the sinusoidal reference signal.

The frequency of the triangular waveform f_{pwm} is the frequency of the inverter. The frequency of the reference is the fundamental output frequency. For a grid connected PV, it is the frequency of the grid 50 Hz.

The ratio of those two frequencies gives the frequency modulation index:

$$m_f = \frac{\text{PWM frequency } f_{\text{pwm}}}{\text{fundamental frequency } f_1} \quad (5.11)$$

The line to neutral fundamental frequency output voltage of the inverter is defined by: [19]

$$U_{\text{an},1} = \frac{m_a V_{\text{DC}}}{2} \sin (2\pi f_0 . t) \quad (5.12)$$

$$U_{\text{bn},1} = \frac{m_a V_{\text{DC}}}{2} \sin (2\pi f_0 . t - \frac{2\pi}{3}) \quad (5.13)$$

$$U_{\text{cn},1} = \frac{m_a V_{\text{DC}}}{2} \sin (2\pi f_0 . t + \frac{2\pi}{3}) \quad (5.14)$$

Where: f_0 is the desired frequency.

The line-to-line voltage rms value at the fundamental frequency is obtained by multiplying the fundamental line to neutral fundamental frequency with $\sqrt{3}/\sqrt{2}$.

The switching frequency should be higher to reduce the harmonics at the output. Thus, less filter harmonics will be used. However, switching losses increase in proportion to the switching frequency.

In PV system, the DC voltage that is the output from the boost converter is the input for the inverter. A controller should be implemented in order to maintain the DC voltage in a constant manner. In addition, the voltage reference determines the output frequency and amplitude desired.

The function of inverter DC/AC is to generate AC output current i_{ac} in phase with the AC grid voltage v_{ac} . Switching frequency f_{PWM} is much greater than the AC line frequency (60Hz or 50Hz). By controlling the switch duty ratio D of the inverter, it is possible to generate a sinusoidal current i_{ac} in phase with the AC line voltage. The input DC voltage V_{DC} must be greater than the peak AC line voltage.

5.3.2 Simulation and validation the sine PWM by using Psim

In figure (5.14) is shown the inverter is composed of six switches S_1 through S_6 with each phase output connected to the middle of each “inverter leg”. Two switches in each phase are used to construct one leg. The AC output voltage from the inverter is obtained by controlling the semiconductor switches ON and OFF to generate the desired output. Pulse width modulation (PWM) techniques are widely used to perform this task. In the simplest form, three reference signals are compared to a high frequency carrier waveform. The result of that comparison in each leg is

used to turn the switches ON or OFF. It should be noted that the switches in each leg should be operated interchangeably, in order not to cause a short circuit of the DC supply. In figure (5.15) shown the waves of three phase voltage source inverter (VSI) simulation in Psim: I_{RL1a} , I_{RL1b} , I_{RL1c} , V_{car} , V_a .

Insulated Gate Bipolar Transistors (IGBTs) and power MOSFET devices can be used to implement the switches. Each device varies in its power ratings and switching speed. IGBTs are well suited for applications that require medium power and switching frequency.

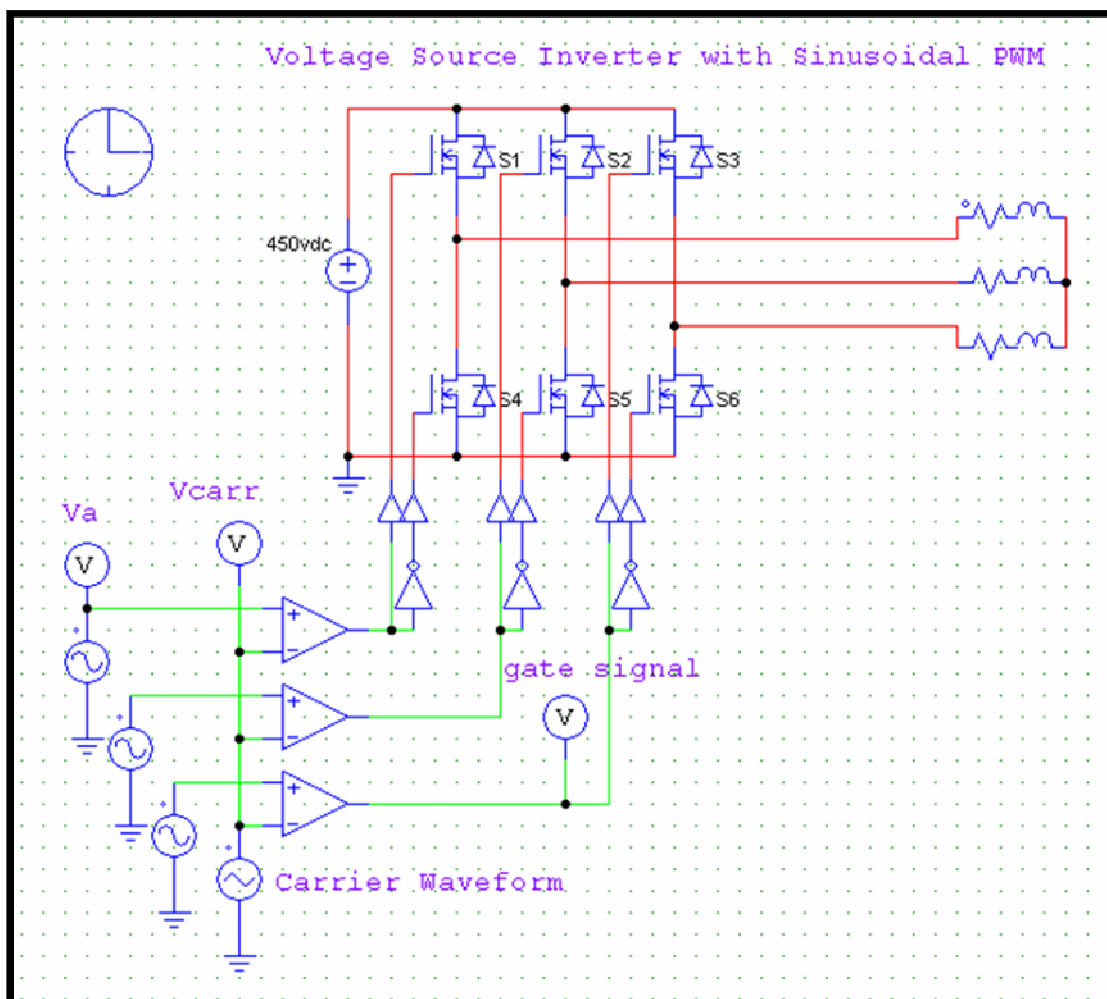


Figure (5.14): Three phase voltage source inverter (VSI) simulation in Psim.

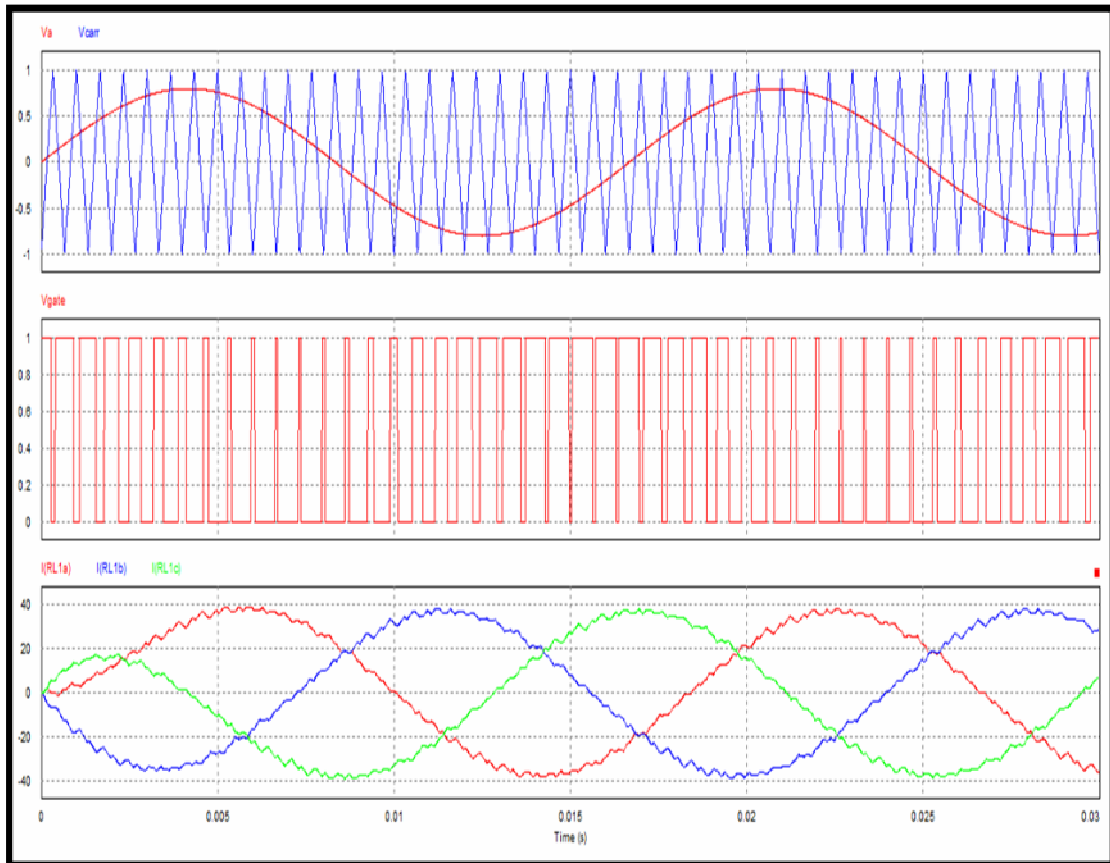


Figure (5.15): The waves of three phase voltage source inverter (VSI) simulation in Psim in figure(5.14) : I_{RL1a} , I_{RL1b} , I_{RL1c} , V_{car} , V_a , V_{gate} .

Chapter Six

Design of PV

System for Electrification

of a Household in Palestine

Chapter Six

Design of PV System for Electrification of a Household in Palestine

6.1 Introduction

Since the area of Palestine is relatively small and the solar radiation (W/m^2) doesn't change significantly within such short distance ($31^\circ 10' - 32^\circ 30' \text{ N}$), the measuring data for all regions (West-Bank & Gaza Strip) may considered to be the same. Table (6.1) shows the measurement of the global radiation on a horizontal surface in the Tulkarm[22]. They have been done by horizontally oriented measuring devices, and done on a 10-minute interval basis.

Table (6.1): Hourly average solar radiation of typical summer day (31/7/2012)[22].

Hours	Solar Radiation (W/m^2)	Hours	Solar Radiation (W/m^2)
1:00	0	13:00	875
2:00	0	14:00	822
3:00	0	15:00	712
4:00	0	16:00	559
5:00	0	17:00	376
6:00	16.5	18:00	199
7:00	113	19:00	43
8:00	288	20:00	0.25
9:00	502	21:00	0
10:00	669	22:00	0
11:00	788	23:00	0
12:00	850	24:00	0

From table (6.1) & figure (6.1), it is obvious that the solar radiation is more than $750 \text{ W}/\text{m}^2$ during the hours: 11, 12, 13 and 14, pm and it is also more than $135 \text{ W}/\text{m}^2$ in the morning hours 8, 9 and 10 am, and it also the

solar radiation is more than 300 W/m² in the evening hours 15, 16, 17, and 18 pm. This means that we have enough potential for solar radiation and we can obtain electric energy even in the morning or evening.

So it is very suitable for electricity generation from solar energy through PV systems. This encourages us to start to build proper centralized or decentralized PV-Systems to solve the main problem of Palestine in general (the lack of supply, and the peak demand of electricity). It is useful also to take a look at the advantages of PV system. It has high reliability, because source is free and abundant – the sunlight source. It needs little maintenance, because there are no moving parts. It has virtually no environmental impact, no air pollution, no noise, and no hazardous waste. It's produced domestically, no need for liquid or gaseous fuels to be transported or composted. Strengthening the national economy & reducing the trade deficit, by creating new jobs for relatively young, high tech industry. It is Modular & thus flexible, in terms of sizing and applications. It meets the demand and capacity challenges facing energy service providers, capability to produce the exact needed power and near the point of use. Figure (6.1) shows the daily irradiation-curve plotted from data of table (6.1).

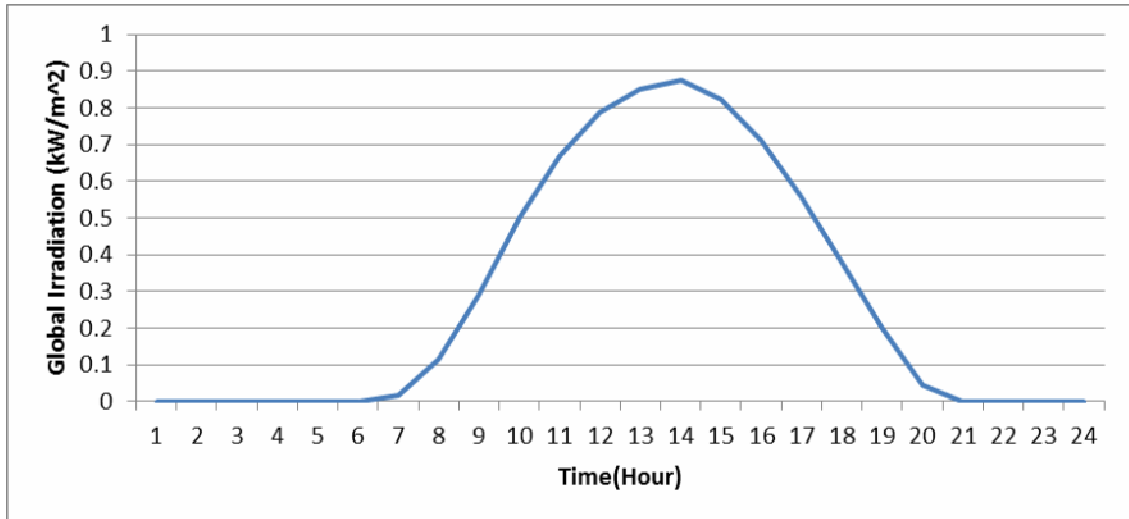


Figure (6.1): The global irradiation (kW/m²) versus time (hours)-2012[22].

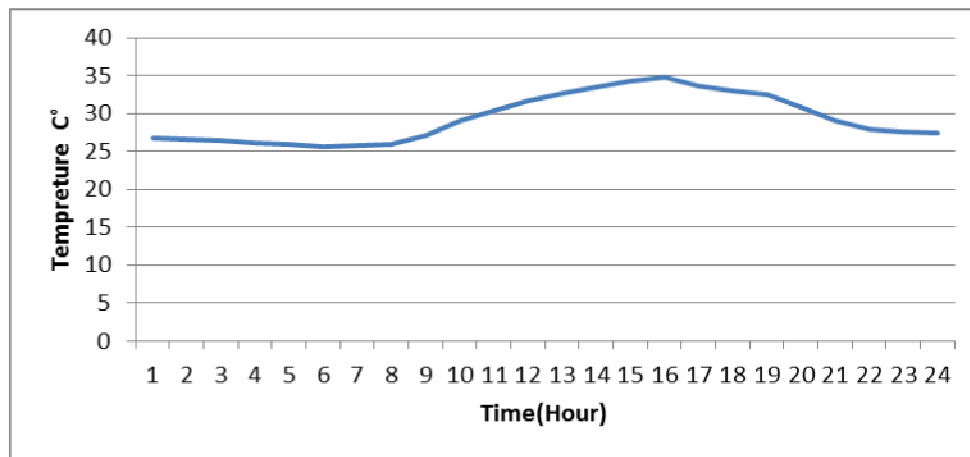
6.2 Ambient Temperature in Palestine

As we mentioned before, temperature affects the PV generators efficiency. The relation between temperature and efficiency is inversed. The ambient temperature is the main factor that affects the PV generator's temperature. Table (6.2) shows, for an example, the ambient temperature of the target area. The shown data is the average of one day measurement in July 2012. The original measurements are done on a 10-minute interval basis[22].

Table (6.2): Ambient temperature in Tulkarm[22].

Hours	Ambient temperature (C°)	Hours	Ambient temperature (C°)
1:00	27	13:00	33
2:00	27	14:00	33
3:00	26	15:00	34
4:00	26	16:00	35
5:00	26	17:00	34
6:00	26	18:00	33
7:00	26	19:00	33
8:00	26	20:00	31
9:00	27	21:00	29
10:00	29	22:00	28
11:00	30	23:00	28
12:00	32	24:00	27

Figure (6.2) shows the daily curve of the ambient temperature drawn from the data table (6.2). It shows that the maximum temperature occurs around noon time (32°C), and the minimum temperature occurs in the early morning (21°C).

**Figure (6.2): The daily ambient temperature curve-2012[22].**

6.2 Solar Energy in Palestine

Palestine has high potential of solar energy. It has around 3000 sunshine hours / year and high annual average solar energy radiation which is about 5.45 kWh / m² - day.

As shown in table (6.3), the lowest average solar energy is in December which is about 2.84 kWh/m² - day and the highest one is in June which is about 8.245 kWh/m² - day.

Table (6.3): Monthly solar energy on horizontal surface for Tubas District [23].

Month	kWh/m ² -day	Month	kWh/m ² -day
January	2.885	July	8.167
February	3.247	August	8.099
March	5.226	September	6.304
April	6.247	October	4.700
May	7.565	November	3.562
June	8.245	December	2.840

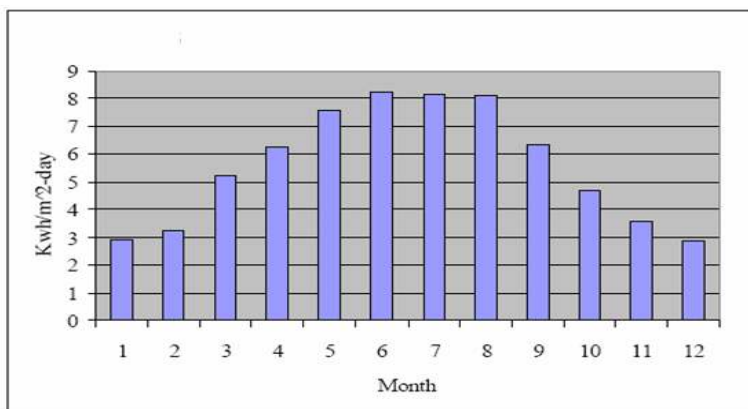


Figure (6.3): Monthly solar energy for Tubas district on horizontal surface.

6.3 Calculation Electricity Consumption

The fluctuation in the irradiation during the year requires stand-alone PV system with a storage system of enough energy capacity. The consumption has to be calculated in different irradiation durations such as in different seasons or in different months or at least between the extreme values of summer and winter when estimating the consumption.

The calculation of the solar energy is based on the average month of the year based on the location and global irradiation data. The radiation

calculation for different geographical latitude and inclination angles will be calculated in the following section. The first step in stand-alone system design should start by calculating the energy consumptions of all the appliances and other equipment and their power range should be listed in Table 6.4 For instance the list for individual power consumers will be as follow.

Table (6.4): The electrical load for typical household

Type of appliances				
	Number	Power (W)	Hour/day	Energy (Wh/day)
Compact Fluorescent Lamps	15	15×11	4	660
Computer with Accessories	1	125	4	500
Fridge	1	200	8	1600
TV and Recorder	1	125	6	750
Iron	1	1000	4/7	571
Washing machine	1	245	3/7	105
Total				4186 approximate d-to 4500Wh/ day/house

The daily load energy consumption for house is about **4.5kWh**.

The electrical loads in the house are small appliances such as TV, radio, small washing machine, lighting and refrigerator, as was noted in table (6.4).

6.4. The Average Daily of Solar Radiation Intensity

Palestine has a high solar energy potential, where the daily average solar radiation intensity is **5.4 kWh/m²**, and the peak sun hours (PSH) equal 5.4.

6.5 Installation of the PV System

To install the PV system, a poly-crystalline PV module type (Kyocera KC130GHT-2), is used in this system with the following specifications in table (6.5) and appendix (D.1)

Table (6.5): Specification of Kyocera KC130GHT-2 module at standard conditions

Electrical Data	
Maximum Power	130W
Maximum Power Voltage	17.6V
Maximum Power Current	7.39A
Open Circuit Voltage (Voc)	21.9V
Short Circuit Current(Isc)	8.02A
Area	0.9291m ²

6.5.1. PV generator sizing

The peak power (Wp) of the PV generator (PPV) is obtained from the following equation [24]:

$$P_{PV} = \frac{E_L}{\eta_V \eta_R PSH} S_f \quad (6.1)$$

where E_L (energy consumption per day) = 4.5 kWh ; PSH (the peak sun hours) = 5.4 ; η_R efficiency of charge regulator = 0.92 ; η_V efficiency of inverter = 0.9 ; S_f (the safety factor, for compensation of

resistive and PV-cell temperature losses = 1.15, Substituting these values in equation (6.1) to get the peak power (Wp) of the PV generator one obtains:

$$P_{PV} = \frac{4.5}{0.9 \times 0.92 \times 5.4} \times 1.15 = 1.15 \text{ kWp}$$

To obtain this peak value, we select to install multicrystalline-36 rectangular cells module type KC 130 GHT-2 of a 0.929 m² area, rated at 12 VDC , and P_{mpp} = 130W as shown in appendix(2). The number of necessary PV modules (No. PV) is obtained as:

$$No_{.PV} = \frac{P_{PV}}{P_{mpp}} \quad (6.2)$$

$$No_{.PV} = \frac{1150}{130} = 8.84 \text{ PV modules.}$$

We know all loads are operated by 220V AC loads and the input of the inverter will be 48V DC rather than 12V DC in order to reduce the PV array current output requirements, thus reducing wire size from array to inverter. Note that the same number of modules will still be required, since the same total power must be produced by the array. So we select the nominal voltage of the PV generator to be V_{nominal} 48 V, so number of modules in series is 4 module since each module is designed to charge a battery with 12 V nominal voltage

And

$$No_{.PV \text{ series}} = \frac{V_{pv}}{V_{mpp}} = \frac{8.84}{4} = 2.21 \approx 3 \text{ modules.}$$

We select 3 PV parallel strings constitution a generator of 12 modules with 1560W which increase the safety factor to be 1.56 and hence improving the system reliability.

The configuration will be as shown in Figure (6.1). The area of the array is $(0.9291)*(3)*(4) = 11.15 \text{ m}^2$

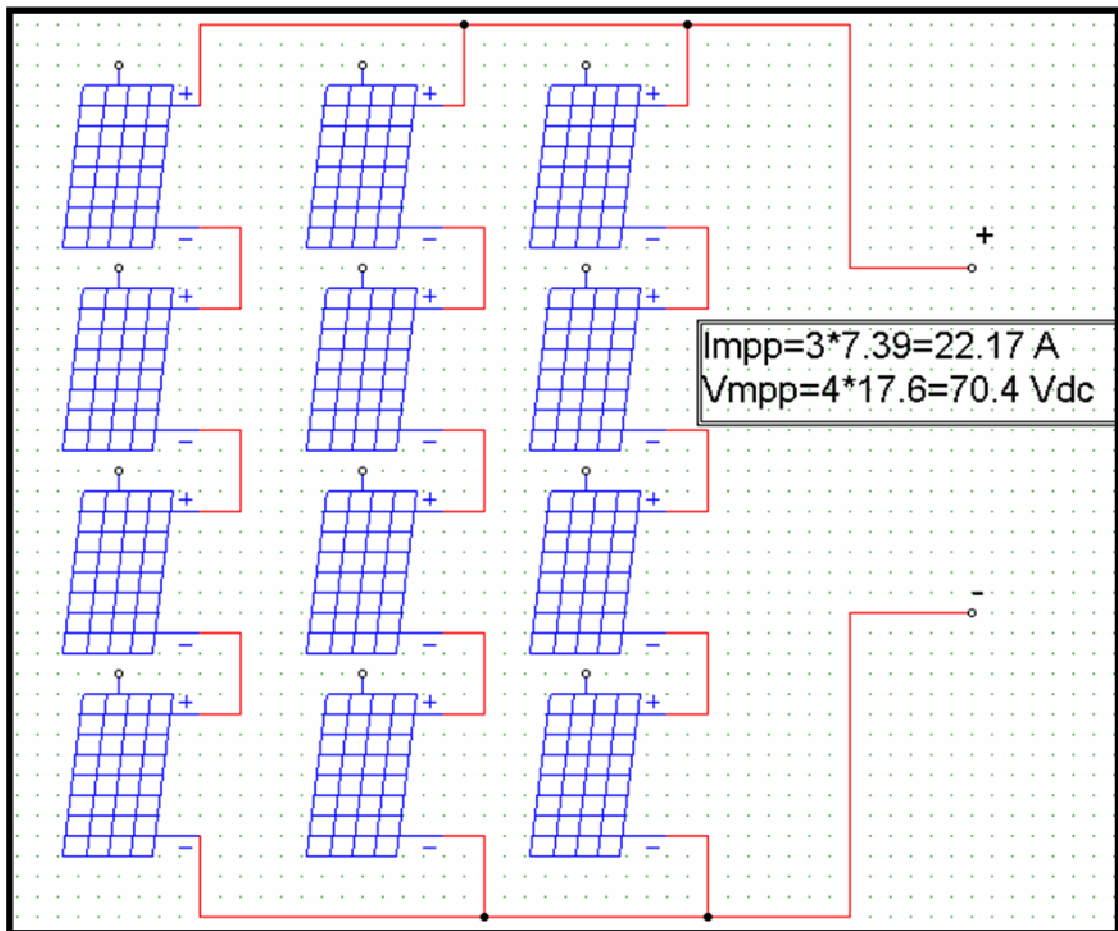


Figure (6.4): The configuration of PV generator for household.

For Palestine area, the optimum tilt angle of PV generator that captures the maximum amount of solar radiation over the whole year is 32° directed towards south .

6.5.2 Selection of the battery block

The storage capacity of battery block for such system is considerably large. Therefore, special lead-acid battery cells (block type) of long life time (> 10 years), high cycling stability rate (>1000 times), and capability of standing very deep discharge is selected.

The number of days of autonomy required for critical need applications depends on the location of the system. In locations with relatively high average insolation, even during the worst part of the year, less storage is needed. The number of days of autonomy required for household is 1.5 days.

The next choice is to determine the type of batteries to use and the allowable depth of discharge. In this design, deep discharge batteries allowing 80% discharge are not unreasonable, since under most conditions, the batteries will not discharge nearly this amount. Hence, the battery life will be relatively long. Battery size is thus determined from[13]:

$$C_{Ah} = \frac{1.5 \times E_L}{V_B \times DOD \times \eta_B \eta_V} \quad (6.3)$$

$$C_{wh} = C_{Ah} V_B \quad (6.4)$$

Where V_B and η_B are voltage and efficiency of battery block, while DOD is the permissible depth of discharge rate of a battery cell. Assuming realistic values of $\eta_B = 0.85$, $DOD = 0.75$ and $V_B = 48V$, by substituting these values in Equation (6-3) and Equation (6-4), then:

$$C_{Ah} = \frac{1.5 \times 4.5 \text{ kWh}}{48 \times 0.75 \times 0.85 \times 0.9} = 245.1 \text{ Ah.}$$

$$C_{wh} = 245.1 \times 48 = 11.7 \text{ kWh.}$$

Lead acid battery (block type) is typically designed to take 10 hours from zero charge to full charge. Hence, if 10 hours times the PV charging rate in amperes exceeds the battery capacity in Ah, it means the PV array is capable of fully charging the batteries in less than 10 hours[13]. Once the battery capacity is determined, the number of batteries required for the system is determined by dividing the total capacity require by the capacity of a single battery.

To install this capacity, we need 24 block batteries in series (each battery rated at 2 V / 250 Ah as shown in Figure (6.5) to build a battery block of an output rated at 48 V DC /250Ah.

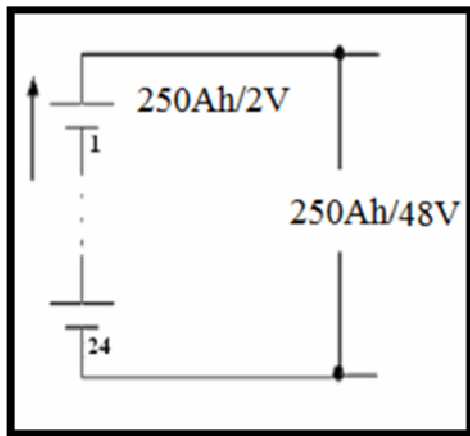


Figure (6.5): The configuration of battery blocks of the PV system for household.

6.5.3 Charge regulator (CR) sizing

It's a DC/DC converter, used to regulate the output current of PV generator going to the inverter, and to protect the battery block against deep

discharge and over charge, input/output rating of CR are fixed by the output of the PV array and V_B [24] .

The specifications of CR are:

❖ V input , must equal to the $V_{o.c} (PV) = (4*12) \sim (4*21.9)$

$$= (42 \sim 88) \text{ V DC.}$$

❖ V output , must equal to nominal (PV) $V = (48*1) \sim (48*1.2)$

$$= (48 \sim 57.6) \text{ V DC.}$$

❖ The appropriate rated power of CR, must be equal to $P_{PV} = 1.56\text{kW} \approx 2$ kW. It's recommended that the CR should have a maximum power control unit.

❖ The efficiency must be not less of 92 %.

❖ Controller sizing = Module short circuit x modules in parallel x 1.25(factor of safety).

$$= 8.02\text{A} \times 3 \times 1.25 = 30.1 \text{ A}$$

❖ 30A – 48V charge regulator have been selected for household.

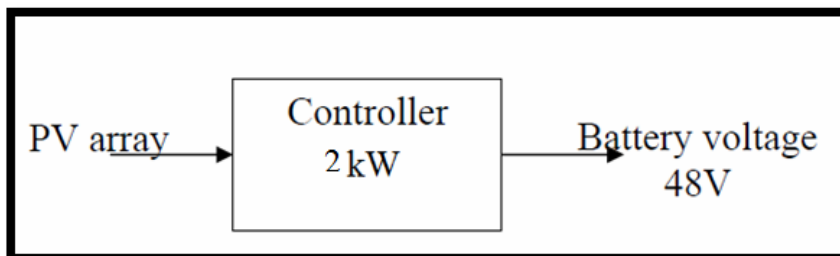


Figure (6.6): Charge controller specifications.

Figure (6.6) is shown the specifications of the Charge controller.

6.5.4. Inverter sizing

The inverter has to be capable of handling the maximum expected power of AC loads. The input of the inverter have to be matched with the battery block voltage which is 48V while its output should fulfill the specifications of the electric grid of the grid which is 220V, 1 Φ .Figure (6.7) shows the specifications of the inverter .

In order to size the inverter suitable to PV system the main parameters should be determined from:

- ❖ V_{input} should be located in the inverter MPPT voltage range (42~57.6V DC) and $V_{rated} = 52.5VDC$.
- ❖ V_{output} should fulfill the specification of the electric grid of the household specified as: $V_{rated} = 220V \pm 5\%$ AC, three phase 50 Hz, sinusoidal wave voltage.
- ❖ Power of inverter's size nominal power to be greater than total power of appliances that may run at the same time is given by the following formula:

$$P = (10 \times 11 + 125 + 200 + 1000) = 1435 \text{ W}$$

And the appliances with large surge currents that include motors are $245 \times 3 = 735 \text{ W}$. To allow the system growth, we add 25% of the previous two values to get total power

$$P_{Total} = (\text{power of appliances running simultaneously} + \text{power$$

of large surge current appliances) $\times 1.25$

$$P_{\text{Total}} = (1435 + 735) \times 1.25$$

$$= 2712 \text{ W}$$

- ❖ The maximum inverter output current is found by dividing the total load power by the system voltage:

$$\text{Inverter to load current} = 3 \text{ kW} / 220\text{V} = 13.6\text{A.}$$

- ❖ The efficiency = 95% - 97%.

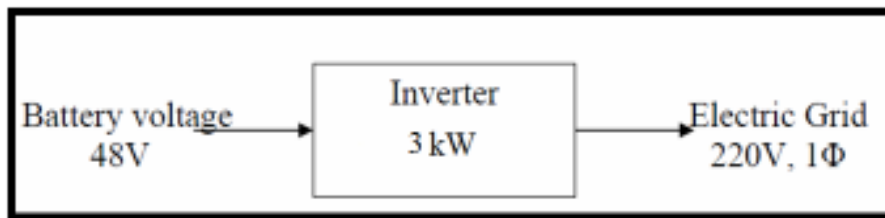


Figure (6.7): Inverter specifications.

Figure (6.7) shows the specifications of the inverter.

6.6 Types of Solar PV Systems

PV systems can be classified into two categories; stand-alone systems and grid-connected systems.

6.6.1 Stand-alone PV

A stand-alone PV system is shown in Figure (6.8) with all necessary components such as PV panels, DC-AC inverter, DC-DC converters, MPPT controller and battery.

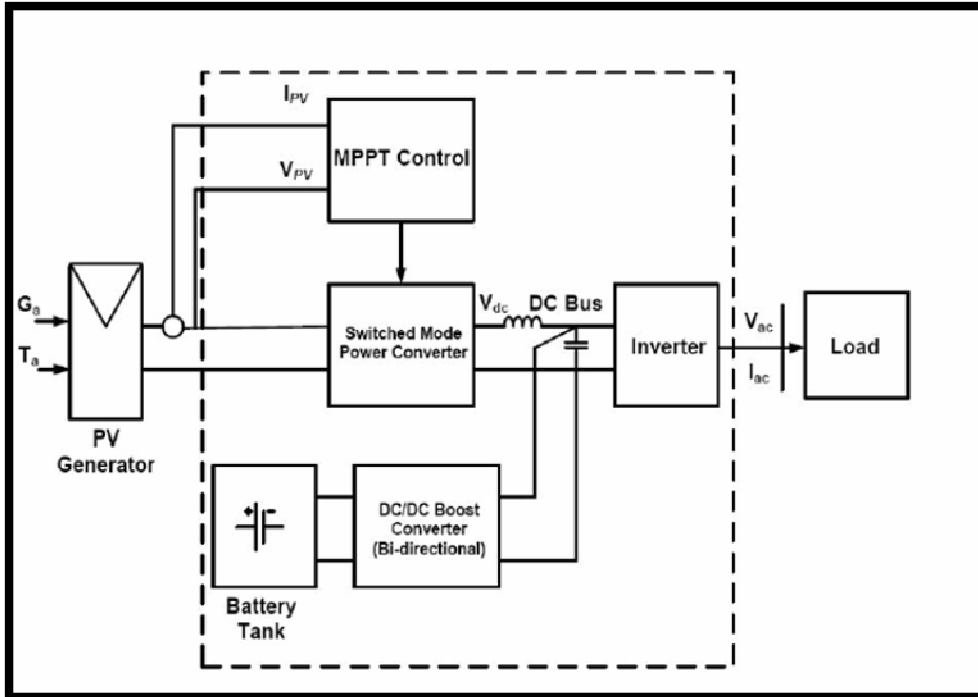


Figure (6.8): Stand - alone PV operation [25].

Where, G_a is irradiation and T_a is the ambient temperature.

The PV panels are connected in series and parallel combinations to achieve the desired power capacity. DC-AC inverter is used to convert DC input from the PV generator to AC output at certain voltage level and frequency to be used for consumers. By the use of the battery, the excess power generated by the PV system is stored to be used when required. The DC-DC bidirectional converter is boosting the voltage level from the battery side to the higher level of inverter input side or it lowers the voltage from the inverter side to battery input side in order to be able to charge the battery in an appropriate voltage level. The MPPT controller is used to get the maximum power from the PV generator during the operation[26].

6.6.2 Grid tie inverter

A grid-tie inverter (GTI) is a special type of inverter that converts direct current (DC) electricity into alternating current (AC) electricity and feeds it into an existing electrical grid. GTIs are often used to convert direct current produced by many renewable energy sources, such as solar panels or wind turbines, into the alternating current used to power homes and businesses. The technical name for a grid-tie inverter is "grid-interactive inverter". Grid-interactive inverters typically cannot be used in standalone applications where utility power is not available[27].

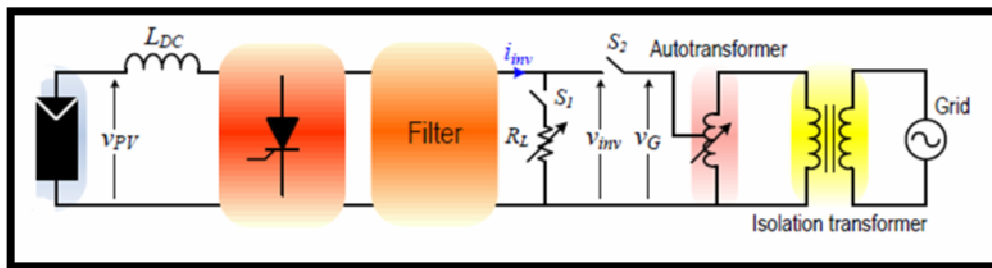


Figure (6.9): Grid tie inverter[28].

The connection between the solar array and the utility grid is a bit more complex than that. The following are the required components for a grid-connected solar PV system[29]:

- ❖ Solar panels
- ❖ Inverter
- ❖ DC disconnect
- ❖ AC breaker panel

- ❖ Utility disconnect
- ❖ Electrical wiring in your home

Inverters take DC power and invert it to AC power so it can be fed into the electric utility company grid. The grid tie inverter must synchronize its frequency with that of the grid (e.g. 50 or 60 Hz) using a local oscillator and limit the voltage to no higher than the grid voltage.

A high-quality modern GTI has a fixed unity power factor, which means its output voltage and current are perfectly lined up, and its phase angle is within 1 degree of the AC power grid. The inverter has an on-board computer which will sense the current AC grid waveform, and output a voltage to correspond with the grid[27].

Grid-tie inverters are also designed to quickly disconnect from the grid if the utility grid goes down to prevent the energy produced from harming any line workers who are sent to fix the power grid [27].

Properly configured, a grid tie inverter enables a home owner to use an alternative power generation system like solar or wind power without extensive rewiring and without batteries. If the alternative power being produced is insufficient, the deficit will be sourced from the electricity grid[27].

Chapter Seven

**Economic Analysis of the
Standalone and Grid Tie PV
system**

Chapter Seven

Economic Analysis of the Standalone and Grid Tie PV system

7.1 Economic study of the Standalone PV Systems

This section shows the calculation of the cost of generated energy by Standalone and Grid Tie PV Systems and the economical comparison between them.

7.1.1 Determining the cost of producing one kWh from Standalone PV System

The economic analysis used in this work is based on the use of life cycle cost, cost annuity (NIS/kWh).

- **Life cycle cost (LCC)**

The life cycle cost (LCC) is defined as the sum of the PWs of all system components. It may contain elements pertaining to original purchase price, maintenance costs, operation costs, and salvage values.

A) Initial cost of standalone PV system

The initial cost includes the costs of equipment represented in PV-panels, inverter, charge regulator, batteries, wires and other components used in installation. It includes also labor and technicians costs for installation. These costs depend on the size and type of a component. All these costs are summed to give the overall initial cost.

$$\text{Initial cost} = \square (\text{components cost} + \text{installation cost}) \quad (7.1)$$

- **Initial cost of photovoltaic modules**

PV-modules are available in different sizes and types, the size of PV is characterized by their peak watt at STC (rated power). The price of peak watt is almost the same for mono or poly crystalline, but the installation or Structure cost will differ depending on the installed PV area. The (NIS/W_p) will decrease as the size of module increases.

- **Initial cost of standalone PV inverter, charge controller and batteries**

Inverter, charge controller and batteries available in different sizes and types. The price of these components depends on their capacities, efficiencies, protection features and types.

- **Other initial costs**

Shipping costs and accessories needed for installation and system protection, wiring, rooms, should be also considered. These costs depend on the system size and vary with the kind of the project; if it is for public use (may be land available free), or for private use.

B) Operation and maintenance cost of standalone PV system

The operation costs considered are incurred after installation in order to run the system for a certain number of years (system life time).

C) Salvage value

The salvage value is considered as the value of the project components after the system life time is finished.

Figure (7.1) shows the cash flow which represents the initial, maintenance cost and salvages revenue.

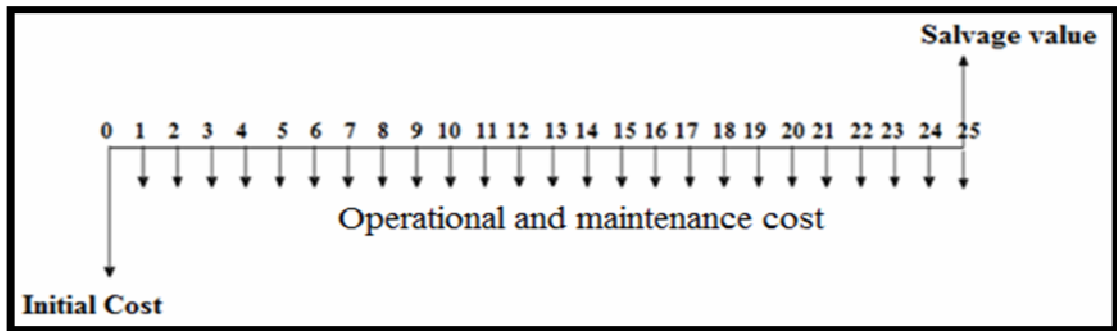


Figure (7.1): The cash flow which represent initial, operational cost and salvage value.

7.1.2 Economic factors

In order to calculate the equivalent uniform annual series (A_w) of cash flow in figure (7.1), the most important fact to remember is to first convert everything to its present worth.

The life cycle cost of grid tie system = initial cost of PV system + present worth of maintenance and operation – present worth of salvage value.

The life cycle cost of grid tie system = initial cost of PV system + Operation and maintenance $\times (P/A, i, n)$ – salvage value $\times (P/F, i, n)$.

The term $A (P/A,i,n)$ is called the uniform-series present worth factor.

This expression determines the present worth P of an equivalent uniform annual series A , which begins at the end of year 1 and extends for n years at an interest rate i , and (P/A) can be found by equation (7.2):

$$P = A \left[\frac{(1+i)^n - 1}{i(1+i)^n} \right] \quad i \neq 0 \quad (7.2)$$

The term $F (P/F,i,n)$ is known as the single-payment present-worth factor, or the P/F factor. This expression determines the present worth P of a given future amount F after n years at interest rate i , and (P/F) can be found by equation (7.3):

$$P = F \left[\frac{1}{(1+i)^n} \right] \quad (7.3)$$

In order to simplify the routine engineering economy calculations involving the factors, tables of factors values have been prepared for interest rates from 0.25 to 50% and time period from 1 to large n values, depending on the interest value 10% and interest table in appendix (F).

The equivalent annual worth AW is obtained with appropriate A/P , as follows: $AW = PW (A / P i , n)$

Then the energy unit price is calculated from equation (7.4)

$$(\text{NIS/kWh}) = \frac{Aw}{\text{Total yearly kWh produced}} \quad (7.4)$$

7.1.3 Cost of producing one kWh from standalone PV system for a house

The price of the PV system and its installation are important factors in the economics of standalone PV systems. These include the prices of PV modules, inverter, charge regulator, batteries and all other auxiliaries as shown in table (7.1). The cost of installation must be taken into consideration. The technical specification was determined in chapter six for a household load. The company specifications and datasheets are in Appendix D.

Table (7.1): Cost of elements and installation of standalone PV system.

Component material or work	Quantity	Price (NIS)	Specifications Design
PV – module	12	16800	1.56 KW _P for a PV array
Inverter	1	5500	Input:48V Output:220VAC, 50 Hz
Charge Regulator	1	1500	Nominal battery voltage: (12-72) V
Battery	24	30000	48V / 250Ah
Installation		1000	

Before starting calculations one should consider the following:

- 1- The energy consumption for a house hold is 4.5kWh/day (as mentioned in chapter six).
- 2-The lifecycle of the system components will be considered as 25 years.
- 3- The interest rate is about 10%.

The initial cost of the PV system = PV array cost + inverter cost + charge regulator cost + battery cost + installation cost.

$$\begin{aligned} \text{The initial cost of the PV system} &= 16800 + 5500 + 1500 + 30000 \\ &+ 1000 \\ &= \underline{\underline{54800\text{NIS}}}. \end{aligned}$$

The annual maintenance and operation costs are about 2% of initial cost which is equal to 44NIS/year, salvage value after 25 years is taken 15% from initial cost and it is equal to 8220 NIS.

The life cycle cost of standalone PV system is obtained by drawing cash flow as in figure (7.2):

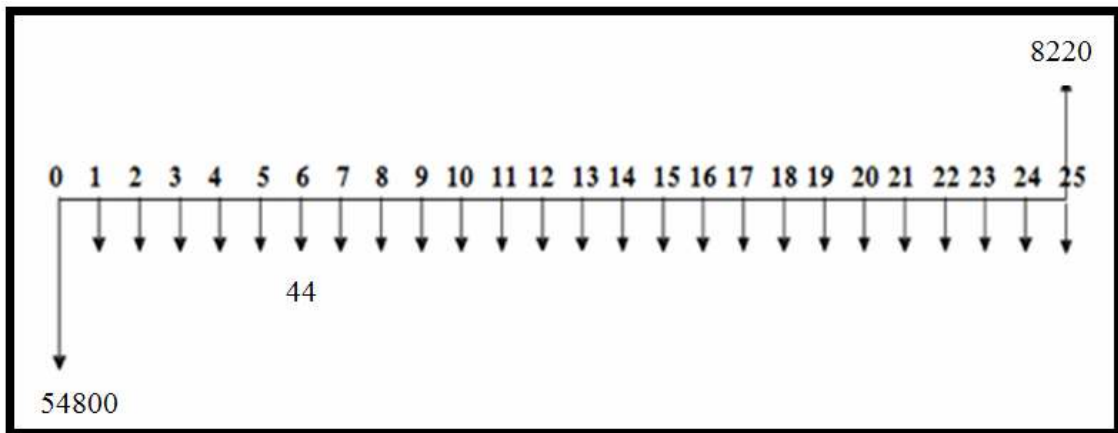


Figure (7.2): Cash flow of standalone PV system for a house.

The life cycle cost of PV system = $54800 + 44 (P/A, i, n) - 8220(P/F, i, n)$.

$$PW = 54800 + 44 (P / A 10\%, 25) - 8220(P / F 10\%, 25).$$

The factors in the above equation are taken from appendix (F):

$$PW = 54800 + 44 \times 9.0770 - 8220 \times 0.0923 = \underline{\underline{54441\text{NIS}}}.$$

$$AW = PW (A/P i, n) = 54441 (A/P 10\%, 25).$$

From appendix (F), the term (A/P 10%, 25) is equal to 0.11017, then:

$$AW = 54441 (A / P 10\%, 25).$$

$$AW = 54441 \times 0.11017 = \underline{\underline{5998\text{NIS}}}.$$

Energy produced from the standalone PV system yearly = PV model power output \times PSH \times $_{INV}$ \times $_{C.R}$ \times $_{BAT}$ \times 365(day).

$$\text{Energy produced from the standalone PV system yearly} = 1.56\text{kW} \times 5.4 \times 0.9 \times 0.92 \times 0.85 \times 365 = \underline{\underline{2947.1 \text{ kWh}}}.$$

$$\begin{aligned} \text{The cost of 1 kWh from the PV generator} &= 5998\text{NIS}/2947.1 \\ \text{kWh} &= \underline{\underline{2.1 \text{ NIS/kWh}}}. \end{aligned}$$

7.2 Grid Tie System Tariffs

Electricity delivered to the grid can be compensated in several ways such as net metering or feed-in tariff.

7.2.1 Net metering tariff

A solar PV system generates electricity by converting sunlight into electricity that can be used in your home or business. This reduces the amount of electricity you need to purchase from your utility. If your system produces more electricity than you need at any given time, it will actually spin your meter backwards to supply the grid. Your utility keeps track of

how much electricity you supply to the grid as well as how much you purchase, and bills you only for your net electricity consumption (via net metering). At the end of any billing period, if overall electricity production exceeds consumption (indicated by a negative meter read), a billing credit is applied to your next bill[27]. Figure (7.3) shows grid tie net metering tariff.

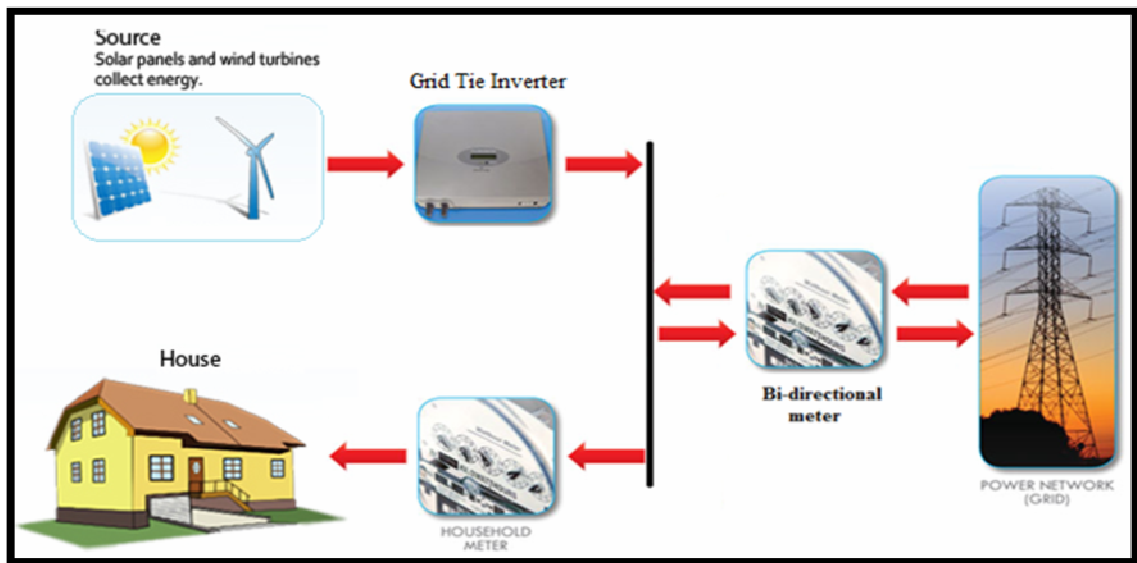


Figure (7.3): Grid tie net metering tariff.

7.2.2 Feed in tariff

A feed-in tariff (FIT) encourages a new renewable energy development by creating a long-term financial incentive to customers who generate renewable electricity, offering a standardized and streamlined process, and easing the entry for new systems. Under a feed-in tariff, a utility is contractually obligated to connect the renewable energy generator to the grid and pay that generator for electricity at a fixed rate for the life of the FIT contract, typically 10-20 years. The goal of a FIT is to create a robust market for renewable energy to lower technology costs and increase

development of such resources for the duration of the program, and potentially pave the way for future growth. The design of FITs can vary considerably in how rates are calculated, eligibility of different technologies and resource sizes, and the contract terms[27]. Figure (7.4) shows grid tie feed in tariff.

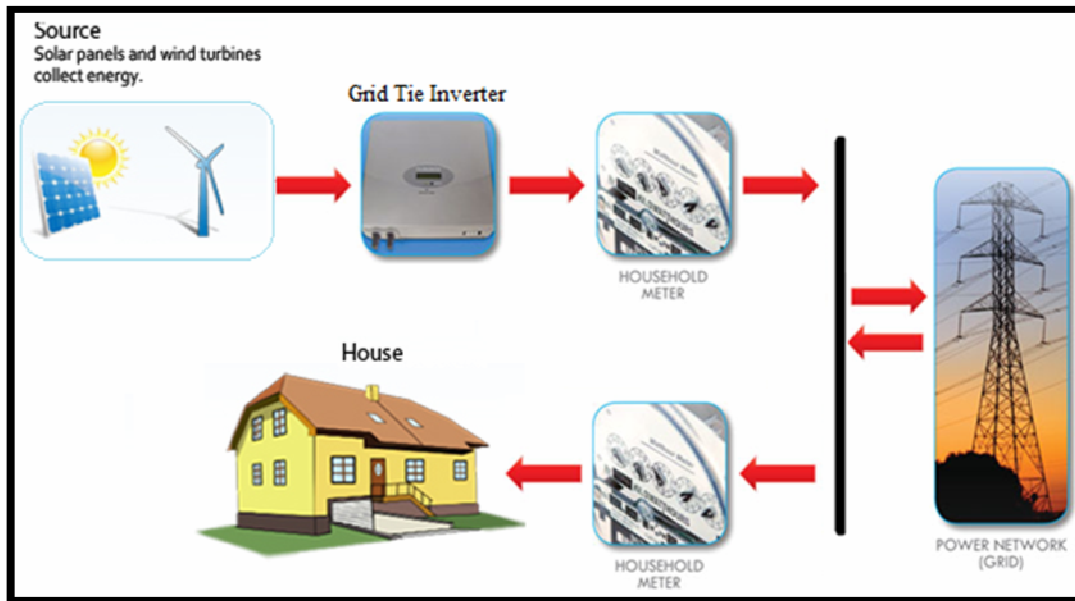


Figure (7.4): Grid tie feed in tariff.

7.2.3 Evaluation the economic impact of a house grid tie feed in tariff PV system

The Palestinian Energy and Natural Resources Authority (PENRA) started this year to implement the one thousand home projects which is based on the production of electricity from solar cells mounted on rooftops, to exploitation the solar energy in Palestine. PENRA encourage citizens to participate in this project by contributing in 30% from the total PV modules price. They will install 1.56 kW_p for one home after which implementing an audit to know if there is a feasibility of installing PV modules or not.

PENRA will determine a feed in tariff for 1kWh production from the house at motivational price equal to 1.07 NIS.

For that we will perform an economic study to know if this is project feasible or not returns for the citizens.

For 1.56kW_p we need 12 PV modules and don't need battery and charge regulator.

The initial cost of the PV system = PV array cost + inverter cost + installation cost.

The initial cost of the PV system = $(12 \times 1400 \times 70\%) + 5500 + 1000$

$$= \underline{\underline{18260\text{NIS.}}}$$

The annual maintenance and operation costs = $(2\% \times 18260) / 25$

$$= \underline{\underline{15\text{ NIS.}}}$$

Salvage value after 25 years = $15\% \times 44720\text{ NIS} = \underline{\underline{2739\text{ NIS.}}}$

The life cycle cost of grid tie PV system is obtained by drawing cash flow as in figure (7.5):

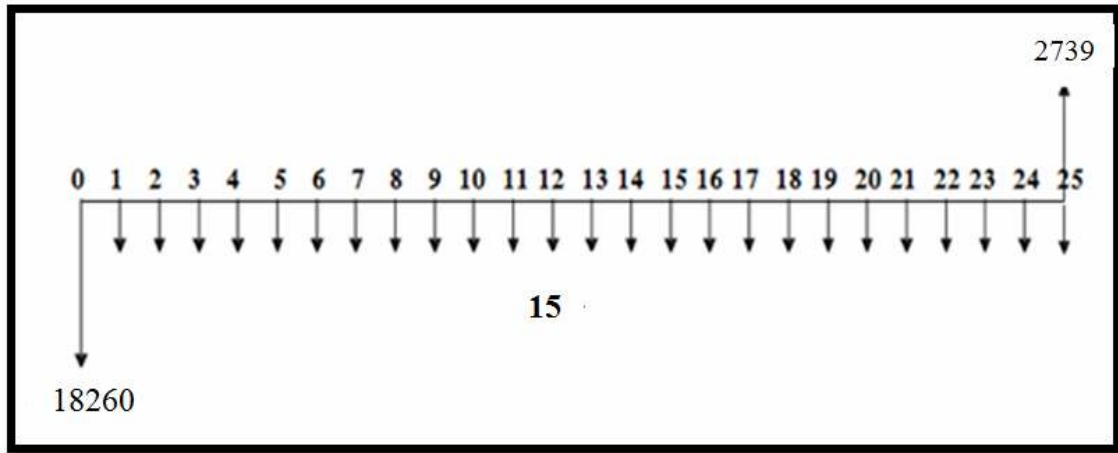


Figure (7.5): Cash flow of grid tie PV system for a house.

The life cycle cost of PV system = $18260 + 15 (P/A 10\%, 25) - 2739(P / F 10\%, 25) = \underline{\underline{18143.3 \text{ NIS.}}}$

$$AW = PW (A/P i, n) = 18143.3 (A/P 10\%, 25) = 2000 \underline{\underline{\text{NIS.}}}$$

Annual energy produced from the grid tie PV system = PV model power output \times PSH \times $I_{NV} \times 365$ day

Annual energy produced from the grid tie PV system = $1.56\text{kW} \times 5.4 \text{ hour} \times 0.9 \times 365 \text{ day} = \underline{\underline{2767 \text{ kWh.}}}$

The cost of 1 kWh from the PV generator = $2000 \text{ NIS} / 2767 \text{ kWh}$

$$= \underline{\underline{0.72 \text{ NIS/kWh.}}}$$

Annual benefit money = cost of annual total revenue after PV installation - cost of annual total bill before PV installation = $(2767\text{kWh} \times (1.07 - 0.72) \text{ NIS/kWh}) - (4.5\text{kWh/day} \times 365\text{day} \times 0.55\text{NIS/kWh}) = \text{NIS. (i.e the annual Profit from grid tie PV system} = 1858\text{NIS}).$

$$\text{S.P.B.P} = \text{investment} / \text{saving} = 18260\text{NIS} / (1858\text{NIS}/\text{year}) =$$

9.76years.

We show from the last calculations there is feasible revenue but there is a high initial cost.

7.3Environment impact of PV system

In the long term, environmental benefits may be the most important reason for the implementation of grid off and grid-tied PV system. The environmental impact of small PV plants prevents the production of huge quantities of CO₂ when compared with nonrenewable energy sources producing coal and oxides of sulfur and nitrogen. Of course, CO₂ is inherent in the combustion process and cannot be avoided. Scrubbers can reduce, but not eliminate sulfur and particulate emissions. Gas fired plants are cleaner than coal plants, but still produce greenhouse gases. Atmospheric emissions from nuclear plants are negligible, but radioactive waste is an incessant problem with no clear cut solution.

1 kWh of electricity produced from a coal powered station emits 0.97kg of CO₂ to the atmosphere[32].

Chapter Eight
Modeling of the Standalone and
Grid Tie PV system

Chapter Eight

Modeling of the Standalone and Grid Tie PV system

8.1 Introduction

In this chapter we focus on the two type of PV system: standalone PV system and grid tied PV system. We will simulate a standalone and grid tie PV system by Simulink.

The parameters of the components of the PV system for the house designed are chosen as mentioned in chapter six to apply it in matlab Simulink to verify and show how the system will response.

8.2 Standalone PV System

In the stand alone PV system the battery energy storage is necessary to help get a stable and reliable output from PV generator. In this case we need a battery charge regulator to protect the battery against overcharge and deep discharge which shorten the battery life time [30].

Figure (8.1) shows a charge controller system it consist a PV system, filter and battery charger. A PV system block contains a PV array, a buck-boost converter with MPPT algorithm controller. A buck-boost converter with MPPT algorithm controller is to adjust photovoltaic interfaces so that the operating characteristics of the load and the photovoltaic array match at the maximum power point (MPP) considering some criteria like cell temperature, shadowing etc. Here Photovoltaic voltage is a preferable control variable in case of MPPT since current is heavily dependent of

weather conditions. Buck boost converter is implemented to the system to maintain the output voltage at the desired value. When the PV gets the maximum or minimum voltage from the sunlight, this converter will use to control the output voltage at the desired value to charging the battery. In figure (8.2) shows a PV system consists: PV panel, MPPT (P&O) controller and buck-boost converter and in figure (8.3) shows the voltage output from PV system before charge controller. In appendix C show perturb and observe Algorithm by m-file code.

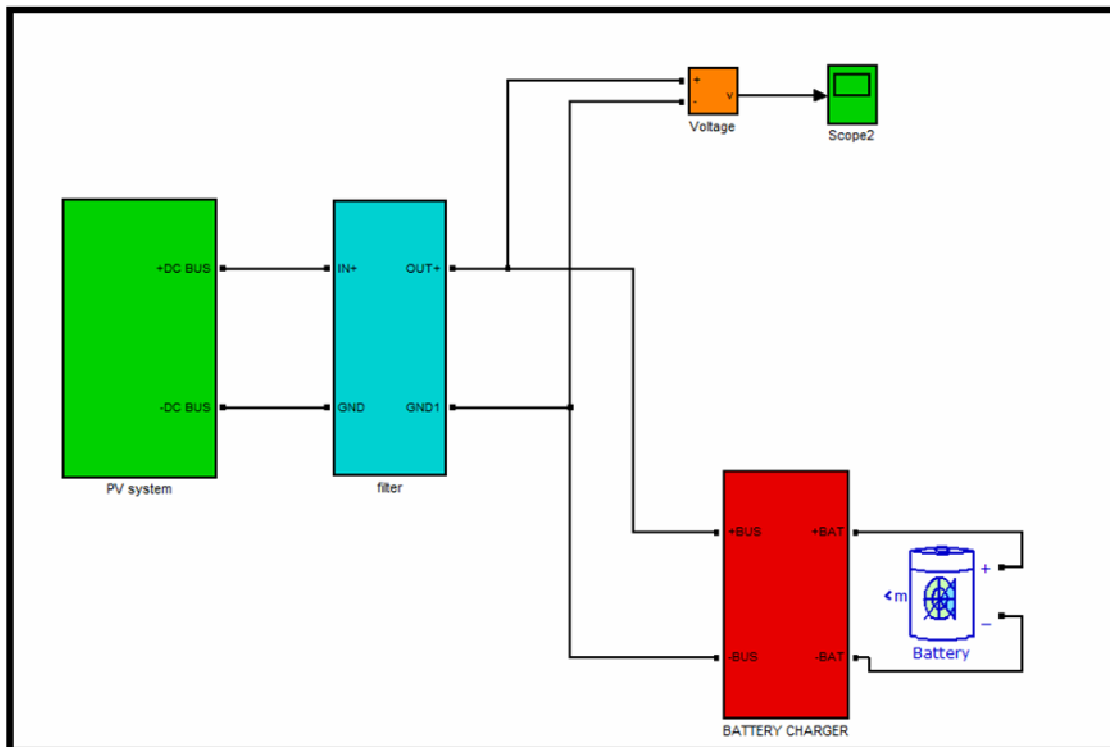


Figure (8.1): Charge controller system.

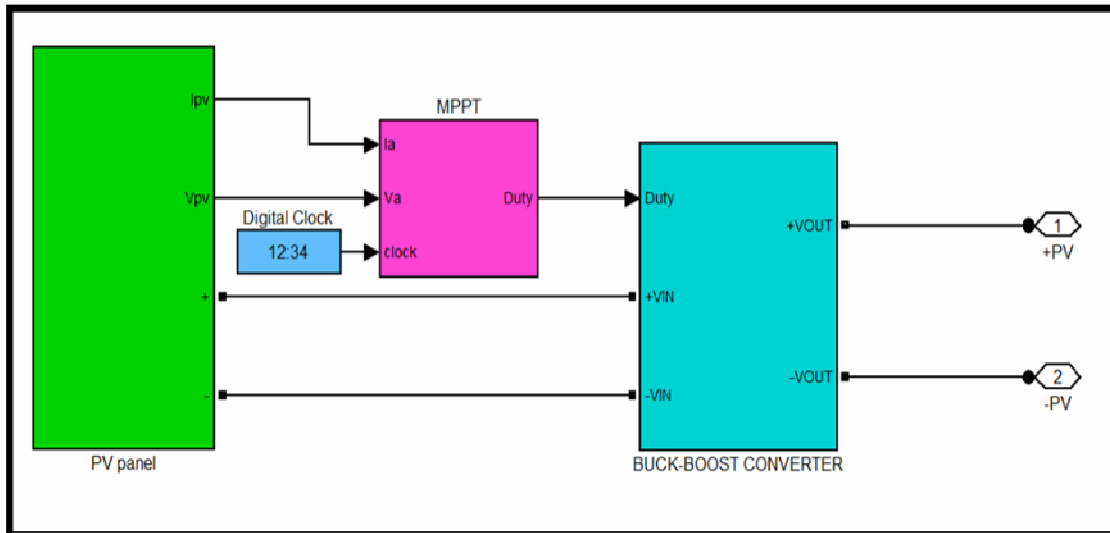


Figure (8.2): PV system consists: PV panel, MPPT (P&O) controller and buck-boost converter.

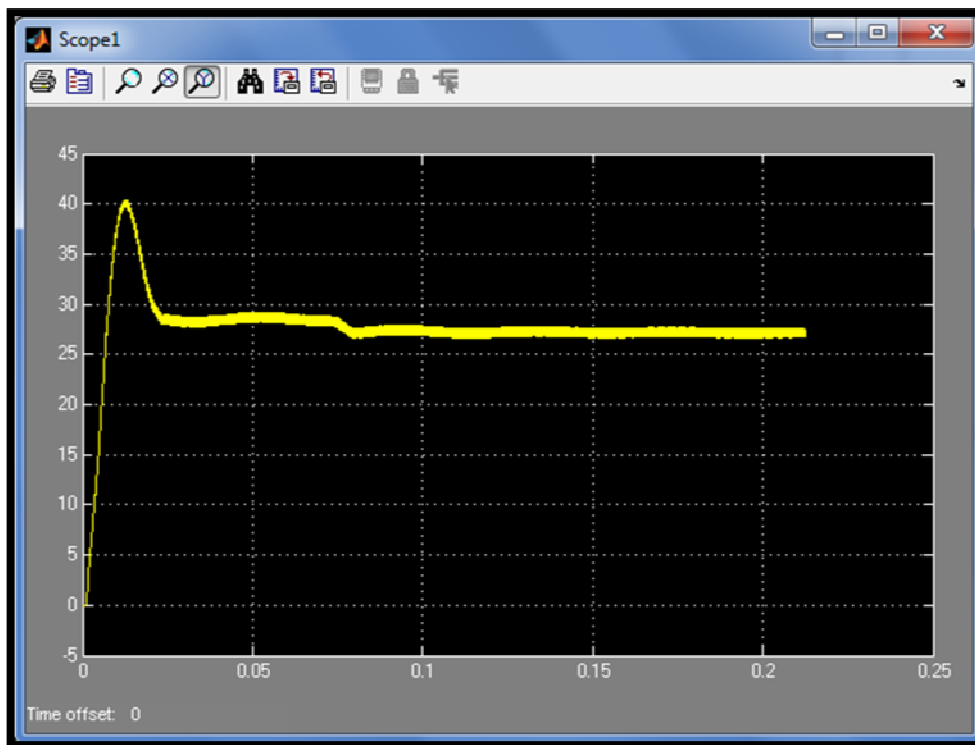


Figure (8.3): Voltage output from PV system before charge controller [Y- axis: voltage(volt), X –axis: time (sec)] .

In figure (8.4) shows a Battery Charger block is consist a boost converter with controller. The output circuit connected to the PV system is usually dc-dc converter mainly boost chopper in order to boost the voltage

to the predetermined levels. Figure (8.5) show a boost converter in battery charger.

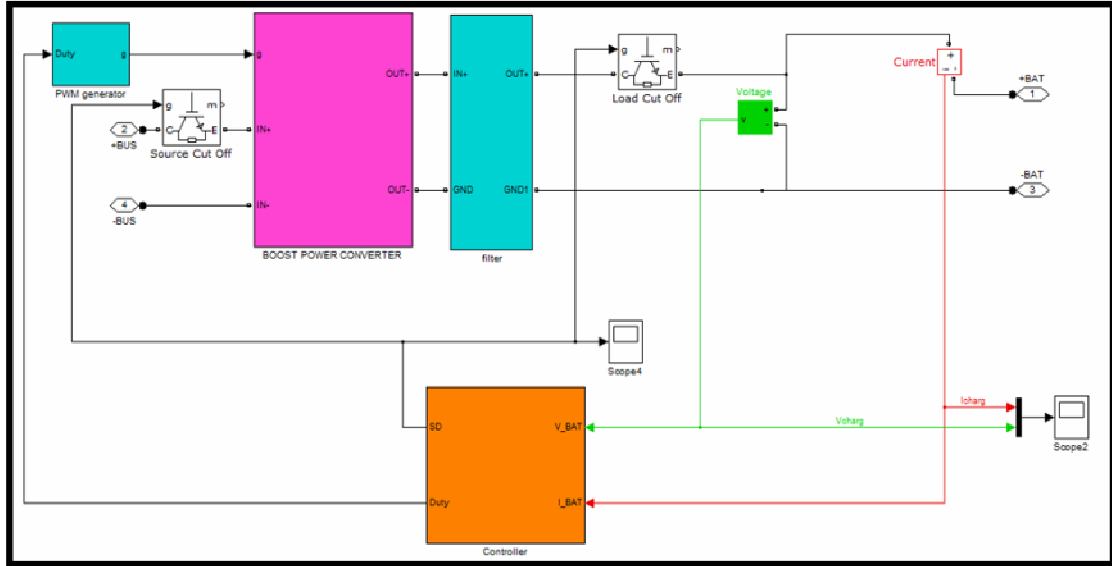


Figure (8.4): Battery charger.

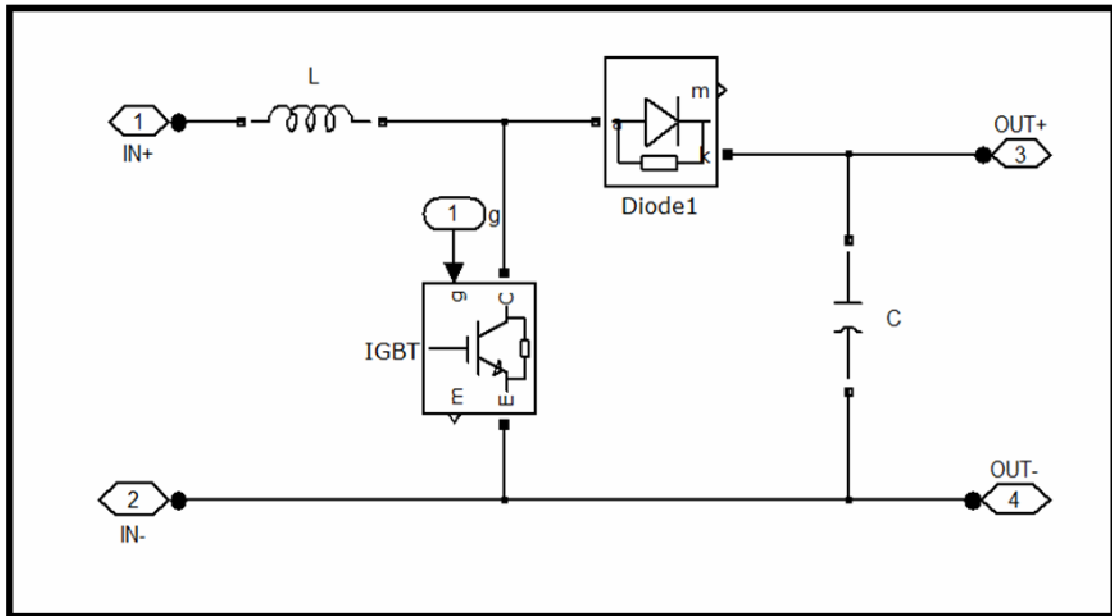


Figure (8.5): Boost power converter, $L=10e-6$, $C=100e-6$.

8.2.1 Battery charging algorithm

The complete battery charging demands a complex control strategy, in which it would be possible to charge the battery, between its limits, in

the faster possible way because the daily period of energy generation of the PV panel is limited. To achieve a fast, safe and complete battery lead-acid charge, some of the manufacturers recommend dividing the charging process in four stages that are designated by: (i) trickle charge, (ii) bulk charge, (iii) over charge and (iv) float charge. Figure (7.6) show the curves of current and voltage applied to the battery during a correct charging cycle [31].

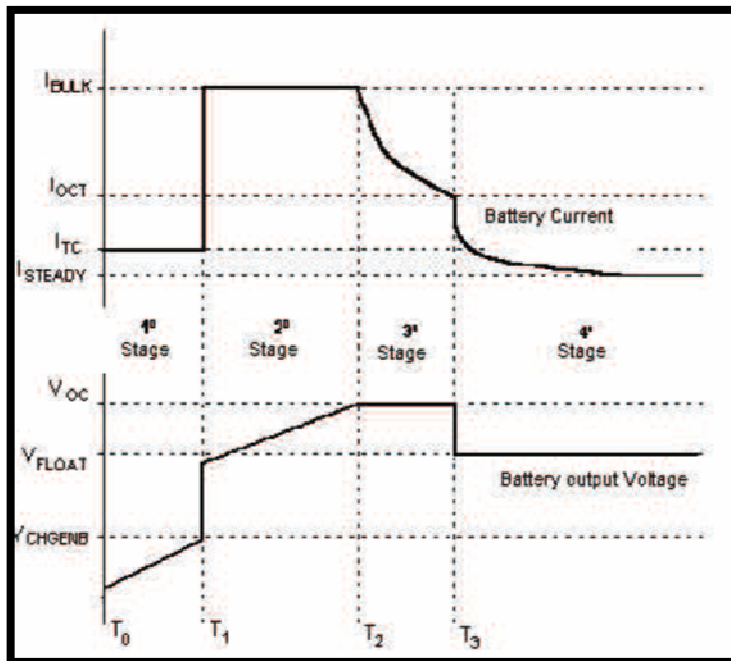


Figure (8.6): Current and voltage curves in the four stages of battery charge [31].

8.2.1.1 Trickle charge – 1st stage (from T_0 to T_1)

This first stage is active when the battery voltage is below the value V_{CHGENB} . This voltage value, specified from the manufacturers, shows that the battery arrives at its critical discharge capacity. In this condition the battery should receive a small charge current defined by I_{TC} that has a

typical value of $C/100$ where C is the normal battery capacity with a 10 hours charging process.

This small current I_{TC} is applied until the battery voltage reaches the value of V_{CHGENB} .

8.2.1.2 Bulk charge - 2nd stage (from T_1 to T_2)

After the battery voltage reaches the value V_{CHGENB} it should be applied to the battery a constant current I_{BULK} . I_{BULK} is the maximum charge current that battery supports without losing amount of water. Its value is specified by the manufacturers. This current is applied until the battery voltage reaches the maximum value of over charge voltage, defined by V_{OC} which is also specified by the manufacturers.

8.2.1.3 Over charge – 3rd stage (from T_2 to T_3)

During this stage the control algorithm should regulate the battery voltage V_{OC} until the complete charge has been reached. When the charging current fall down to a pre-established value I_{OTC} and the voltage stays in the value V_{OC} , the charge process should go to the next, and final, stage. The value of I_{OCT} is around 10% of the I_{BULK} .

8.2.1.4 Float charge – 4th stage (from T_3 until the end)

In this stage the control algorithm will apply to the battery a constant voltage V_{FLOAT} which is specified by the battery manufacturers. This voltage is applied to the battery with the objective of avoiding its auto-

discharge. During the discharging process the battery voltage will fall down and when it reaches $0.9 V_{\text{FLOAT}}$ the control algorithm will execute again the 2nd stage providing the I_{BULK} current.

The control algorithm only returns to the 2nd stage if the PV panel is capable of delivering energy. If it is not the case the battery will continue the discharge process. If the voltage goes below the value V_{CHGENB} the control algorithm should restart the charging process in 1st stage as soon as the PV panel is capable of delivering energy.

In this work some simplifications have been introduced in the implementation of the four different charging stages of a lead-acid battery. The 1st stage was not implemented because the discharge battery voltage, with this model, does not go below V_{FLOAT} . The possible applied load is disconnected from the battery by the control algorithm avoiding reaching the critical discharge.

The 4th stage was not implemented but the 3rd stage is continued until the charge current reach I_{STEADY} and finally the charging process is ended. When the PV panel has energy to deliver and the battery voltage is below V_{OC} , the control algorithm executes the 2nd stage.

The battery charging algorithm can be seen in figure (8.7). The values V_b and I_b are the battery voltage and delivered current respectively while T_b is the battery temperature. The maximum value of V_{OC} depends of the battery temperature. The temperature of the battery T_b is

measured by using a NTC temperature sensor and its linearization is made in software using a conversion table. From figure (8.7) is clear that only the 2nd and the 3rd stages are performed.

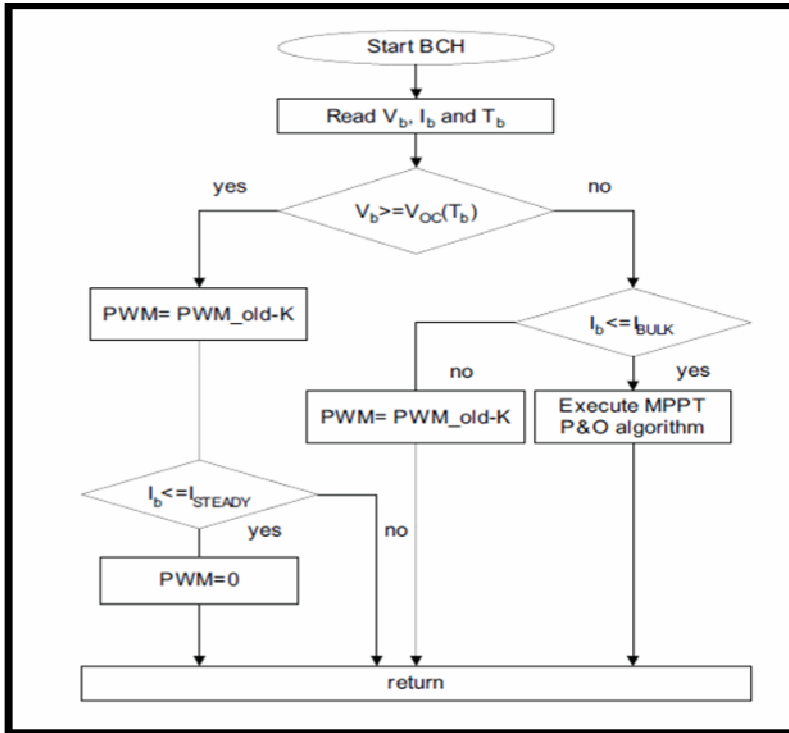


Figure (8.7): Battery charging algorithm with two main stages.

Figure (8.8) shows battery charging controller blocks with two main stages by Simulink and in Appendix E shows the m-file charge controller algorithm in CHARGER block.

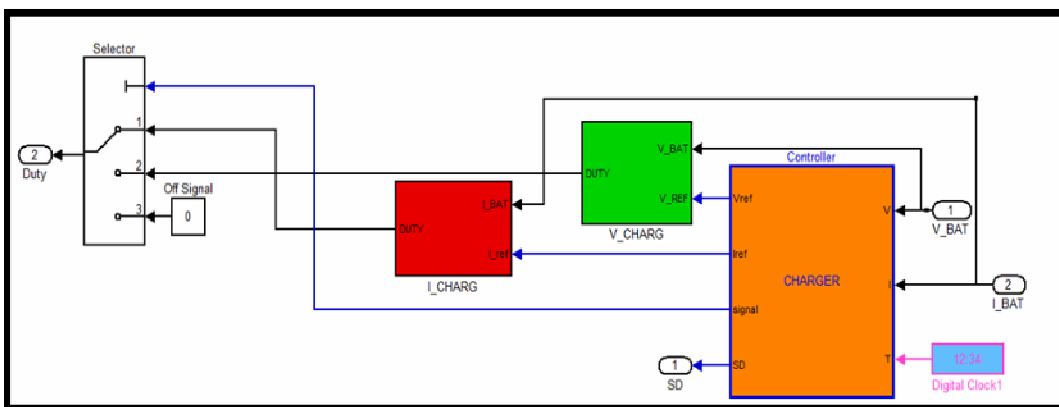


Figure (8.8): Battery charging controller blocks.

In simulation we apply a charging in two modes: **Constant voltage mode** and **Constant current mode**:

Constant voltage mode: In a constant voltage charge mode voltage is kept at 48 Volt and current cut off is 5A. Figure (8.9) shows V-Charge block contents. Charger controller block determine the V_{REF} which is equal one to make a voltage applied in the battery around 48 volts. Figure (8.10) shows the battery charging voltage in function of time.

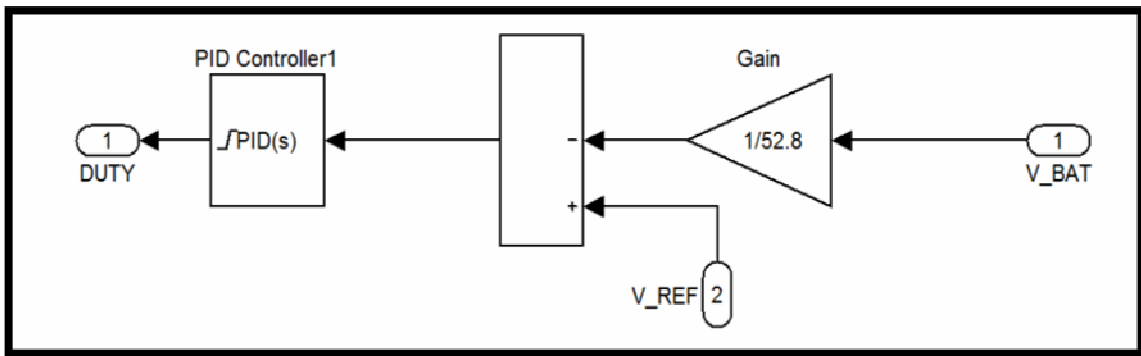


Figure (8.9): V-Charge block, values PID controller is (P= 0.65, I=150, D= 2.7e-06).

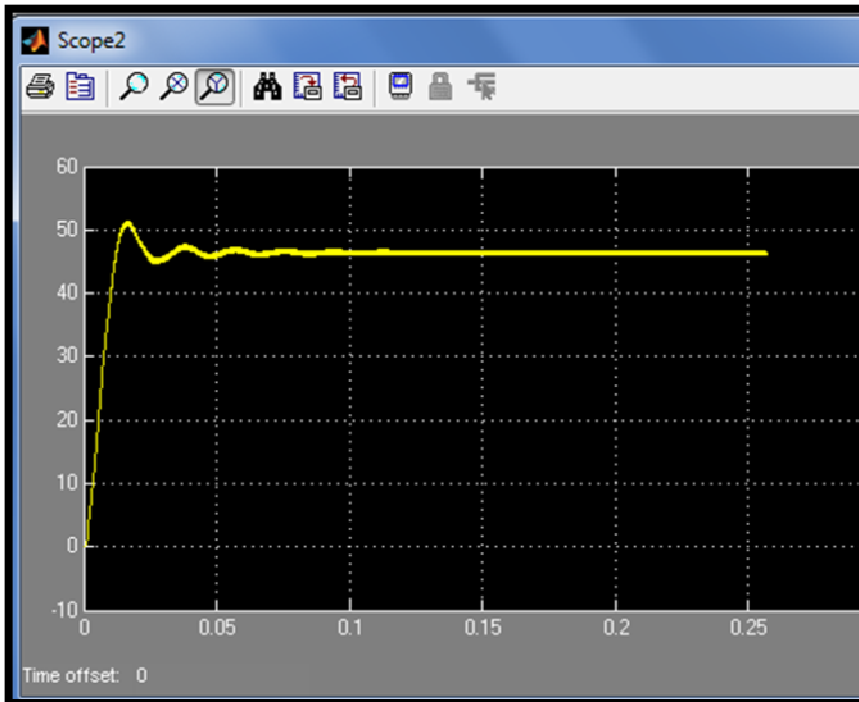


Figure (8.10): Battery charging at voltage constant mode (V=48volts) [Y- axis: voltage(volt), X -axis: time (sec)].

Constant current mode: In a constant current charge mode, current is kept at 100A and voltage limit is 52.8V. In figure (8.11) shows I-Charge block contents. CHARGE controller block determine the I_{REF} is equal one to make a current charging battery is 100A. This mode varies the voltage applied to the battery to maintain a constant current flow, switching off when the voltage reaches the level of a full charge.

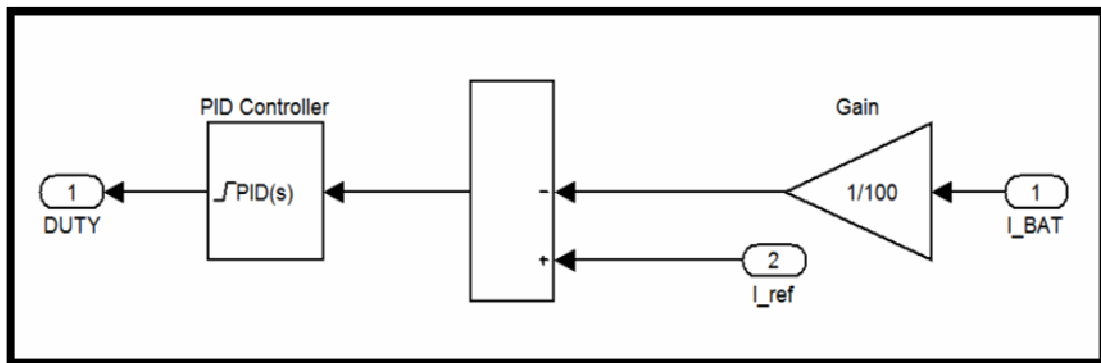


Figure (8.11): I-Charge block, values PID controller is (P = 0.75, I = 50, D = $3 \times 2.7 \times 10^{-6}$).

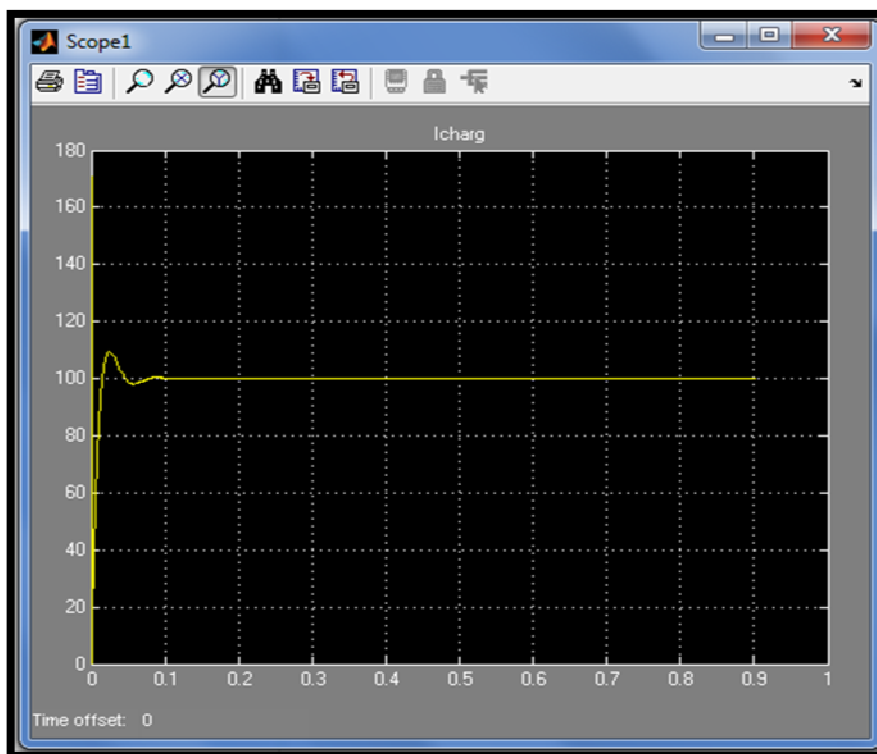


Figure (8.12): Battery charging at current constant mode ($I=100A$) [Y- axis: current(A), X -axis: time (sec)].

8.2.2 Off - grid inverter

In chapter five we discussed and analyzed the types, parameters and control strategy of inverter. In this section we will show how to implement an off- grid system in Matlab Simulink.

Figure (8.13) shows the inverter design for a PV system. The first stage contains a battery regulator with the value 48 Volts and a boost converter to amplify the battery voltage to the desired value amounting to 192 V dc. The boost converter parameters are $L=100 \times 10^{-3}$ H, $C= 1000 \times 10^{-6}$ F, $f_{\text{switching}}=100$ kHz, Duty cycle=75% .Figure (8.14) show the dc link voltage signal.

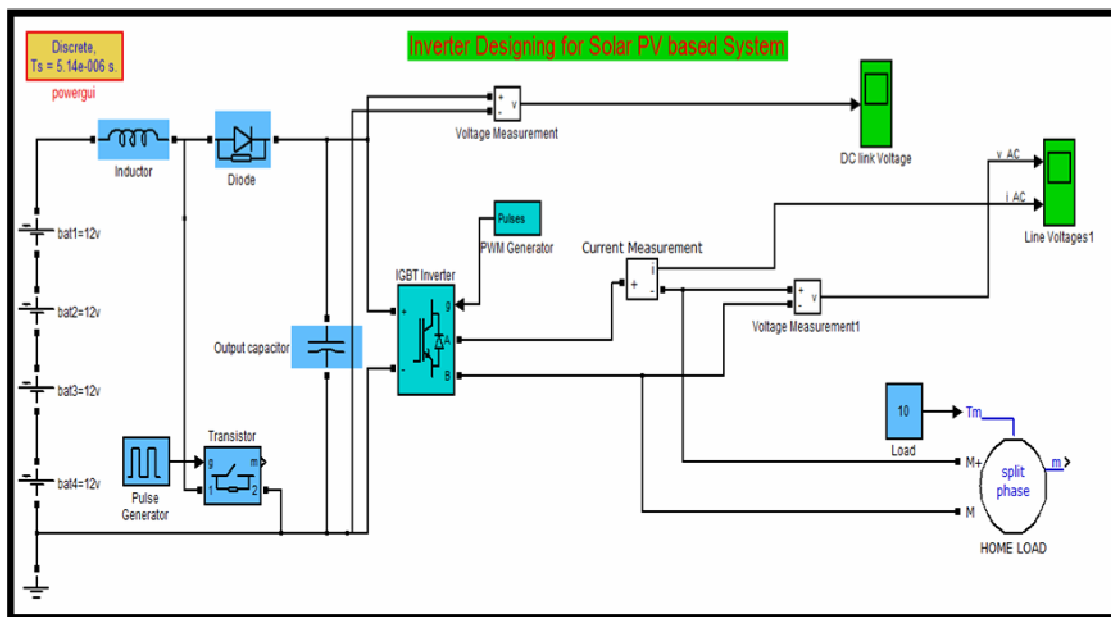


Figure (8.13): Inverter designing for solar PV system.

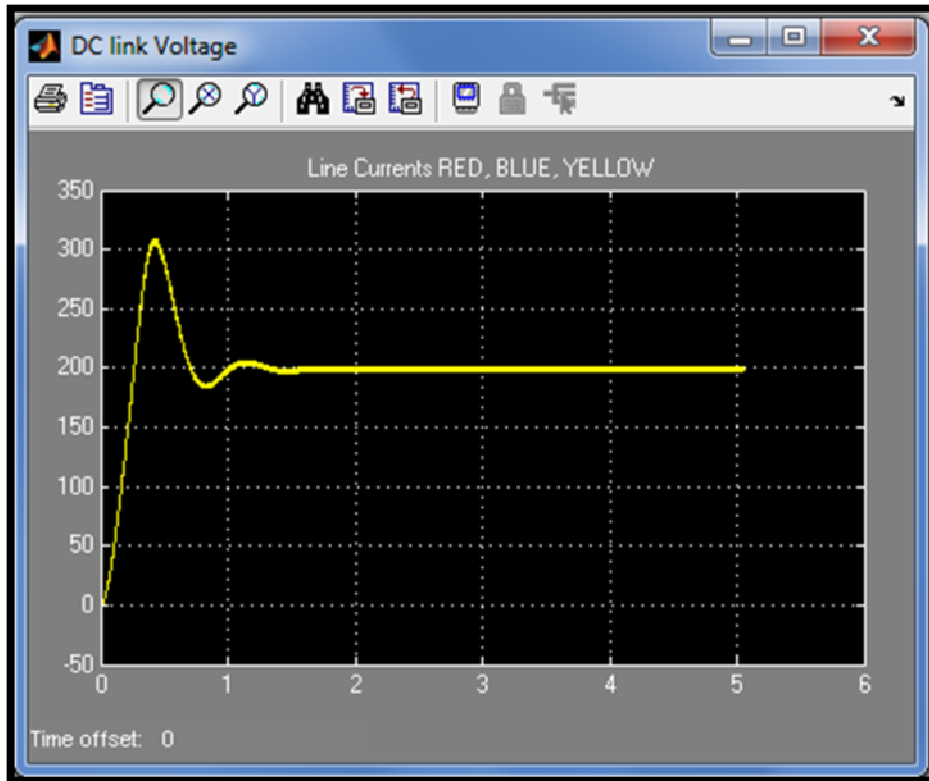


Figure (8.14): Dc link voltage after boost-converter $V_{STEADY} \approx 192$ volts [Y- axis: voltage(volt), X –axis: time (sec)].

The dc voltage applied at the dc link will be converted to single phase AC voltage by using IGBT inverter. We use sine PWM technique, represented by PWM generator block which contains 2-arms (4- pulses), Carrier frequency=900Hz, Modulation index ($0 < m_a < 1$) = 0.9, Frequency of output voltage =50Hz. Figure (8.15) shows the output voltage amounting to 220VAC and current 25A AC from off-grid inverter.

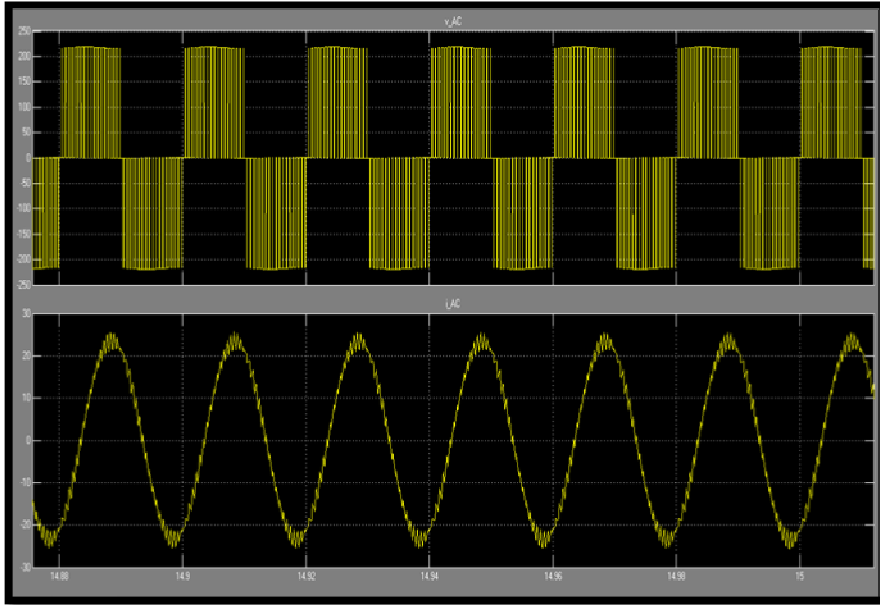


Figure (8.15): Output voltage v-AC [Y- axis: voltage(volt), X –axis: time (sec)] And current i-AC[Y- axis: current(A), X –axis: time (sec)] from off-grid inverter.

8.3 Grid Tie PV System

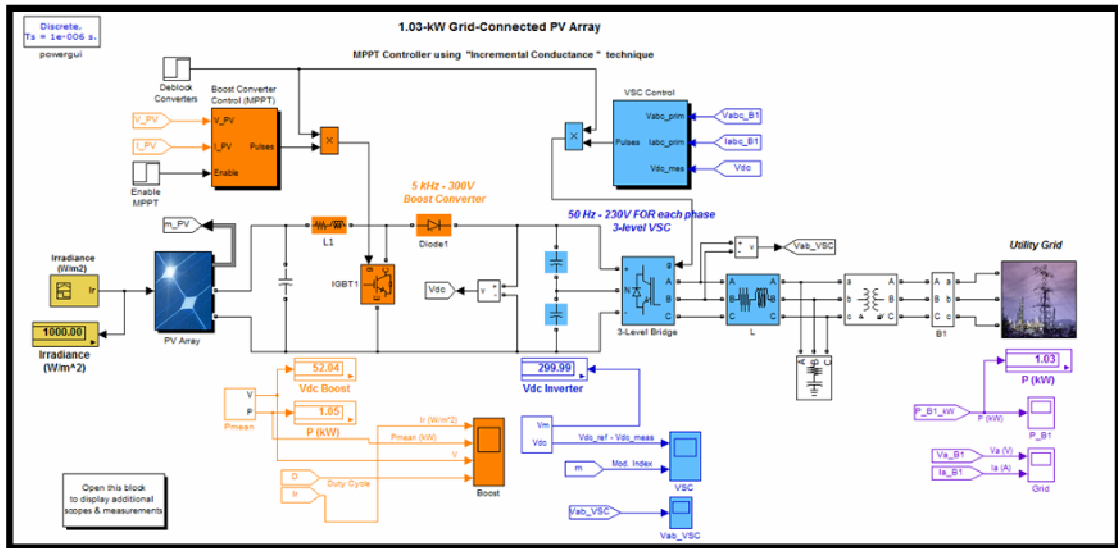


Figure (8.16): One phase on grid inverter.

In figure (8.16), the system consists of 1.15kW PV array, 1kW load. These conditions are applied to the system to find the system performance.

- 1-The input temperature of the PV array equals 25 °C.

2-The input radiation of the PV array equals is variations from (1000 to 250) W/m^2 with time from (0-2.25) sec.

The PV system under study is shown in figure (8.16). A photovoltaic array is used to convert sunlight into DC current. The output of the array is connected to a boost DC converter that is used to perform MPPT functions and increase the array terminal voltage to a higher value so it can be interfaced to the distribution system grid at 220 V. The DC converter controller is used to perform these two functions. A DC link capacitor is used after the DC converter and acts as a temporary power storage device to provide the voltage source inverter with a steady flow of power.

The capacitor's voltage is regulated using a DC link controller that balances input and output powers of the capacitor. The voltage source inverter is controlled in the rotating dq frame to inject a controllable three phase AC current into the grid. To achieve unity power factor operation, current is injected in phase with the grid voltage. A phase locked loop (PLL) is used to lock on the grid frequency and provide a stable reference synchronization signal for the inverter control system, which works to minimize the error between the actual injected current and the reference current obtained from the DC link controller. An adjustable speed drives (ASD) and an RL load is connected to the grid to simulate some of the loads that are connected to a distribution system network. An LC low pass filter is connected at the output of the inverter to attenuate high frequency harmonics and prevent them from propagating into the power system grid.

A second order LCL filter is obtained if the leakage inductance of the interfacing transformer is referred to the low voltage side. This provides a smooth output current which is low in harmonic content.

Figure (8.17) show the block VSC main controller that convert from dc bus voltage input to ac voltage grid.

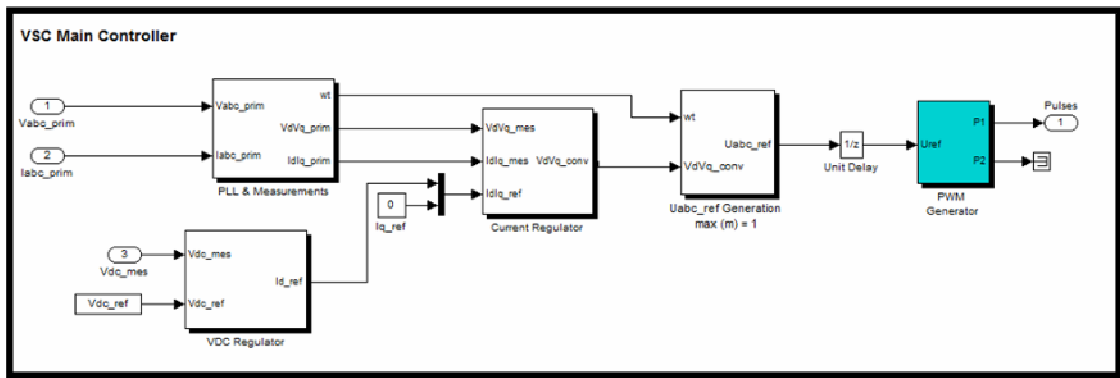


Figure (8.17): VSC main controller block.

Figure (8.18) and (8.19) show the Incremental conductance mppt block and algorithm.

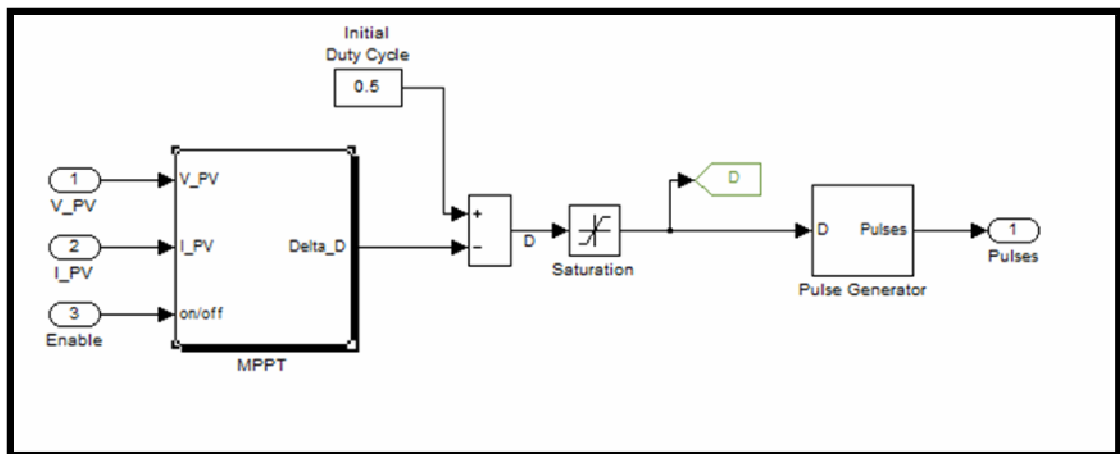


Figure (8.18): IC conductance mppt controller block.

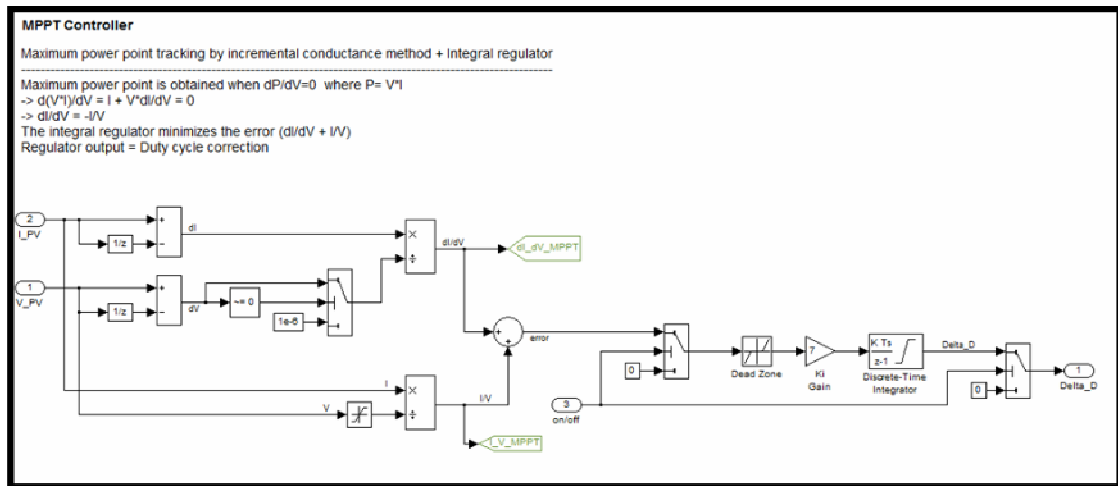


Figure (8.19):IC conductance mppt algorithm.

Figure (8.20) shows that the output power from PV array is still 1 kW for 0.7s, and then from 0.7s to 1.3s the PV power decrease to 0.25kW because the radiations decrease from (1000 to 250) W/m^2 . After 1.3s the output power from PV is increased to 1kW with increased radiation. The voltage PV is be stabilized because variation the duty cycle with changing radiation and the effective of changing radiation is few in PV voltage array.

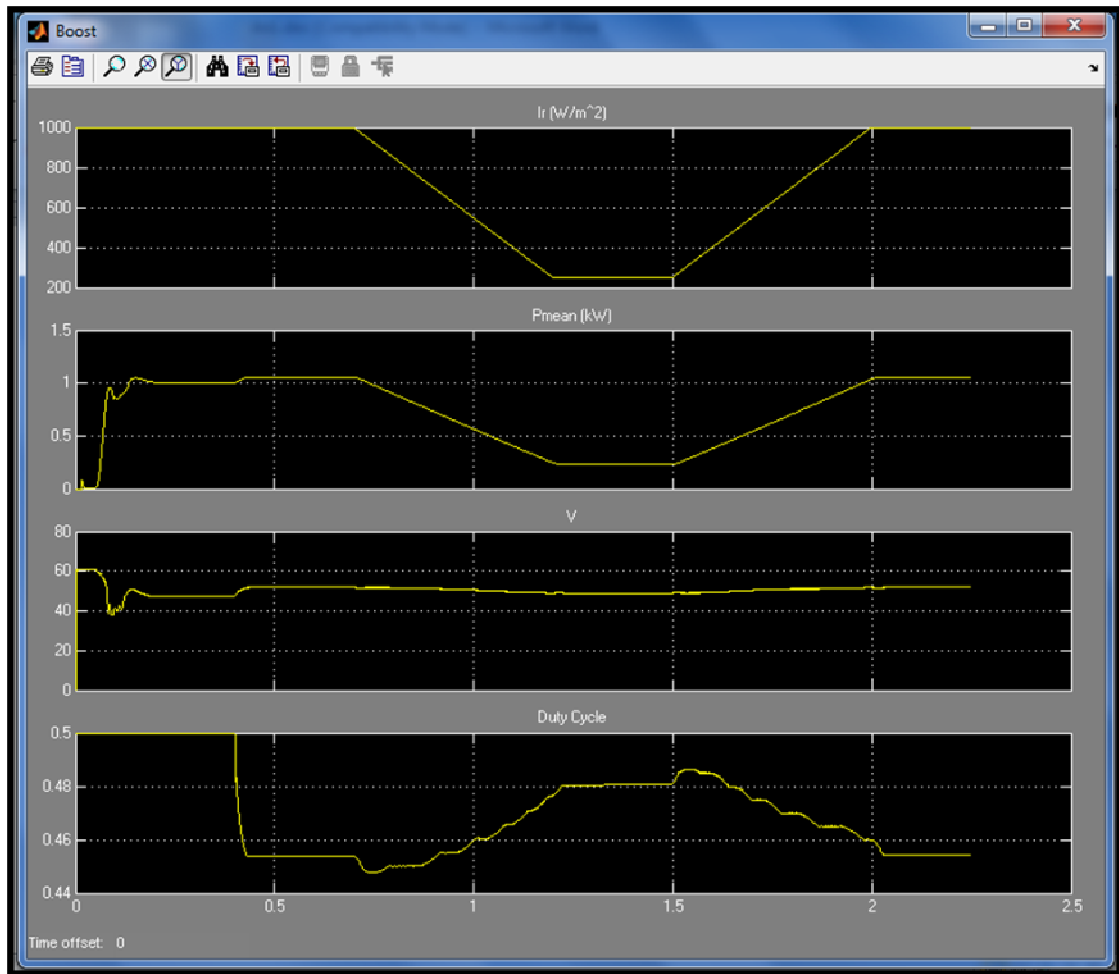


Figure (8.20): Output power (kW), output voltage(volt) from PV array and Mppt duty cycle with changing a radiation(Kw/m^2), [X –axis: time (sec)].

Figure (8.21) show that the output power from grid tie PV system with variable radiation as mentioned above.

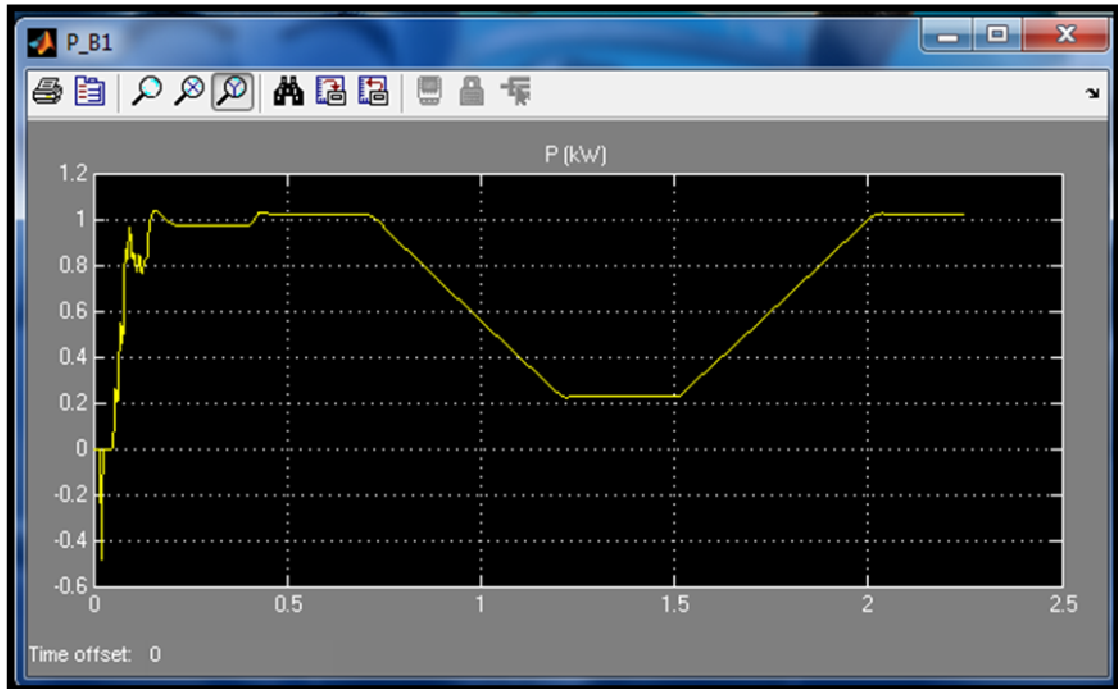


Figure (8.21): Output power (kW) from the grid tie PV system with variable radiations, [X –axis: time (sec)].

Figure (8.22) and figure (8.23) show the output voltage and current that produced from grid tie PV system with changing radiation.

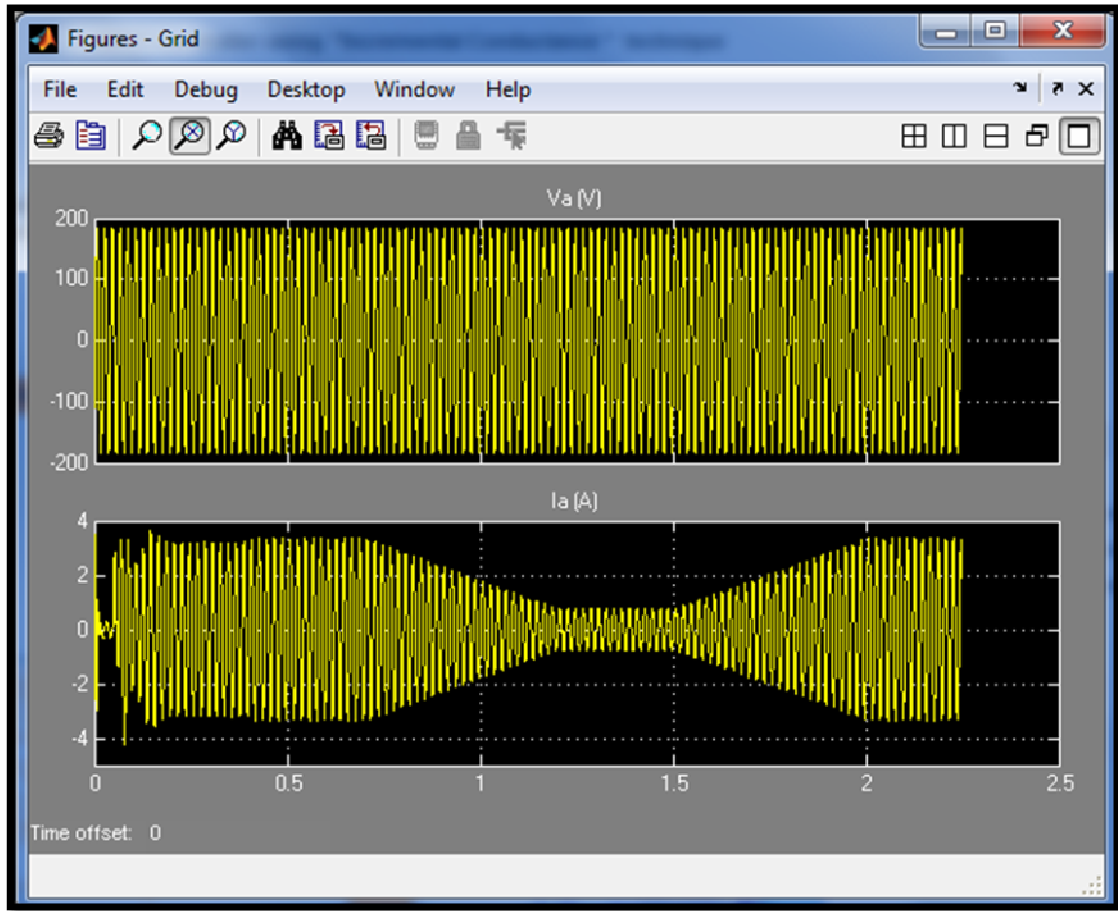


Figure (8.22): Grid tie voltage (volt) and current (A) output with deffirence radiation, [X -axis: time (sec)].

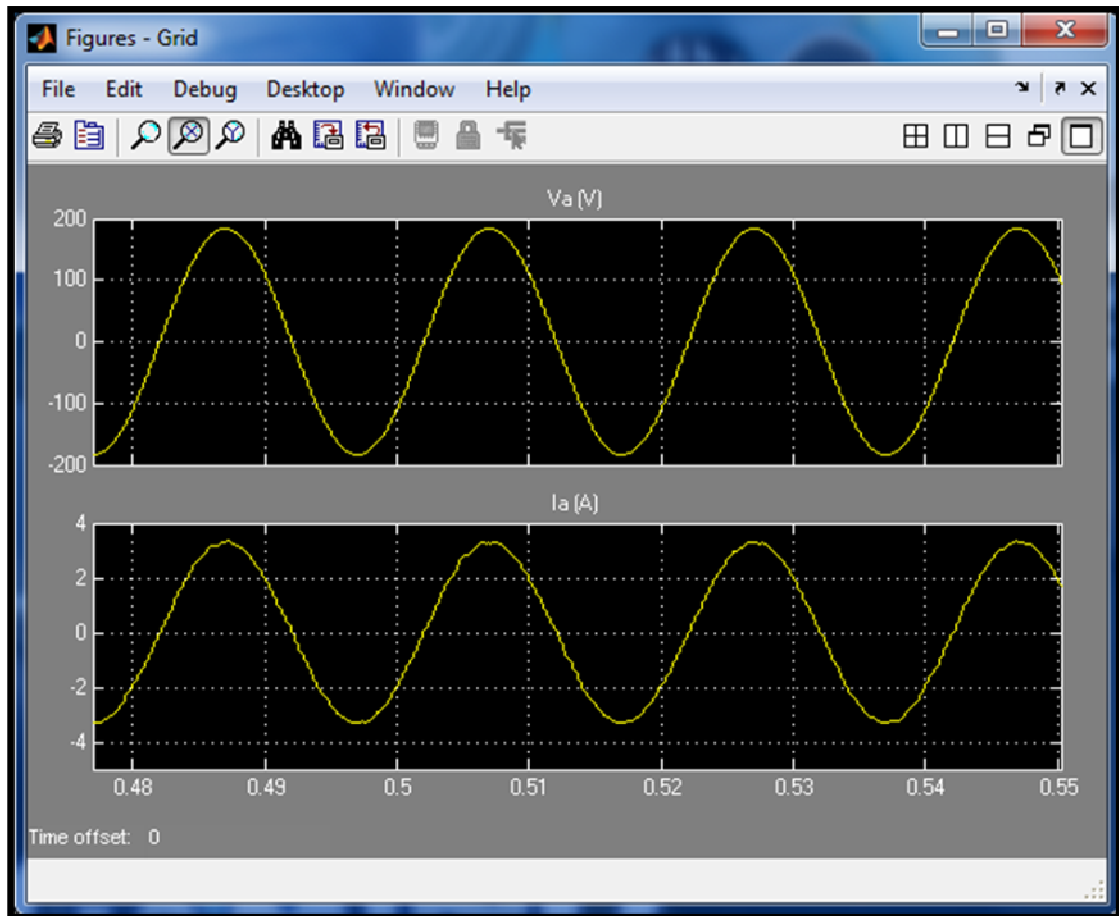


Figure (8.23):50Hz Voltage and current output of grid tie PV system, [X –axis: time (sec)].

Figure (8.24) shows the voltage dc bus is constant with changing the radiation and how modulation index is responded with changing radiation.

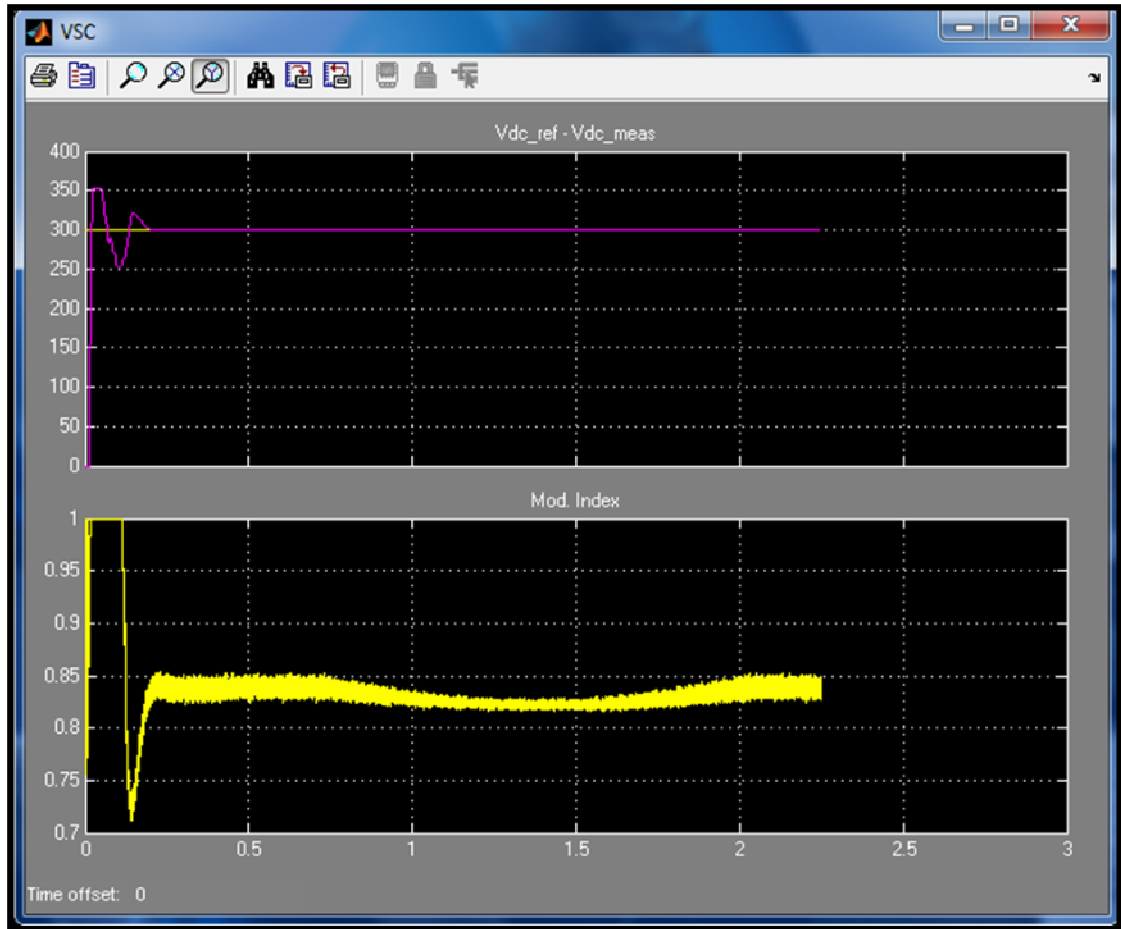


Figure (8.24): Vdc mean and Vdc ref with modulation index, [X-axis: time (sec)].

Conclusions and Future Scope of Work

Conclusions

-This study presents a simple but efficient photovoltaic standalone PV system. It models each component and simulates the system using MATLAB Simulink and Psim software's. The result shows that the PV model using the equivalent circuit in moderate complexity provides good matching with the real PV module. Simulations perform comparative tests for the two MPPT algorithms with using DC-DC converter after that design and simulate a full system standalone PV system to produce AC current for a home load.

-The design and calculation the rated value of a PV system units (PV array, battery, charge controller and inverter) for a load home and makes an economic study for a standalone PV system and grid tie PV system, the cost of energy generated by a standalone PV system is 2.1 (NIS/kWh) and the cost of energy generated by grid tie PV system is 0.72 (NIS/kWh).

- Design a grid tie PV system by using matlab Simulink and observe how the system works with a dynamics behavior of the changing radiations.

-The design of a control system for one phase grid connected photovoltaic arrays. The open loop maximum power point tracking technique aimed at solving the problems present in two of the most common techniques used for that purpose: the perturb and observe (P&O) and incremental conductance algorithms. The main drawbacks of the P&O

technique are its poor dynamic response and swinging around the maximum power point during steady state operation.

The incremental conductance technique suffers also from a relatively slow dynamic response time.

The open loop MPPT technique employed in this thesis aims at providing an improved dynamic response time as compared to the previously mentioned techniques. It does not suffer from high implementation complexity as well. The PV array maximum power point was approximated using test PV cells that kept track of the current weather conditions.

Scope for Future Work

After the completion of my studies and investigations, the scope is been identified as:

- ❖ Design a real low-cost power source (single phase,50Hz) using a standalone PV system with all power electronics component, current and voltage sensors, interface circuits and programming MPPT algorithm and SPWM strategy on a dsPIC controller to be more efficient for the Palestine conditions.
- ❖ Study and design a smart PV system that contains grid tied system with storage battery, where the smart system can decide when it should feed the energy in grid or storage in battery or connect the load home on the grid based on economic and technical consideration.

References

1. **"Introduction to Photovoltaic Systems"**, in Renewable Energy The Infinite Power of Texas: <http://www.infinitepower.org/pdf/FactSheet-11.pdf> [Access Date 20-09- 2012].
2. Cristina Ventura, **"Theoretical and Experimental Development of a Photovoltaic Power System for Mobile Robot Applications"**, in Ph.D. Thesis Electrical Engineering. December 2011.
3. <http://www.agrissolar.coop/technology/photovoltaics.html> [Access Date 9-09- 2012].
4. Basem Alsayid and Jafar Jallad, "*Modeling and Simulation of Photovoltaic Cells/Modules/Arrays*". *International Journal of Research and Reviews in Computer Science (IJRRCS)*, December 2011. Vol. 2, No. 6.
5. Marcelo Gradella Villalva, J.R.G., Ernesto Ruppert Filho., "*Comprehensive Approach to Modeling and Simulation of Photovoltaic Arrays*". *Power Electronics, IEEE Transactions on*, May 2009. 24 (5): p. 1198 - 1208
6. SINGH, J., "**STUDY AND DESIGN OF GRID CONNECTED SOLAR PHOTOVOLTAIC SYSTEM AT PATIALA**", in Thesis submitted in the partial fulfillment for the award of the degree of

Master of Engineering in Power Systems & Electric Drives, Thapar university Patiala,2010.

7. Ramaprabha Ramabadran "***MATLAB Based Modelling and Performance Study of Series Connected SPVA under Partial Shaded Conditions***" *journal of sustainable development* /vol.2.no.3/November 2009 (Tamilnadu, India).
8. Mermoud, A., "***PARTIAL SHADINGS ON PV ARRAYS: BY-PASS DIODE BENEFITS ANALYSIS*** ". *European Photovoltaic Solar Energy Conference* – Valencia, Spain, 6-10 September 2010.
9. M. G. Villalva, J.R.G., E. Ruppert "***MODELING AND CIRCUIT-BASED SIMULATION OF PHOTOVOLTAIC ARRAYS***". *IEEE*, F.University of Campinas - UNICAMP, Brazil.
8. André Mermoud., "***PARTIAL SHADINGS ON PV ARRAYS: BY-PASS DIODE BENEFITS ANALYSIS*** ". *European Photovoltaic Solar Energy Conference* – Valencia, Spain, 6-10 September 2010.
9. M. G. Villalva, J.R.G., E. Ruppert "***MODELING AND CIRCUIT-BASED SIMULATION OF PHOTOVOLTAIC ARRAYS***". *IEEE*, F.University of Campinas - UNICAMP, Brazil.
10. Silje Odland Simonsen, "***Development of a Grid Connected PV System for Laboratory Use***". Master of Science in Energy and Environment, February 2009. Norwegian University of Science and Technology,Department of Electric Power Engineering.

11. Deutsche Gesellschaft Für Sonnenenergie, "**Planning and Installing Photovoltaic Systems**": A Guide for Installers, Architects and Engineers, January 2008.
12. *Asma M. Yasin* "**Optimal Operation Strategy and Economic Analysis of Rural Electrification of Atouf Village by Electric Network, Diesel Generator Photovoltaic System**" A thesis presented to the University of An-Najah National University, Nablus, Palestine, 2008.
13. Marwan M. Mahmoud, Lectures of renewable energy 2, Tuesday, May 24, 2010, at An - Najah National University.
14. AKIHIRO OIE "**Design and Simulation of Photovoltaic Water Pumping System**" A Thesis Presented to the Faculty of California Polytechnic State University, San Luis Obispo, Requirements for the Degree of Master of Science in Electrical Engineering, 2005
15. Balakrishna S, Thansoe, Nabil A, Rajamohan G, Kenneth A.S., Ling C. J, "**The Study and Evaluation of Maximum Power Point Tracking Systems**" School of Engineering & Science, Curtin University of Technology, Sarawak Campus, Malaysia.
16. Ghislain Remy, Olivier Bethoux, "**Review of MPPT Techniques for Photovoltaic Systems**" Laboratoire de Génie Electrique de Paris (LGEP)/ SPEE-Labs, Université Paris-Sud 11, France.

17. ROBERTO FARANDA, S.L., "**Energy comparison of MPPT techniques for PV Systems**". WSEAS TRANSACTIONS on POWER SYSTEMS.
18. Yen-Jung Mark Tung, Dr. Aiguo Patrick Hu, Dr. Nirmal-Kumar Nair," *Evaluation of Micro Controller Based Maximum Power Point Tracking Methods Using dSPACE Platform*" Australian University Power Engineering Conference 2006.
19. Abu-hamdeh, Muthanna S, "**Modeling of Bi-directional Converter for Wind Power Generation**", The Ohio State University 2009, available from ohiolink.edu
20. Falinirina F. Rakotomananandro "**Study of Photovoltaic System**" Master thesis presented to the Ohio State University, 2011.
21. Miss. Sangita R Nandurkar , Mrs. Mini Rajeev "**Design and Simulation of three phase Inverter for grid connected Photovoltaic systems**", Proceedings of Third Biennial National Conference, NCNTE- 2012, Feb 24-25 80 .
22. AL-MAQDESI LAB Project Measurments in PALESTINE TECHNICAL UNIVERSITY"KHADOORI" (PTUK),2012.
23. Bassam Ahmed A.Abdel-Ghani,"**TECHNO-ECONOMIC EVALUATION OF ELECTRIFICATION OF SMALL VILLAGES IN PALESTINE BY CENTRALIZED AND DECENTRALIZED PV SYSTEM**",A thesis presented to the

University of An-Najah National University, Nablus, Palestine, 2008.

24. Buresch M. , "**Photovoltaic energy systems design and installation**", New York ; McGraw-Hill ; 1998
25. Ali Keyhani, Integration of Green, "**Renewable Energy in Electric Power Systems**", Dec 2009, Wiley-VCH.
26. Eyup Taymur ,"**Photovoltaics Systems Sizing**"A thesis presented toThe Ohio State University ,2009.
27. http://en.wikipedia.org/wiki/Grid-tie_inverter [Access Date 3-2-2012].
28. Gurhan Ertasgin ,"**Low-Cost Current- Source 1-ph Photovoltaic Grid- Connected Inverter**",a thesis subbmited in partial fulfillment for the dsgree of Doctor of Philosophy, August 2010.
29. <http://www.sunpirate.com/photovoltaic-system-types.html> [Access Date 9-6- 2012].
30. http://en.wikipedia.org/wiki/Charge_controller [Access Date 2-4-2012].
31. José António Barros Vieira, Alexandre Manuel Mota, "**Maximum Power Point Tracker Applied in Batteries Charging with PV Panels**",2008.
32. http://www.esru.strath.ac.uk/EandE/Web_sites/0102/RE_info/C02.htm [Access Date 1-11- 2012].

APPENDICES

Appendix A: Specifications of the MSX-50 Photovoltaic Module

Appendix B: M-file code that calculate R_s and R_p

Appendix C: Perturb and Observe Algorithm

Appendix D: Specifications of the Standalone PV system elements

Appendix E: Charge controller algorithm BY M-file

Appendix F: Table of interest at $i = 10\%$

APPENDIX (A)

Specifications of the MSX-50 Photovoltaic Module

MSX-50 Photovoltaic Modules



The MSX-50 is a midsize photovoltaic module in Solarex's Megamodule™ series, a product line which is the industry standard for reliability, durability and value. It is well-suited to applications requiring the ruggedness and other premium characteristics—such as the 20-year warranty—of Solarex's larger MSK modules, but needing 50 watts peak output. Typical uses include remote habitations, instrumentation systems, security sensors, and navigation aids.

With 36 polycrystalline silicon solar cells in series, the MSX-50 charges batteries efficiently in virtually any climate. It may be used in single-module arrays or deployed in multiple-module arrays, wired in series/parallel combinations as required to meet current and voltage requirements. The MSX-50 is engineered under Solarex's IntegraSystem™ system integration concept, which ensures full compatibility with other Solarex subsystems and components (support hardware, regulators, etc.) and easy system assembly.

Individually Tested, Labeled and Warranted

As part of the final inspection procedure, every MSX module is tested in a solar simulator and labeled with its actual output—voltage, current, and power at maximum power point (P_{max})—at Standard Test Conditions and Standard Operating Conditions. Furthermore, the MSX-50 is covered by our industry-leading limited warranty, which guarantees:

- that no module will generate less than its guaranteed minimum P_{max} when purchased;
- at least 80% of the guaranteed minimum P_{max} for twenty years.

Contact Solarex's Marketing Department for full terms and limitations of this unparalleled warranty.

Reliable and Versatile

The Megamodule series has proved its reliability at thousands of installations in every climate on Earth. Among the features that contribute to its versatility:

Great Voltage Capability

These modules consist of 36 polycrystalline silicon solar cells electrically configured as two series strings of 18 cells each. The strings terminate in the junction box on the module back. Shipped in 12V configuration, modules may easily be switched to 6V configuration in the field by moving leads in the junction box. This design also allows

installation of bypass diodes on 18-cell strings, which can improve reliability and performance in systems with nominal voltage 24V and above.

High-Capacity Multifunction Junction Box

The size of the junction box (25 cubic inches, 411cc) and its six-terminal connection block allow most system array connections (putting multiple modules in series or parallel) to be made right in the J-box. The box also can accommodate bypass or blocking diodes or a small regulator. In many instances, this saves the expense and labor of fitting additional boxes. The box is nontight (IP54 rated) and accepts 1/2" nominal or PG13.5 conduit or cable fittings. The standard terminals accept wire as large as AWG #10 (6mm²); an optional terminal block accepts wire up to AWG #4 (25mm²). Both blocks accept preformed terminations or bare wire.

Proven Materials and Construction

Megamodule materials reflect Solarex's quarter-century of experience with solar modules and systems installed in virtually every climate on Earth.

- Polycrystalline silicon solar cells: efficient, attractive, stable.
- Modules are rugged and weatherproof; cell strings are laminated between sheets of ethylene vinyl acetate (EVA) and tempered glass with a durable Tedlar backsheet.
- Tempered glass superstrate is highly light-transmissive (low iron content), stable, and impact-resistant.
- Corrosion-resistant, bronze-anodized extruded aluminum frame is strong, attractive, compatible with Solarex mounting hardware and most other mounting structures.

Safety Approved

The MSX-50 module is listed by Underwriter's Laboratories for electrical and fire safety (Class C fire rating), certified by TÜV Rheinland as Class II equipment, and approved by Factory Mutual Research for application in NEC Class 1, Division 2, Group C & D hazardous locations.



More than 20 years ago, Solarex made the first polycrystalline silicon solar cell, advancing photovoltaics beyond the first generation monocrystalline technology designed for electronics. Designed specifically for photovoltaics, polycrystalline silicon is used in Solarex's Mega™ series to provide a wide range of attractive, efficient modules. They require substantially less energy to manufacture and generate substantially more energy per raised watt than other crystalline silicon modules.



Options

- Blocking and bypass diodes
- Solarstate™ charge regulator

Quality certified

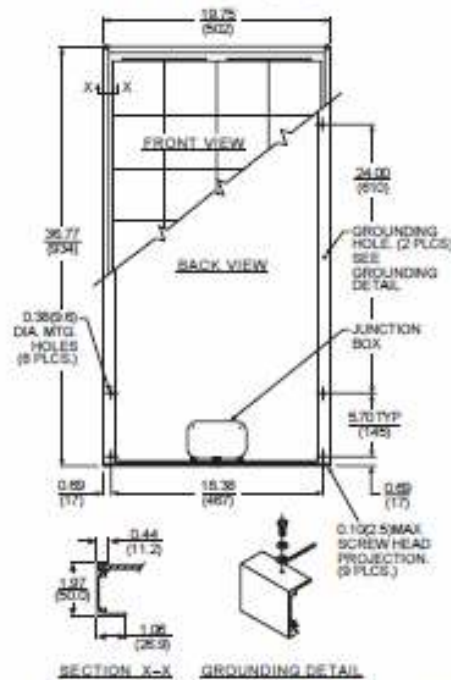
MSX-50 modules are manufactured in our ISO 9001-certified factories to demanding specifications, and are designed to comply with IEC 1215, IEEE 1262 and CEC 503 test requirements, including:

- repetitive cycling between -40°C and 90°C;
- repetitive cycling between -40°C and 85°C at 85% relative humidity;
- simulated impact of one-inch (25 mm) hail at terminal velocity;
- 2700 VDC frame/cell string isolation test;
- performance at low light levels;
- a "damp heat" test, consisting of 1000 hours of exposure to 85°C, and 85% relative humidity;
- a "hot-spot" test, which determines a module's ability to tolerate localized shadowing (which can cause reverse-biased operation and localized heating);
- resistance to UV degradation;
- robustness of electrical terminations;
- simulated wind loading of 125 mph (200 kph).

Mechanical Characteristics

Weight: 11.8 pounds (5.35 kg)

Dimensions: Dimensions in brackets are in millimeters. Unbracketed dimensions are in inches. Overall tolerances ±1/8" (3mm)

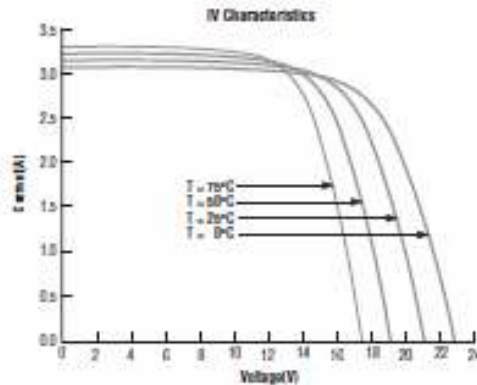


Typical Electrical Characteristics¹

Maximum power (P_{max})	50W
Voltage at P_{max} (V_{mp})	17.1V
Current at P_{max} (I_{mp})	2.92A
Guaranteed minimum P_{max}	47.5W
Short-circuit current (I_{sc})	3.17A
Open-circuit voltage (V_{oc})	21.1V
Temperature coefficient of I_{sc}	(0.065±0.015)%/°C
Temperature coefficient of V_{oc}	-(80±10)mV/°C
Temperature coefficient of power	-(0.5±0.05)%/°C
NOCT ²	47±2°C

Notes

- (1) These modules are tested, labeled and shipped in 12V configuration. These data represent the performance of typical 12V modules as measured at their output terminals, and do not include the effect of such additional equipment as fuses and cabling. The data are based on measurements made in a solar simulator at Standard Test Conditions (STC), which are:
 - illumination of 1 kW/m² (1 sun) at spectral distribution of AM 1.5;
 - cell temperature of 25°C or as otherwise specified (on curves)
 Operating characteristics in sunlight may differ slightly. For characteristics of modules in 6V configuration, divide the 12V voltage characteristics by 2 and multiply current characteristics by 2. Power values are unchanged.
- (2) Under most climatic conditions, the cells in a module operate hotter than the ambient temperature. NOCT (Nominal Operating Cell Temperature) is an indicator of this temperature differential, and is the cell temperature under Standard Operating Conditions: ambient temperature of 25°C, solar irradiation of 0.8 kW/m², and wind speed of 1 m/s.



[Download MSX-50 IV XLS](#)

[Download CAD](#)

For more information, contact:



Appendix (B)**M-file code that calculate R_s and R_p**

```

% Matlab script for modeling a photovoltaic array

%% Load PV device data

data_MSX50

%% Adjusting algorithm

a = 1.3;

% Reference values of  $R_s$  and  $R_p$ 

 $R_{s\_max} = (V_{ocn} - V_{mp}) / I_{mp}$ ;

 $R_{p\_min} = V_{mp} / (I_{scn} - I_{mp}) - R_{s\_max}$ ;

% Initial guesses of  $R_p$  and  $R_s$ 

 $R_s = 0$ ;

 $R_p = R_{p\_min}$ ;

% The model is adjusted at the nominal condition

 $T = T_n$ ;

 $G = G_n$ ;

 $V_{tn} = k * T_n / q$ ;          %Thermal junction voltage (nominal)

 $V_t = k * T / q$ ;           %Thermal junction voltage (currenttemperature)

 $I_{on} = I_{scn} / (\exp(V_{ocn} / a / N_s / V_{tn}) - 1)$ ;  % Nominal diode saturation current

 $I_o = I_{on}$ ;

perror = Inf; %dummy value

```

```

% Iterative process for Rs and Rp until Pmax,model = Pmax,experimental
ni = 0;
while (perror>tol) && (Rp > 0) && (ni < nimax)
ni = ni + 1;
% Temperature and irradiation effect on the current
dT = T-Tn;
Ipvn = (Rs+Rp)/Rp * Iscn;    % Nominal light-generated current
Ipv = (Ipvn + Ki*dT) *G/Gn;  % Actual light-generated current
Isc = (Iscn + Ki*dT) *G/Gn;  % Actual short-circuit current
% Increments Rs
Rs = Rs + Rsinc;
Rp_ = Rp;
Rp = Vmp*(Vmp+Imp*Rs)/(Vmp*Ipv-
Vmp*Io*exp((Vmp+Imp*Rs)/Vt/Ns/a)+Vmp*Io-Pmax_e);
% Solving the I-V equation for several (V,I) pairs
clear V
clear I
V = 0:Vocn/nv:Vocn;    % Voltage vector
I = zeros(1,size(V,2)); % Current vector
for j = 1 : size(V,2) %Calculates for all voltage values
% Solves g = I - f(I,V) = 0 with Newton-Raphson
g(j) = Ipv-Io*(exp((V(j)+I(j)*Rs)/Vt/Ns/a)-1)-(V(j)+I(j)*Rs)/Rp-I(j);

```

```

while (abs(g(j)) > 0.001)
g(j) = Ipv-Io*(exp((V(j)+I(j)*Rs)/Vt/Ns/a)-1)-(V(j)+I(j)*Rs)/Rp-I(j);
glin(j) = -Io*Rs/Vt/Ns/a*exp((V(j)+I(j)*Rs)/Vt/Ns/a)-Rs/Rp-1;
I_(j) = I(j) - g(j)/glin(j);
I(j) = I_(j);
end
end % for j = 1 : size(V,2)

% Calculates power using the I-V equation
P = (Ipv-Io*(exp((V+I.*Rs)/Vt/Ns/a)-1)-(V+I.*Rs)/Rp).*V;

Pmax_m = max(P);

perror = (Pmax_m-Pmax_e);

end % while (error>tol)

%% Outputs

% I-V curve

figure(1)

grid on

hold on

title('Adjusted I-V curve');

xlabel('V [V]');

ylabel('I [A]');

xlim([0 Vocn*1.1]);

ylim([0 Iscn*1.1]);

```

```

plot(V,I,'LineWidth',2,'Color','k') %
plot([0 Vmp Vocn ],[Iscn Imp 0
], 'o','LineWidth',2,'MarkerSize',5,'Color','k')
% P-V curve
figure(2)
grid on
hold on
title('Adjusted P-V curve');
xlabel('V [V]');
ylabel('P [W]');
xlim([0 Vocn*1.1]);
ylim([0 Vmp*Imp*1.1]);
plot(V,P,'LineWidth',2,'Color','k') %
plot([0      Vmp      Vocn      ],[0      Pmax_e      0
], 'o','LineWidth',2,'MarkerSize',5,'Color','k')
disp(sprintf('Model info:\n'));
disp(sprintf(' Rp_min = %f,Rp_min));
disp(sprintf('   Rp = %f,Rp));
disp(sprintf(' Rs_max = %f,Rs_max));
disp(sprintf('   Rs = %f,Rs));
disp(sprintf('   a = %f,a));
disp(sprintf('   T = %f,T-273.15));

```

```
disp(sprintf(' G = %f',G));  
disp(sprintf(' Pmax,m = %f (model)',Pmax_m));  
disp(sprintf(' Pmax,e = %f (experimental)',Pmax_e));  
disp(sprintf(' tol = %f',tol));  
disp(sprintf('P_error = %f',perror));  
disp(sprintf(' Ipv = %f',Ipv));  
disp(sprintf(' Isc = %f',Isc));  
disp(sprintf(' Ion = %f',Ion));  
disp(sprintf('\n\n'));
```

Appendix (C)

Perturb and Observe Algorithm

```

function D = PO(V,I,T)
% MPPT controller based on the Perturb &
Observe algorithm.
% D output = Duty cycle of the boost converter
(value between 0 and 1)
% Enabled input = 1 to enable the MPPT
controller
% V input = PV array terminal voltage (V)
% I input = PV array current (A)
% Param input:
Dinit = 0.5; %Initial value for D output
Dmax =0.9; %Maximum value for D
Dmin = 0.1; %Minimum value for D
deltaD =0.01; %Increment value used to
increase/decrease the duty cycle D
% ( increasing D = decreasing Vref )
%
persistent Vold Pold Dold n P;
dataType = 'double';
if isempty(Vold)
    Vold=0;
end
if isempty(n)
    n=1;
end
if isempty(Pold)
    Pold=0;
end
if isempty(Dold)
    Dold=Dinit;
end
%%%%%%%%%%%%%%
if (T > n*0.02) %0.02s
    P= V*I;
    dV= V - Vold;
    dP= P - Pold;
    if dP ~= 0
        if dP < 0

```

158

```
    if dV < 0
        D = Dold - deltaD;
    else
        D = Dold + deltaD;
    end
else
    if dV < 0
        D = Dold + deltaD;
    else
        D = Dold - deltaD;
    end
end
else D=Dold;
end
    if D >= Dmax || D<= Dmin
        D=Dold;
    end
Dold=D;
Vold=V;
Pold=P;
end
```

APPENDIX (D)

Specifications of the Standalone PV system elements

(D.1): Solar PV module technical specifications

THE NEW VALUE FRONTIER





KC130GHT-2

High efficiency multicrystal photovoltaic module



CUTTING-EDGE TECHNOLOGY

Exhaustive research work, continuous further development of production processes and highly automated production enable polycrystalline Kyocera solar modules to attain an exceptional standard of quality and markedly high levels of efficiency.

The integrated Kyocera high-performance solar cells with a standard size of 15 cm x 15.5 cm achieve over 16% efficiency, guaranteeing an extremely high annual yield of energy from the photovoltaic system.

To protect against the harshest weather conditions, the cells are embedded between a reinforced glass covering (halloform resistance complying with IEC 61215, tested by TÜV) and EVA foil, and are sealed with a PET foil backing. The laminate is set in a sturdy aluminum frame which is easy to assemble.

The back of the junction box is equipped with bypass diodes that eliminate the risk of the individual solar cells overheating (hot spot effect). Many series-connected photovoltaic modules can be easily wired using pre-assembled solar cables and multi-contact plugs.

Kyocera manufactures all the components at its own production sites – without buying in semi-finished products – to ensure consistently high product quality.

EXAMPLES OF APPLICATION

- Off-grid systems, for e.g.
 - Residential Solar Power Systems
 - Public and Industrial Solar Power Systems
 - Solar power stations

TÜV-certified Solar Inverter platform for tested quality and safety
 TÜV-certified 000007356
 IEC 61215 and Safety Class II
 Kyocera is ISO 14001 and ISO 14001 certified and registered.



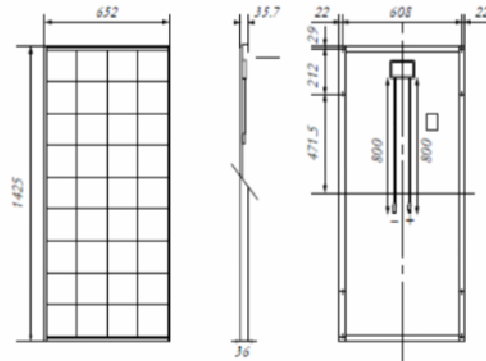



KYOCERA SOLAR

We care!

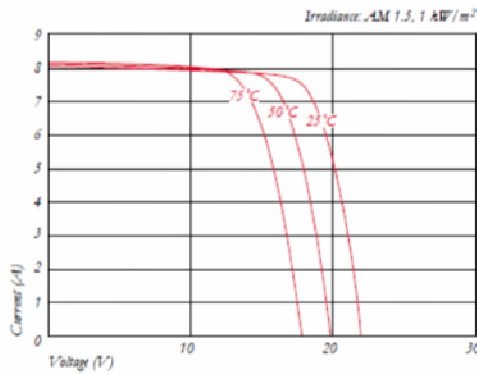
SPECIFICATIONS

in mm

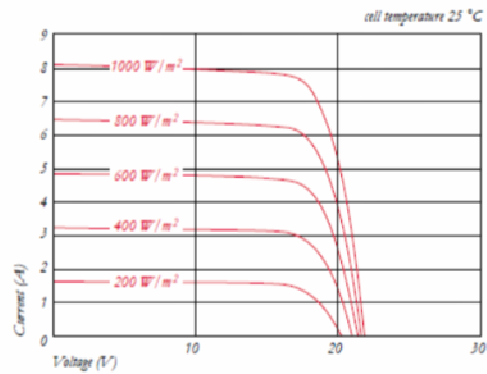


ELECTRICAL CHARACTERISTICS

Current-Voltage characteristics at various cell temperatures



Current-Voltage characteristics at various irradiance levels



ELECTRICAL PERFORMANCE

PV module type	KC130GHT-2	
At 1000 W/m² (STC)*		
Maximum Power	[W]	130
Maximum System Voltage	[V]	1000
Maximum Power Voltage	[V]	17.6
Maximum Power Current	[A]	7.39
Open Circuit Voltage (V _{oc})	[V]	21.9
Short Circuit Current (I _{sc})	[A]	8.02
At 800 W/m² (NOCT)**		
Maximum Power	[W]	92
Maximum Power Voltage	[V]	15.5
Maximum Power Current	[A]	5.94
Open Circuit Voltage (V _{oc})	[V]	19.9
Short Circuit Current (I _{sc})	[A]	6.47
Temperature Coefficients		
NOCT	[°C]	47
Power tolerance	[%]	+10 / -5
Temperature Coefficient of V _{oc}	[V/°C]	-0.21×10 ⁻²
Temperature Coefficient of I _{sc}	[A/°C]	3.18×10 ⁻³
Reduction of efficiency (from 1000 W/m ² to 200 W/m ²)	[%]	4.3

DIMENSIONS

Length	[mm]	1425
Width	[mm]	652
Depth / incl. junction box	[mm]	36 / 36
Weight	[kg]	12.2
Cable	[mm]	(+)800 / (-)800
Connection type		MC-PV3
Junction box	[mm]	113.6x76x9
IP Code		IP65

GENERAL INFORMATION

Performance guarantee	10*** / 20 years****
Warranty	2 years

CELLS

Number per module	36
Cell Technology	multicrystal
Cell Shape (rectangular)	[mm] 150x155
Cell Bonding	3 busbar

* Electrical values under standard test conditions (STC): irradiance of 1000 W/m², air mass AM 1.5 and cell temperature of 25 °C.

** Electrical values under normal operating cell temperature (NOCT): irradiance of 800 W/m², air mass AM 1.5, and wind of 1m/s and ambient temperature of 20 °C.

*** 10 years on 90% of the minimally specified power P under standard test conditions (STC).

**** 20 years on 80% of the minimally specified power P under standard test conditions (STC).

(D.2): Battery Block specifications

Nickel Iron (Ni-Fe) Battery



Cell Size Info

Please take a look at the cell sizes. There are multiple cell capacities that come in the same size container. We highly recommend using the 300Ah cell size or larger for almost every project.

The **100Ah** cell and the **200Ah** cell are great for a small remote pumping station or somewhere that space is tight. The **300Ah**, **400Ah** and **500Ah** cell containers are nearly identical, and are a very popular size. This container features integrated handles that make setup very

easy. This group of cells contains nearly 4x the volume of electrolyte when compared to the 200Ah cell.

For the **600Ah** and **700Ah** cells, the amount of electrolyte in each cell nearly doubles from the previous group. I really like the design of these cells, and recommend them whenever possible. The largest group of cells **800Ah**, **900Ah** and **1000Ah** share the largest container. All cells 600 Ah and bigger come in a clear case that lets you easily monitor electrolyte levels in the cells. Whereas the smaller cells are easier to setup, the larger cells may be easier to maintain.

The Last Battery You Will Ever Buy

Iron Edison recommends Nickel Iron (Ni-Fe) battery technology for your off-grid or renewable energy storage needs. Vastly out-lasting the 7 year life cycle of their lead-acid counterparts, Nickel-iron battery systems have an expected life of twenty five years or more and are quickly becoming the environmentally sensitive choice for off-grid and renewable energy storage applications.

Over a century ago, Thomas Edison found a battery design that he considered to be nearly perfect. Today, Iron Edison is proud to offer an updated version of this incredible design that is specifically manufactured for Renewable Energy systems.

- **Refillable alkaline electrolyte**
- **Full depth of discharge**

- **12, 24 and 48 Volt applications**
- **Nearly indestructible**

Proven Performance

Iron Edison is the only company to have tested the Nickel Iron batteries at a National Renewable Energy laboratory. The cells were vigorously tested at multiple discharge rates, and in each test the cells delivered more than the rated capacity at the 5, 10 and 20 hour discharge rates.

Charging

The action which takes place in an Edison cell, both in charging and discharging, is a transfer of oxygen from one electrode to the other, or from one group of plates to the other, hence this type of cell is sometimes called an oxygenlift cell. In a charged cell the active material of the positive plates is superoxidized, and that of the negative plates is in a spongy or deoxidized state.

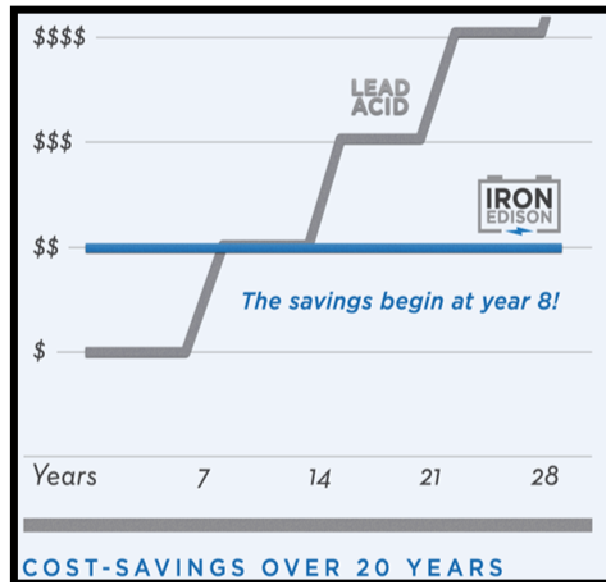
If the normal capacity of the cell is insufficient, short intermediate high rate charges can be given provided that the temperature of the electrolyte does not exceed 115 F. These short charges are very efficient and cause no injury. Rates up to three times normal can be employed for periods of 30 minutes.

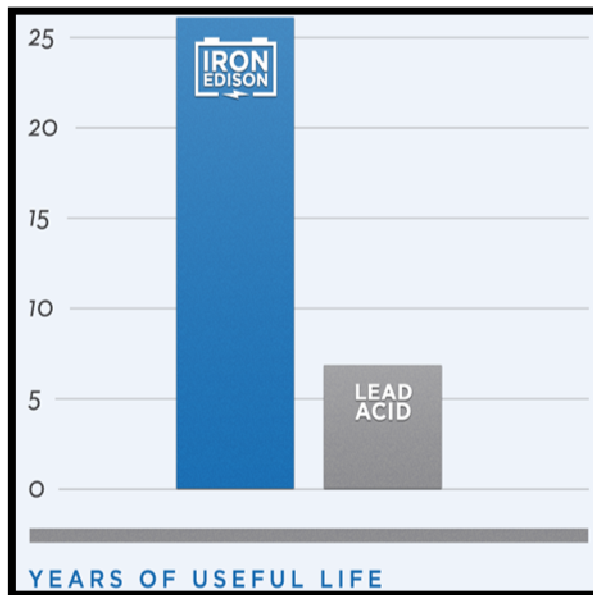
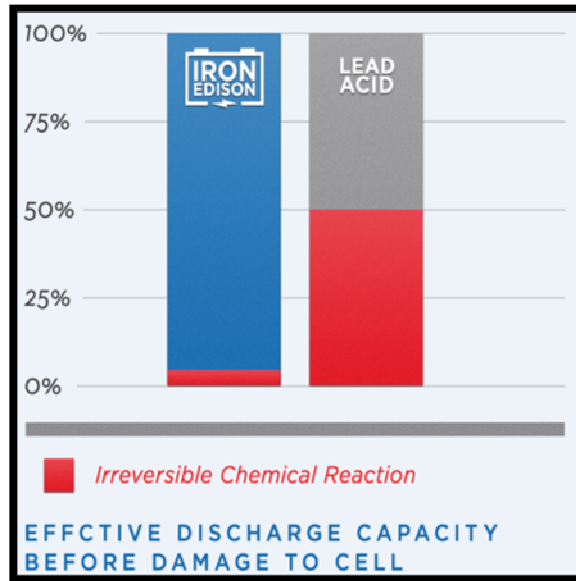
Discharge

In discharging the positive plates deoxidize and the oxygen, with its natural affinity for iron, goes to the negative plates, oxidizing them. It is permissible to discharge continuously at any rate up to 25% above normal, and occasionally for short periods at rates up to six times normal.

Electrolyte

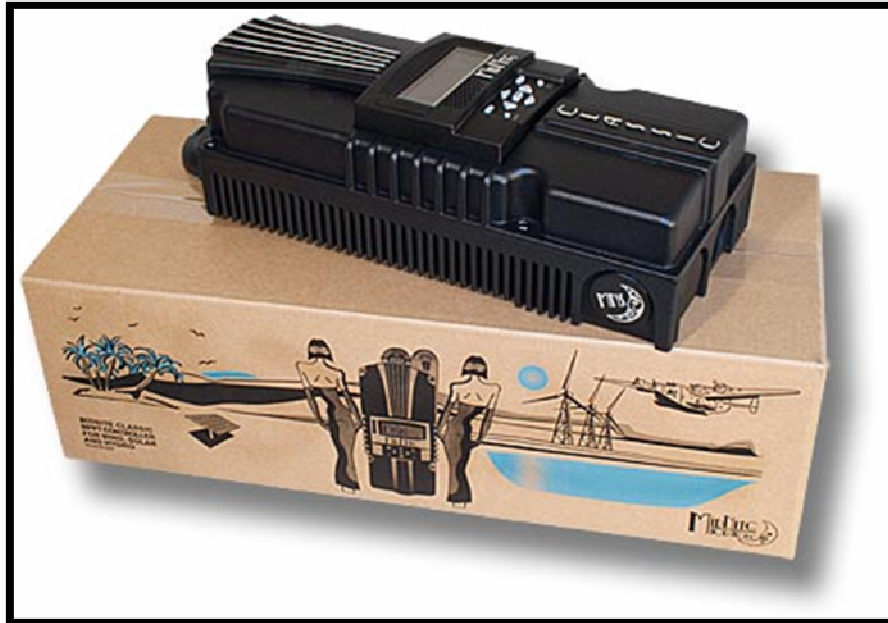
The electrolyte of the Nickel Iron cells does not enter into chemical combination to perform the functions of the cell, but acts merely as a conveyor; it therefore does not change in specific gravity during charge and discharge other than through evaporation and changes in temperature. Considerable variation in specific gravity is permissible, it having influence only on battery efficiency.





(D.3): Charge controller specifications

MidNite Classic MPPT Charge Controllers



Overview

The MidNite Classic charge controller maximizes the flexibility and features available in a charge controller. At this time, the Classic is the only MPPT charge controller that offers arc fault detection. This will soon be required by the NEC.

Features

The The MidNite Classic charge controllers also include ground fault protection so that a separate GFP breaker assembly is not necessary and leaves those breaker spaces free for other uses.

Specific models accommodate solar arrays with up to 150, 200, or 250 VDC of operating voltage.

Open circuit voltage (Voc) is based on operating voltage plus the battery voltage. This is called the HyperVOC zone.

They have MPPT modes for solar, wind or hydro with user adjustable power curves, and a learning mode for self optimization. No hub is required for stacking Classics to act as one large controller.

Specifications

They have two auxiliary outputs, a dry contact relay and a 12V output.

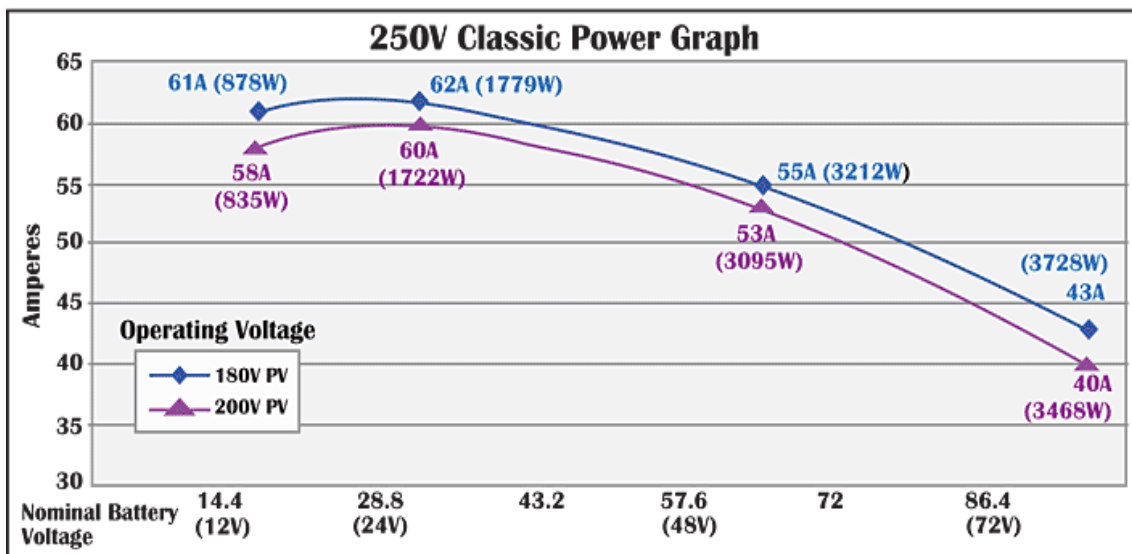
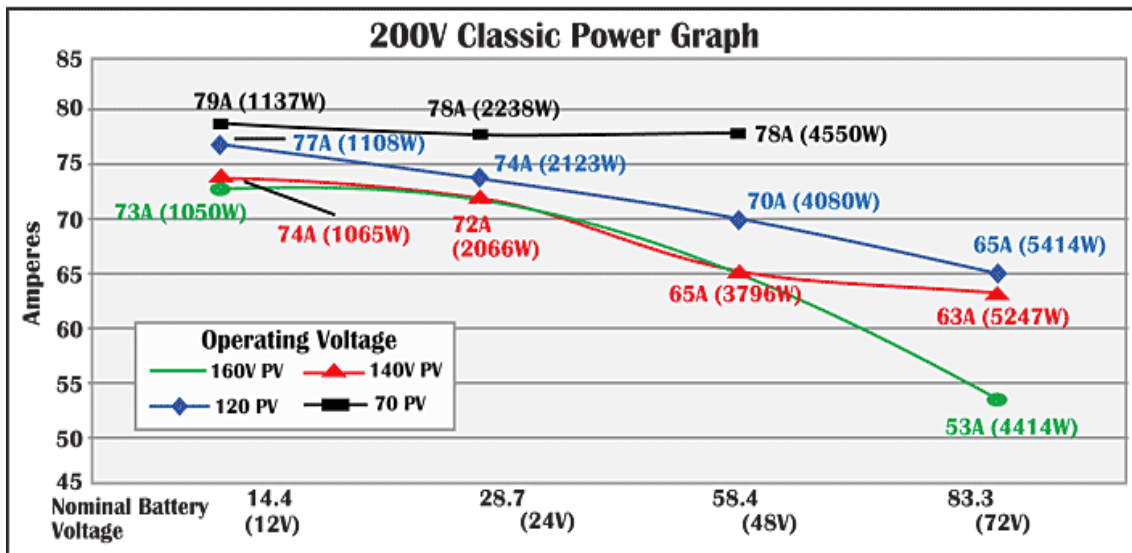
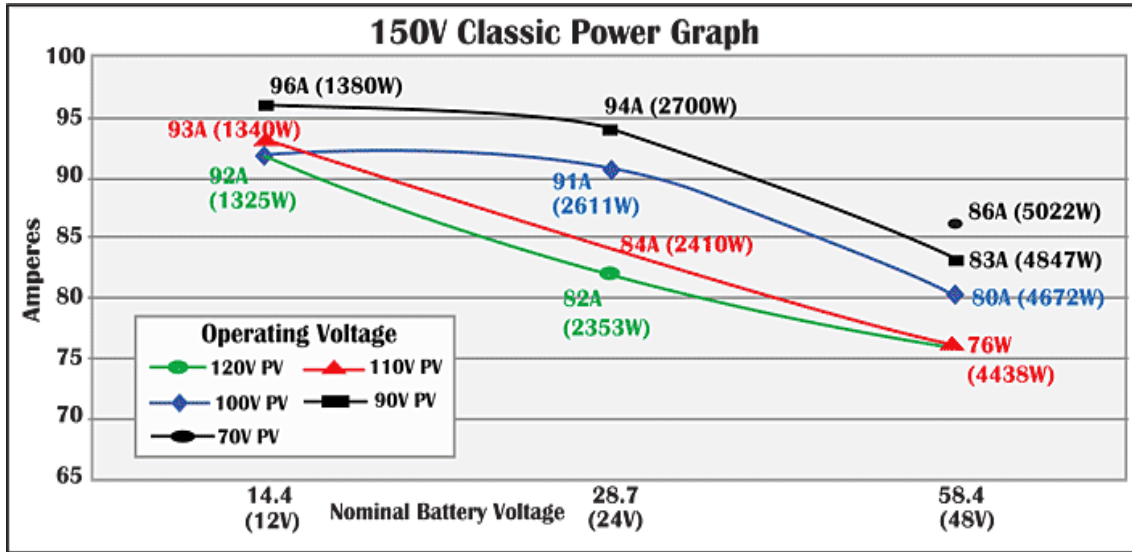
Each unit includes snap-on covers and hole plugs for sealing openings in dusty or salt-air environments, but about 20% reduction in output will result when used in sealed mode.

The Classic has built-in Ethernet, USB and RS-232 ports for two-way communications.

An internal IP address allows the Classic to be a mini web server when hooked up to broadband. It has 32 MB of memory for data storage.

A wizard driven setup covers battery bank size, string voltage, wind turbine selection, power and wire loss chart, PV breaker sizing and more.

Model	Classic 150	Classic 200	Classic 250	Classic 250KS
Operating Volts in	150VDC	200VDC	250VDC	250VDC
*Max Hyper VOC	150+battery	200+battery	250+battery	250+battery
Nominal Battery Volts	12-72 volts	12-72 volts	12-72 volts	12-120 volts
**Absolute Current Output at 25° C	96a at 12v battery 94a at 24v battery 83a at 48v battery	74a at 12v battery 70a at 24v battery 65a at 48v battery	60a at 12v battery 62a at 24v battery 55a at 48v battery	40a at 120v battery
De-rate current at 40°C+	80 amperes	66 amperes	52 amperes	33 amperes
Environment	-40c to 40c			
Dimensions of Classic	14.87" x 5.95" x 4.00" 378mm x 151mm x 102mm			
Dimensions of Box	19.00" x 8.50" x 5.70" 483mm x 216mm x 145mm			
Shipping Weight	11.5lb 4.9kg			
NOTE: Current output ratings were measured with 75% of the PV array's VOC (Open Circuit Voltage)				
*NOTE: Calculated by adding battery voltage to the maximum input operating voltage (48V battery max)				
**NOTE: Measurement Accuracies: +-0.12v, offset calibration adjustment maybe necessary				



(D.4): Inverter specifications**LCD Powerstar Inverter Charger 1kw-6kw, 12V/24V/48vdc, Pure Sine Wave Inverter****Product Description**

Powerstar inverter charger 1KW-6KW, 12V/24V/48vdc, pure sine wave inverter, 220vac/110vac (LNW series)

LCD digital display panel.

35AMP/70AMP built in charger.

LW Series Pure Sine Wave Inverter takes high frequency converter Device. Zero Voltage(ZV) and soft switch technic, high capability Motorola MCU, digital and dummy combined technics which Complete the

voltage increase in one time and SPWM wave modemed Advanced circuit, high efficiency and compact size, small weight And super stability.

It widely applied in wind generator, Solar battery pack set, house, vehicle, ship, navigation and places where lack of city power, mobile electricity work and telecommunications device, launch Station, Emengency EPS.

Pure sine wave Inverters has no repellency for the load, which can work well with fluorescent lamp, electromotor, microwave ovens, Induction cooker, refrigerator, air conditions and transformer.

With protection fonction like, DC input protect When pole wrong, AC input protection against over and low voltage, Output protection against over load, shor circuit Protection, DC input and AC output completely electric insulation. Please contact with Cathy for more specification and details on it.

(Rated Output Power)	1000w	2000w	3000w	4000W	5000w	6000w
Input Voltage Waveform	Pure Sine Wave (utility or generator)					
Nominal Input Voltage	230Vac					
Low Line Disconnect	184Vac±4%					
High Line Disconnect	253Vac±4%					
Max AC Input Voltage	270Vrms					
Nominal Input Frequency	50Hz/ 60Hz (Auto detection)					
Over-Load Protection (SMPS load)	Circuit breaker					
Output Short Circuit Protection	Circuit breaker					
Efficiency (Line Mode)	>95%					
Transfer Switch Rating	30A					
Transfer Time (Ac to Dc)	20ms (typical)					
Output Voltage Waveform	Sine wave					
Power Factor	0~1.0					
Nominal Output Voltage (V)	230Vac					
Output Voltage Regulation	±10% rms					
Nominal Efficiency	>80%					
Nominal DC Input Voltage	12V/24V	12V/24V	12V/24V/48V	24V/48V	24V/48V	24V/48V
Nominal Charge Current	35A	35A	35A	70A	70A	70A
Charge Current Regulation	± 5A _{dc}					
Battery initial voltage	0 –15.7 V _{dc} (can operate with 0V battery)					
Communication:	RJ11 (Used for factory testing. No customer interface available)					
Safety Certification	Compliance with UL458		CE(EN60950)			
EMI Classification	FCC, CLASS A		EN50091-2, CLASS A			
Operating Temperature Range	0°C to 40°C					
Storage temperature	-15°C ~ 60°C					
Operation humidity	5% to 95%					
Audible Noise	60dB max					
Cooling	Forced air, variable speed fan					

Appendix (E)**Charge controller algorithm BY M-file**

```
function [Vref,Iref,signal,SD] = CHARGER(V,I,T)
persistent temp_i temp_v temp_signal temp_fault CC CV n ;
if isempty(temp_i)
    temp_i=0.2;
end
if isempty(temp_v)
    temp_v=0;
end
if isempty(temp_signal)
    temp_signal=1;
end
if isempty(temp_fault)
    temp_fault=1;
end
if isempty(CC)
    CC=1;
end
if isempty(CV)
    CV=0;
```

```
end

if isempty(n)
    n=0;
end

if (T>n*0.02) % sample time is 0.02s
    n=n+1;
    if CC
        if V<52.8
            temp_i=0.1;
            temp_v=0;
            temp_signal=1;
        else
            CV=1;
        end
    end
end

if CV
    if I>5.0
        temp_i=0;
        temp_v=1;
        temp_signal=2;
    else
```

```
        temp_fault=0;

    end

end

end

signal=temp_signal;

SD=temp_fault;

Iref=temp_i;

Vref=temp_v;

end
```

Appendix (F)

Table of interest at $i = 10\%$

10%		10%						
n	Single Payments		Uniform-Series Payments				Uniform Gradient	
	Compound Amount <i>F/P</i>	Present Worth <i>P/F</i>	Sinking Fund <i>A/F</i>	Compound Amount <i>F/A</i>	Capital Recovery <i>A/P</i>	Present Worth <i>P/A</i>	Gradient Present Worth <i>P/G</i>	Gradient Annual Series <i>A/G</i>
1	1.1000	0.9091	1.00000	1.0000	1.10000	0.9091		
2	1.2100	0.8264	0.47519	2.1000	0.57619	1.7355	0.8264	0.4762
3	1.3310	0.7513	0.30211	3.3100	0.40211	2.4869	2.3291	0.9366
4	1.4641	0.6830	0.21547	4.6410	0.31547	3.1699	4.3781	1.3812
5	1.6105	0.6209	0.16380	6.1051	0.26380	3.7908	6.8618	1.8101
6	1.7716	0.5645	0.12961	7.7156	0.22961	4.3553	9.6842	2.2236
7	1.9487	0.5132	0.10541	9.4872	0.20541	4.8684	12.7631	2.6216
8	2.1436	0.4665	0.08744	11.4359	0.18744	5.3349	16.0287	3.0045
9	2.3579	0.4241	0.07364	13.5795	0.17364	5.7590	19.4215	3.3724
10	2.5937	0.3855	0.06275	15.9374	0.16275	6.1446	22.8913	3.7255
11	2.8521	0.3505	0.05396	18.5312	0.15396	6.4951	26.2965	4.0641
12	3.1384	0.3186	0.04676	21.3843	0.14676	6.8137	29.9012	4.3884
13	3.4523	0.2897	0.04078	24.5227	0.14078	7.1034	33.3772	4.6988
14	3.7975	0.2633	0.03575	27.9750	0.13575	7.3667	36.8005	4.9955
15	4.1772	0.2394	0.03147	31.7725	0.13147	7.6061	40.1520	5.2789
16	4.5950	0.2176	0.02782	35.9497	0.12782	7.8237	43.4164	5.5493
17	5.0545	0.1978	0.02466	40.5447	0.12466	8.0216	46.5819	5.8071
18	5.5599	0.1799	0.02193	45.5992	0.12193	8.2014	49.6395	6.0526
19	6.1159	0.1635	0.01955	51.1391	0.11955	8.3649	52.5827	6.2861
20	6.7273	0.1486	0.01746	57.2750	0.11746	8.5136	55.4069	6.5081
21	7.4002	0.1351	0.01562	64.0025	0.11562	8.6487	58.1095	6.7189
22	8.1403	0.1228	0.01401	71.4027	0.11401	8.7715	60.6893	6.9189
23	8.9543	0.1117	0.01257	79.5430	0.11257	8.8832	63.1462	7.1085
24	9.8497	0.1015	0.01130	88.4973	0.11130	8.9847	65.4813	7.2881
25	10.8347	0.0923	0.01017	98.3471	0.11017	9.0770	67.6964	7.4580
26	11.9182	0.0839	0.00916	109.1818	0.10916	9.1609	69.7940	7.6186
27	13.1100	0.0763	0.00826	121.0949	0.10826	9.2372	71.7773	7.7704
28	14.4210	0.0693	0.00745	134.2099	0.10745	9.3066	73.6495	7.9137
29	15.8631	0.0630	0.00673	148.6309	0.10673	9.3696	75.4146	8.0489
30	17.4494	0.0573	0.00608	164.4940	0.10608	9.4267	77.0766	8.1762
31	19.1943	0.0521	0.00550	181.9434	0.10550	9.4790	78.6393	8.2962
32	21.1136	0.0474	0.00497	201.1378	0.10497	9.5264	80.1078	8.4091
33	23.2252	0.0431	0.00450	222.2515	0.10450	9.5694	81.4856	8.5152
34	25.5477	0.0391	0.00407	245.4767	0.10407	9.6086	82.7773	8.6149
35	28.1024	0.0354	0.00369	271.0244	0.10369	9.6442	83.9872	8.7086
40	45.2593	0.0221	0.00226	442.5926	0.10226	9.7741	88.9525	9.0962
45	72.1925	0.0137	0.00139	718.9068	0.10139	9.8628	92.4544	9.3340
50	112.9909	0.0085	0.00086	1163.91	0.10086	9.9148	94.6889	9.5394
55	189.0591	0.0053	0.00053	1890.59	0.10053	9.9471	96.5619	9.7073
60	304.4816	0.0033	0.00033	3034.82	0.10033	9.9672	97.7010	9.8023
65	490.3707	0.0020	0.00020	4893.71	0.10020	9.9796	98.4705	9.8672
70	789.7470	0.0013	0.00013	7867.47	0.10013	9.9873	98.9870	9.9113
75	1271.90	0.0008	0.00008	12709	0.10008	9.9921	99.3317	9.9410
80	2048.40	0.0005	0.00005	20474	0.10005	9.9951	99.5696	9.9609
85	3298.97	0.0003	0.00003	32980	0.10003	9.9970	99.7126	9.9742
90	5313.02	0.0002	0.00002	53120	0.10002	9.9981	99.8118	9.9831
95	8256.68	0.0001	0.00001	8257	0.10001	9.9988	99.8773	9.9889
96	9412.34	0.0001	0.00001	94113	0.10001	9.9991	99.8874	9.9898
98	11389	0.0001	0.00001		0.10001	9.9994	99.9032	9.9914
100	13781	0.0001	0.00001		0.10001	9.9993	99.9202	9.9927

جامعة النجاح الوطنية
كلية الدراسات العليا

تصميم ومحاكاة نظام خلايا شمسية مع متحكم لإيجاد القدرة القصوى لتغذية الحمل بالتيار المتناوب

إعداد

جعفر سيف الدين عبد الحفيظ جلال

إشراف

أ. د. مروان محمود

قدمت هذه الأطروحة استكمالاً لمتطلبات نيل درجة الماجستير في هندسة الطاقة النظيفة
وإستراتيجية الترشيد بكلية الدراسات العليا في جامعة النجاح الوطنية, نابلس - فلسطين.

2012م

ب

تصميم ومحاكاة نظام خلايا شمسية مع متحكم لإيجاد القدرة القصوى لتغذية الحمل بالتيار المتناوب

إعداد

جعفر سيف الدين عبد الحفيظ جلاد

إشراف

أ. د. مروان محمود

الملخص

تعد دراسة أنظمة الخلايا الشمسية والبحث فيها من المواضيع الهامة الذي يجدر بنا تناولها في فلسطين خاصة لانعدام مصادر الطاقة التقليدية وتوفر إمكانية توليد الطاقة الكهربائية بكميات مجدية من الطاقة الشمسية. يقدم هذا البحث تصميم ومحاكاة لنظام خلايا شمسية مستقل وفعال لتزويد الاحمال الكهربائية المنزلية، كما يتناول دراسة نظرية للوحات الخلايا الشمسية وكيفية نمذجتها على برنامج الماتلاب سيمولنك وبرنامج البي سيم باستخدام المعادلات المتعلقة بها والدوائر الكهربائية المكافئة لها. يتناول هذا البحث أيضا أنواع مختلفة من الخوارزميات التي تعمل على إيجاد نقطة القدرة القصوى لزيادة الطاقة المستفادة من الإشعاع الشمسي و تطبيقها على محول فولتيات لتحويلها من مستوى فولتية الى مستوى اخر يتلائم مع فولتية البطارية لشحنها ومن ثم تحويل تلك الفولتية من فولتية مستمرة الى فولتية مترددة تتناسب والاحمال الكهربائية المنزلية من حيث قيمة الفولتية والتردد باستخدام برنامج الماتلاب سيمولنك.

في هذا البحث تم اختيار حمل منزلي يومي بمقدار 4.5 كيلو واط.ساعة كمثال، لإختيار افضل تصميم لنظام خلايا شمسي مستقل بكافة مكوناته الممثلة في ألواح شمسية قدرتها 1.15 كيلو واط ، بطاريات لتخزين الطاقة سعتها 11.7 كيلو واط.ساعة بالإضافة الى محول فولتيات من مستمر الى متردد قدرته 3 كيلو واط.

بناء على الحمل المنزلي الذي تم اختياره وسعر تكلفة مكونات نظام الخلايا الشمسية

المستقل وتركيبه فقد تبين ان تكلفة سعر الكيلو واط.ساعة المنتج من هذا النظام هو 2.1 شيكل.